AD NUMBER: AD0864287
LIMITATION CHANGES
TO: Approved for public release; distribution is unlimited.
FROM: Distribution authorized to U.S. Gov't. agencies and their contractors; Export Control; 1 Aug 1969. Other requests shall be referred to the Air Force Air Materiels Lab, (MAM), Wright-Patterson AFB, OH 45433.
AUTHORITY
USAF LTR, 12 JAN 1972

AFML-TR-69-224

INVESTIGATION OF THE EFFECTS OF THERMAL MECHANICAL VARIABLES ON THE CREEP PROPERTIES OF HIGH STRENGTH COLUMBIUM ALLOYS

J. A. Cornie
R. T. Begley

Westinghouse Astronuclear Laboratory

Technical Report AFML-TR-69-224

August 1969

Air Force Materials Laboratory
Air Force Systems Command
Wright-Patterson Air Force Base, Ohio

BLANK PAGE

NOTICES

When Government drawings, specifications, or other data are used for any purpose other than in connection with a definitely related Government procurement operation, the United States Government thereby incurs no responsibility nor any obligation whatsoever; and the fact that the Government may have formulated, furnished, or in any way supplied the said drawings, specifications, or other data, is not to be regarded by implication or otherwise as in any manner licensing the holder or any other person or corporation, or conveying any rights or permission to manufacture, use, or sell any patented invention that may in any way be related thereto.

This document is subject to special export controls and each transmittal to foreign governments or foreign nationals may be made only with prior approval of Metals and Ceramics Division (MAM), Air Force Materials Laboratory, Wright-Patterson Air Force Base, Ohio 45433.

The distribution of this report is limited because it contains technology identifiable with items on the strategic embargo lists excluded from export under the U. S. Export and AFSC 80-20.

Copies of this report should not be returned unless return is required by security considerations, contractual obligations, or notice on a specific document.

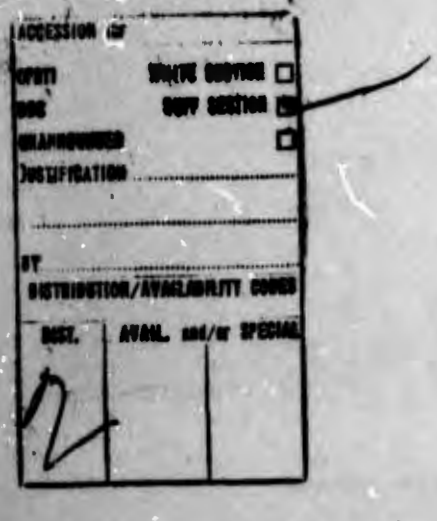

AFML-TR-69-224

INVESTIGATION OF THE EFFECTS OF THERMAL MECHANICAL VARIABLES ON THE CREEP PROPERTIES OF HIGH STRENGTH COLUMBIUM ALLOYS

J. A. Cornie
R. T. Begley

Westinghouse Astronuclear Laboratory

Technical Report AFML-TR-69-224

August 1969

Air Force Materials Laboratory
Air Force Systems Command
Wright-Patterson Air Force Base, Ohio

FOREWORD

The work described in this report was carried out by personnel of the Westinghouse Astronuclear Laboratory under USAF Contract AF33615-67-C-1443, BPSN Nr 67(687351-735101-62405514). The contract is being administered under the direction of the Air Force Materials Laboratory, Wright-Patterson Air Force Base, Ohio with Mr. J. K. Elbaum acting as project engineer.

This report describes the results of research conducted during the period April 1, 1967 to January 30, 1969. The manuscript was released by the authors June 1969 for publication as a technical report.

The authors wish to acknowledge the assistance of E. Vandergrift (Mechanical Property Testing), C. Fitterer (Processing), K. Galbraith (Optical Metallography), R. Harding (Electron Microscopy), and R. Conlin (X-ray Analysis).

This technical report has been reviewed and is approved.

I. Perlmutter
Chief, Metals Branch
Metals and Ceramics Division
Air Force Materials Laboratory

ABSTRACT

A comparison of the properties of two high strength columbium base alloys, Cb-1 (Cb-30W-1Zr-0.06C-0.04N) and B-88 (Cb-28W-2Hf-0.067C) was made to reconcile the reported variation in mechanical properties of the two compositions. Studies of recrystallization, grain growth, and response to thermal-mechanical processing were carried out to characterize the material. The alloys were quite similar in their response to thermal treatment with the exception that Cb-1 showed aging response in the temperature range 1000 - 1200°C. The aging behavior was attributed to the precipitation of a zirconium nitride or carbonitride. The 1315°C (2400°F) creep-rupture properties of the two alloys were quite similar when compared in equivalent structural conditions, with Cb-1 being slightly superior to B-88. The ductile-brittle transition of B-88 was approximately 50°C lower than that of Cb-1.

Studies of methods to increase the intermediate temperature (1200 - 1600°F) yield strength of creep resistant columbium alloys were also carried out. Prestraining was shown to be an effective means of increasing the yield strength in this temperature range. Prestraining a Cb-22W-2Hf-0.06C alloy 9% at 1400°F raised the 1400°F yield strength from 50,000 psi to 95,000 psi. Detailed studies of recovery behavior of prestrained specimens were conducted to permit prediction of the effect of protective coating thermal cycles on residual strain hardening.

The precipitation hardening behavior of a Cb-W-Hf-C-N alloy was also investigated to determine if the intermediate temperature strength of a creep resistant columbium alloy could be increased without degrading high temperature rupture properties. A Cb-22W-2Hf-0.05C-0.04N alloy exhibited pronounced aging response in the 1000 - 1200°C temperature range. A double aging peak was observed. Transmission photomicroscopy studies showed the hardness peaks correlated with the presence of a high density of small coherent precipitates, presumably a hafnium nitride or carbonitride.

TABLE OF CONTENTS

LIST OF FIGURES

LIST OF FIGURES
(continued)

LIST OF FIGURES
(continued)

LIST OF FIGURES
(continued)

LIST OF FIGURES
(continued)

LIST OF TABLES

I. INTRODUCTION

Previous investigations conducted under Contract AF 33(615)-1728[1,2] resulted in the development of the alloy B-88 (Cb-28W-2Hf-0.067C) which has very attractive properties for potential turbine bucket applications. The properties achieved in these initial studies were a density compensated 100 hour rupture strength at 2400°F of 68,500 inches, and 11% room temperature elongation. These properties were achieved by a processing sequence involving high temperature extrusion for ingot breakdown, warm swaging (1300°C) to rod stock, and a final anneal at 1700°C. These initial studies[1,2] demonstrated the pronounced effect of structure, as influenced by prior thermal-mechanical processing, on the creep properties of this alloy. The current study was undertaken with the primary objective of achieving a more detailed understanding of the relationship between structure and mechanical properties of B-88 which would lead to the development of improved properties through proper control of thermal mechanical processing.

An additional objective of the program was to compare the properties of Cb-1 alloy (Cb-30W-1Zr-0.06C-0.04N) investigated by Chang[3] with those of B-88 (Cb-28W-2Hf-0.067C). The high temperature strength of Cb-1 was reported to be significantly superior to B-88 even though the compositions are quite similar. Previous studies at WANL have shown no superiority of zirconium over hafnium as a reactive metal addition in Cb alloys. Hence the difference in mechanical properties may arise from the presence of 0.044% nitrogen in the Cb-1 alloy, or from differences in the processing sequence used to fabricate Cb-1 and B-88. It was thus important to verify the reported high strength of Cb-1 and to determine if the strength difference results from variations in composition or fabrication sequence. A final objective of the program was to evaluate the effects of oxidation resistant coatings on the mechanical properties of B-88.

Following the initiation of this program, attention was focused on the relatively low intermediate temperature (1200-1600°F) yield strength exhibited by B-88 and similar alloys. High yield strength values in this temperature range are critical to avoid plastic

deformation in the root area of a turbine blade. Historically the development of columbium alloys for gas turbine applications has emphasized the improvement of creep properties. As a result, the reference heat treatments were selected to provide the optimum combination of creep resistance and room temperature ductility. For B-88, the optimized condition resulted in a fine grained recrystallized structure. Low and intermediate temperature short time properties, on the other hand, are generally optimized by processing to produce a wrought, recovered structure. Group V_A refractory metal alloys optimized for creep strength do not exhibit their full short-time yield strength potential and conversely, alloys optimized for high strength in the intermediate temperature region have seriously degraded high temperature creep properties. Design studies for columbium alloy turbine blades based on existing superalloy blade geometries call for a minimum yield strength on the order of 70,000 psi at 1200 to 1600°F. The B-88 alloy in the recrystallized condition exhibits a yield strength of only 50,000 psi over this temperature range.

Consequently, at the direction of AFML, the program was redirected to explore methods of developing the required yield strength level in columbium base alloys without serious degradation of high temperature creep properties. Briefly, two approaches were selected:

1. Preferentially cold or warm working the root section in an otherwise creep optimized turbine blade.

2. Age hardening through nitride precipitation.

Approach 1 involved studies of the amount of deformation and allowable temperature of warm work required to provide the required improvement in yield strength and a determination of the kinetics of recovery of the strengthening increment. Approach 2 involved a study of aging response in an alloy similar to B-88 containing a nitrogen addition to determine if nitride precipitation would improve intermediate temperature tensile properties. For the revised program the base alloy was Cb-22W-2Hf-0.06C, modified by the addition of 400 ppm nitrogen for the nitride precipitation studies.

The studies of thermal-mechanical processing of B-88 and the investigation of the effects of protective coating on mechanical properties were terminated to permit incorporation of the work on intermediate temperature strength properties into the program.

II. COMPARISON OF THE PROPERTIES OF B-88 AND Cb-1

The Cb-1 alloy (Cb-30W-1Zr-0.06C-0.04N) investigated by Chang[3] at the General Electric Company has reported strength properties superior to B-88 (Cb-28W-2Hf-0.067C) even though the compositions are quite similar. Previous studies at WANL have shown no superiority of zirconium over hafnium as a reactive metal addition in Cb alloys. Hence, the difference in mechanical properties may arise from the presence of 0.044 w/o nitrogen in the Cb-1 alloy or from differences in processing of Cb-1 and B-88. (Cb-1 was extruded, aged at 2750°F, swaged 75% at 2750°F and swaged an additional 75% at 2500°F. B-88 was swaged from extrusion to final bar stock at 2400°F.) It is therefore considered important to verify the reported high strength of Cb-1 and to determine if the strength difference is due to variations in composition or fabrication sequence.

A. MATERIAL PROCESSING

The material for the B-88/Cb-1 comparison study was consumably melted into 2.6 inch diameter ingots by the double AC vacuum arc melting technique. The electrode fabrication and melting techniques have been described in detail by Begley, Cornie, and Goodspeed[2], and by Ammon and Begley[4]. In order to duplicate the Cb-1 composition reported by Chang[3] it was necessary to make an intentional nitrogen addition. Nitrogen was added as nitrided columbium sheet strips which were of convenient dimensions for easy assembly into the laminated first melt electrode. High purity electron beam melted columbium having approximately 100 ppm total interstitial level was used as the starting material.

The first melt electrodes were melted into 2 inch diameter ingots at power settings of approximately 2200 amps and 28 volts. The melting rate was 1 Kg/min. The pressure in the furnace chamber was less than 5×10^{-5} torr at the commencement of melting and did not exceed 5×10^{-4} torr during melting. The 2 inch diameter ingots were studded and welded together and attached to a columbium adapter to form the second melt electrodes. The B-88 electrode (VAM-88R) was formed by welding sound portions of B-88 extrusions from the

previous program[2]. The final melt electrodes were melted into a 2.6 inch diameter water cooled mold at approximately 2400 amps and 28 volts at a melt rate of 1.4 Kg/min. Pressure rise in the furnace was the same as that for the first melt.

Chemical analyses were performed on top and bottom samples and are given in Table 1.

TABLE 1 - Chemical Analyses of Cb-1 and B-88 Ingots

Alloy	Nominal Composition (w/o)		Chemical Analysis (w/o)					
			W	Hf	Zr	C	O	N
VAM-88R (B-88)	Cb-28W-2Hf-0.067C	Top	27	1.84	---	.066	.0031	.0051
		Bottom	27.1	1.81	---	.077	.0047	.0045
VAM-92 (Cb-1)	Cb-30W-1Zr-0.06C-0.044N	Top	30.0	---	.83	.068	.0024	.035
		Bottom	29.8	---	.77	.064	.0027	.028

The analytical results were reasonably close to the nominal composition for all of the constituents with the exception of nitrogen in the Cb-1 ingot (VAM-92). Nitrogen losses of 15% were observed during an earlier program[1] with columbium alloys containing 22% tungsten. Therefore 20% excess nitrogen over the nominal composition was added to the VAM-92 electrode. The actual nitrogen loss of 35% probably resulted from the higher melting temperature due to the higher tungsten content of the Cb-1 alloy. Taylor's investigations[5] of the Cb-N, Cb-W-N, and Cb-Hf-N systems show that the maximum nitrogen solubility in a Cb-W-Hf matrix such as Cb-1 should be less than 100 ppm at 1315°C (2100°F). Aging studies, which will be discussed in the next section of this report, have shown a potent aging peak at 1200°C. Therefore, the amount of nitrogen (315 ppm, 0.25 atomic %) present in the Cb-1 ingot should be sufficient for the purposes of this evaluation.

During the previous columbium alloy development program[2] all final melts were 2.85 inch diameter which were then conditioned to 2.75 inch diameter and canned in a 0.125 inch thick molybdenum extrusion jacket. Although excellent extrusions were produced initially, subsequent attempts to extrude B-88 utilizing similar billet configuration and extrusion parameters resulted in extrusions which required extensive conditioning due to rupture of the molybdenum jacket. Therefore, the wall thickness of the molybdenum cladding on the billets processed during this program was doubled. Since the O.D. of the billet is limited to 3 inches by the extrusion press container dimensions, the conditioned ingot diameter was reduced to 2.5 inches to allow for the 0.25 inch thick jacket. The thicker wall jackets were apparently responsible for the consistent good quality extrusions. The billets were extruded at 1760°C (3200°F) through 4.4:1 reduction ratio dies at the Air Force Materials Laboratory Facility. The extrusion data for each of the billets are given in Table 2.

Since the objective of this portion of the program was to compare Cb-1 to B-88 under identical processing conditions, one-half of each extrusion was processed by the G.E. sequence used by Chang[3] and the other one-half was processed by the standard sequence developed at WANL for B-88. The processing sequence is shown in Figure 1. The G.E.

TABLE 2 - Extrusion Data

Extrusion Parameter	VAM-88R (B-88) (Cb-28W-2Hf-0.067C)	VAM-92 (Cb-1) (Cb-30W-1Zr-0.06C-0.04N)
Container:		
Size	3.072 in.	3.072 in.
Temperature	800°F	800°F
Die: 60° entry angle, ZrO_2 faced, preheated to 800°F		
Billet Heating (induction)	20 min.	20 min.
time at temperature	5 min.	5 min.
	3200°F	3200°F
Lubricant		
Billet	D. C. 7740	D. C. 7740
Container	MoS_2	MoS_2
Die	MoS_2	MoS_2
Load		
Maximum Stem	485 Tons	495 Tons
Die	370 Tons	380 Tons
Minimum Stem	420 Tons	495 Tons
Die	360 Tons	370 Tons
Ram Speed (ips)		
Maximum	2.25	2.5
Minimum	1.5	1.25
Reduction Ratio	4.4:1	4.4:1
Extrusion Constant		
K Total	88 ksi	90 ksi
K Die Only	63 ksi	69 ksi

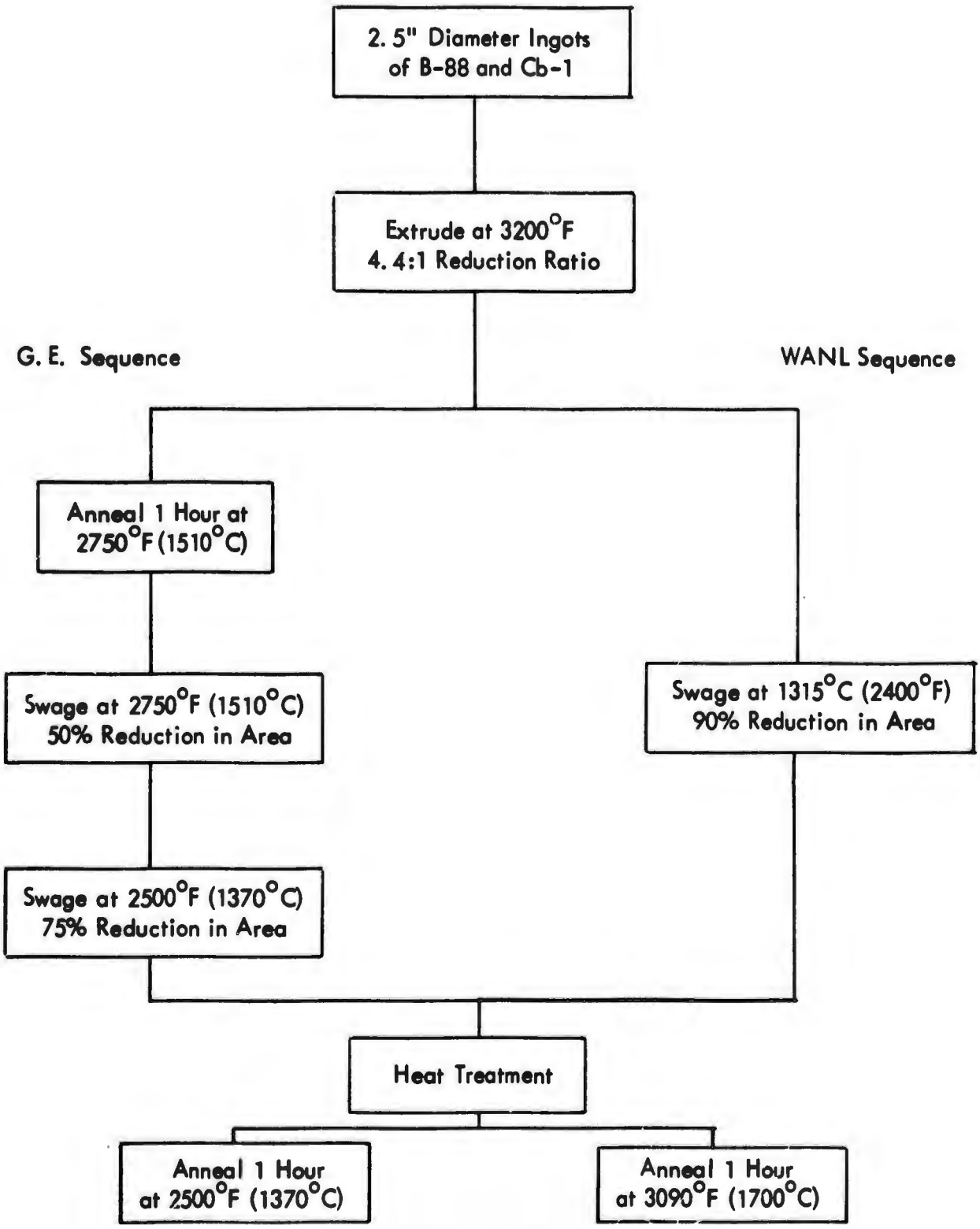

FIGURE 1 - Processing Sequence for B-88 and Cb-1 Comparison Study

processing sequence consists of annealing the extruded alloy 1 hour at 2750°F (1510°C) followed by a 50% reduction in area by swaging at 2750°F (1510°C) and an additional 75% reduction in area at 2500°F (1370°C). The WANL sequence is somewhat simpler in that the material is swaged from extrusion stock directly to specimen blank dimensions (90% reduction in area) at 2400°F (1315°C).

Sound rod was obtained from the B-88 material processed by both the G. E. and the WANL processing sequences. Approximately 15% of the Cb-1 material processed by the G. E. sequence and nearly 50% of the Cb-1 alloy processed by the WANL sequences was scrapped due to end cracking. Much of the Cb-1 processing losses could have been avoided by swaging shorter pieces and utilizing more frequent reheating during each swaging step in order to prevent the actual working temperature from dropping low enough to permit cracking. Never-the-less, sufficient material was obtained for the reference mechanical property evaluation.

B. HEAT TREATMENT AND PHASE EQUILIBRIA STUDIES

Although gross differences in the phase equilibria, microstructure, and recrystallization behavior of B-88 and Cb-1 would not be expected considering their similar compositions, subtle variations may exist due to the higher nitrogen content of Cb-1 or the different processing schedules used which could have an effect on mechanical properties. Therefore, a study was conducted to compare the response to heat treatment of the two alloys, and to determine the effect, if any, of the different processing sequences.

Recrystallization Behavior

The microstructures of Cb-1 processed by the G. E. and WANL sequences, and B-88 processed by the G. E. sequence are illustrated in Figures 2 through 7. No significant structural differences were observed in the Cb-1 alloy processed by both the WANL and G. E. processing sequences after equivalent thermal treatments, as shown in Figures 2, 3, 4, and 5.

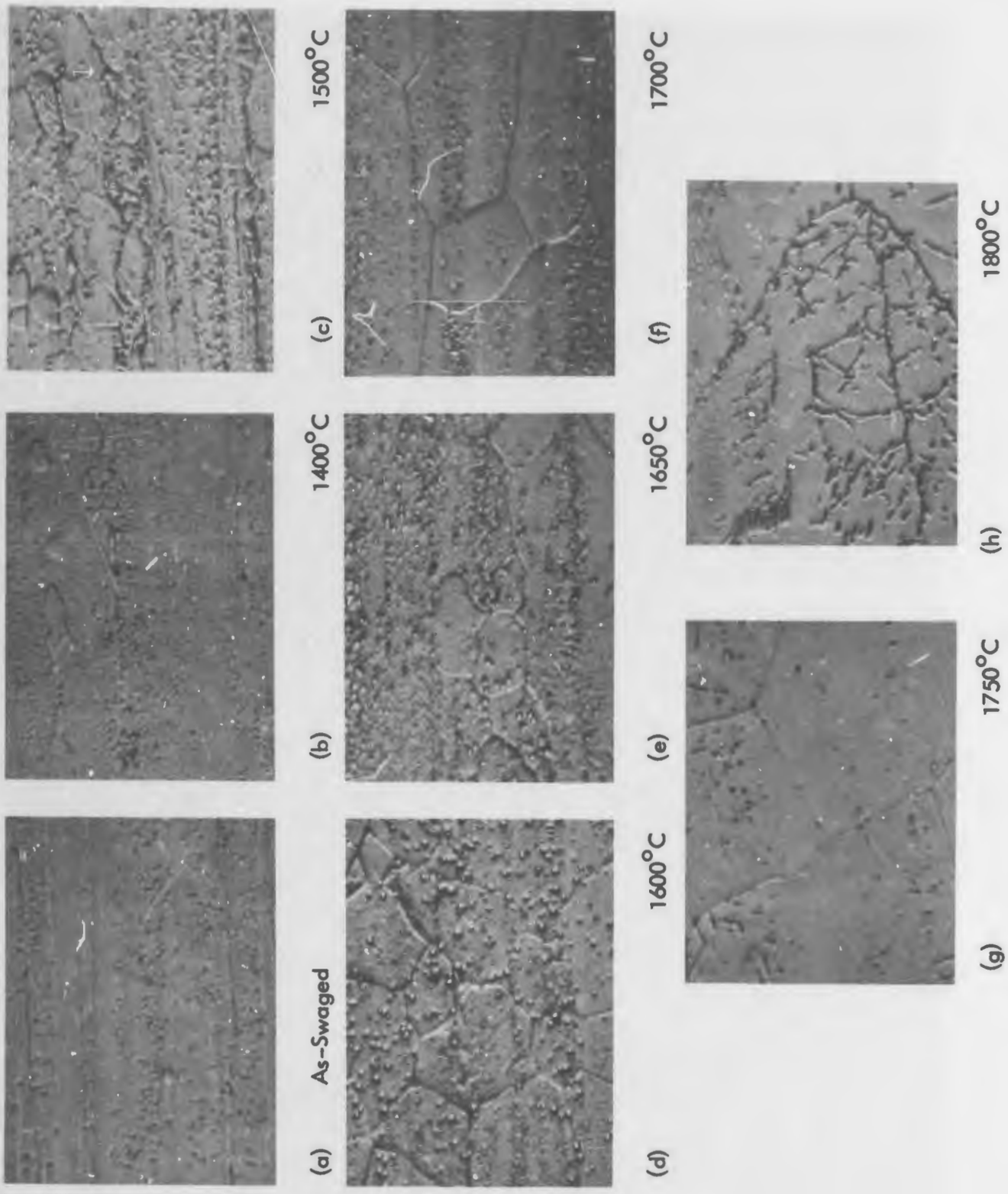

FIGURE 2 - Effect of Annealing on the Microstructure of Cb-1 Processed by G. E. Sequence. 1 Hour Anneals. 1500X

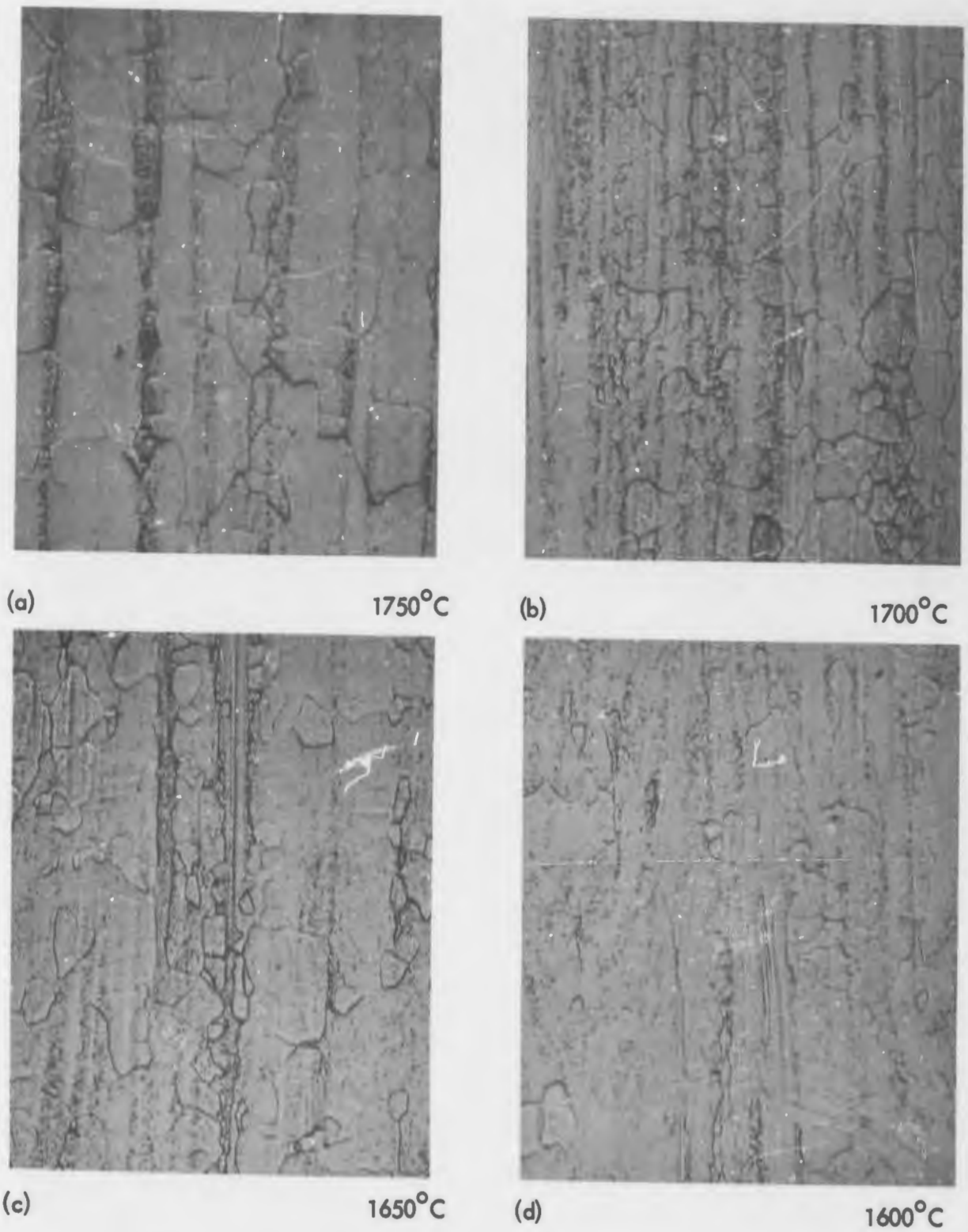

FIGURE 3 - Effect of Annealing on the Microstructure of Cb-1 Processed by G. E. Sequence. 1 Hour Anneals. 400X

NOT REPRODUCIBLE

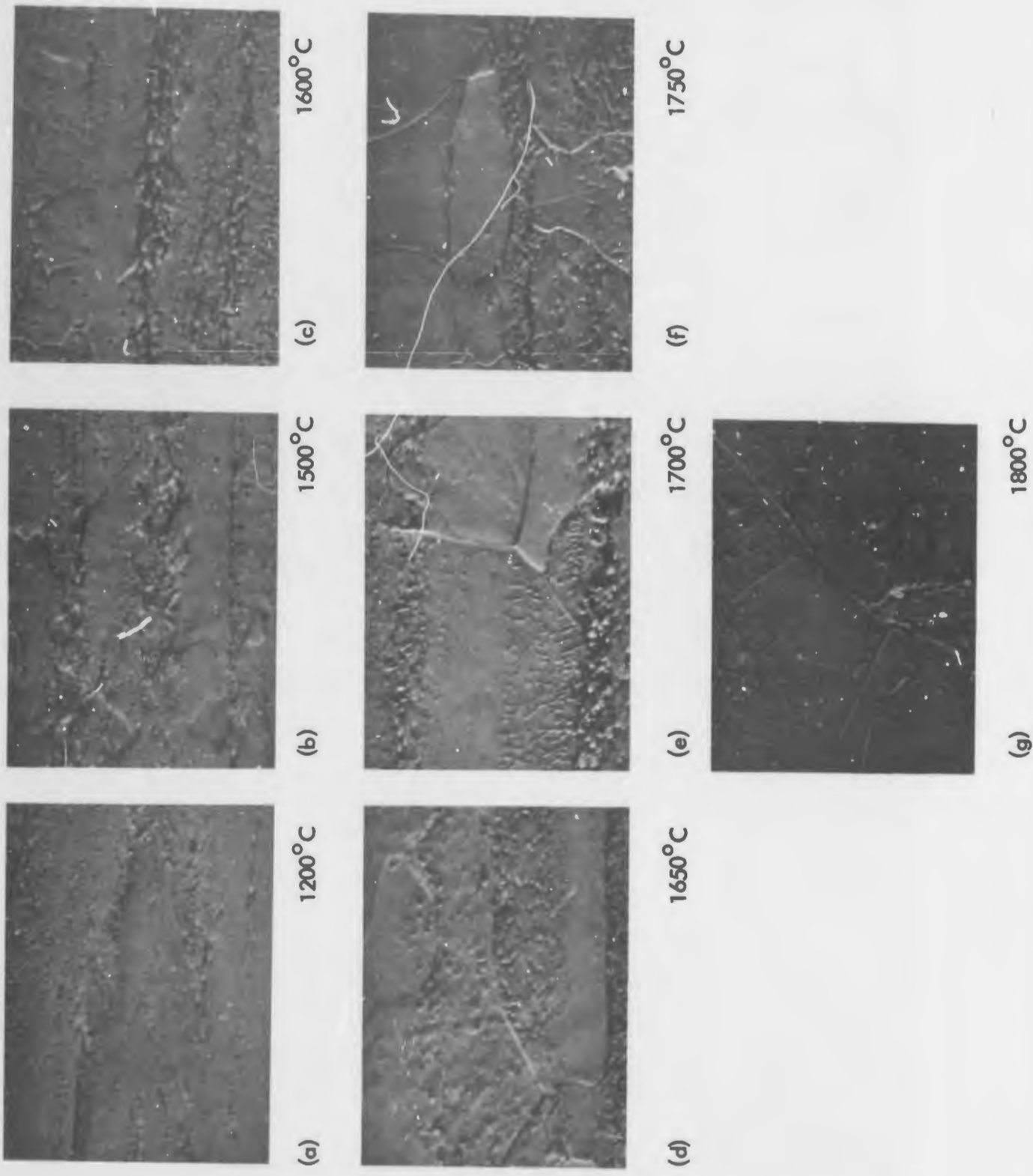

FIGURE 4 - Effect of Annealing on the Microstructure of Cb-1 Processed by WANL Sequence. 1 Hour Anneals. 1500X

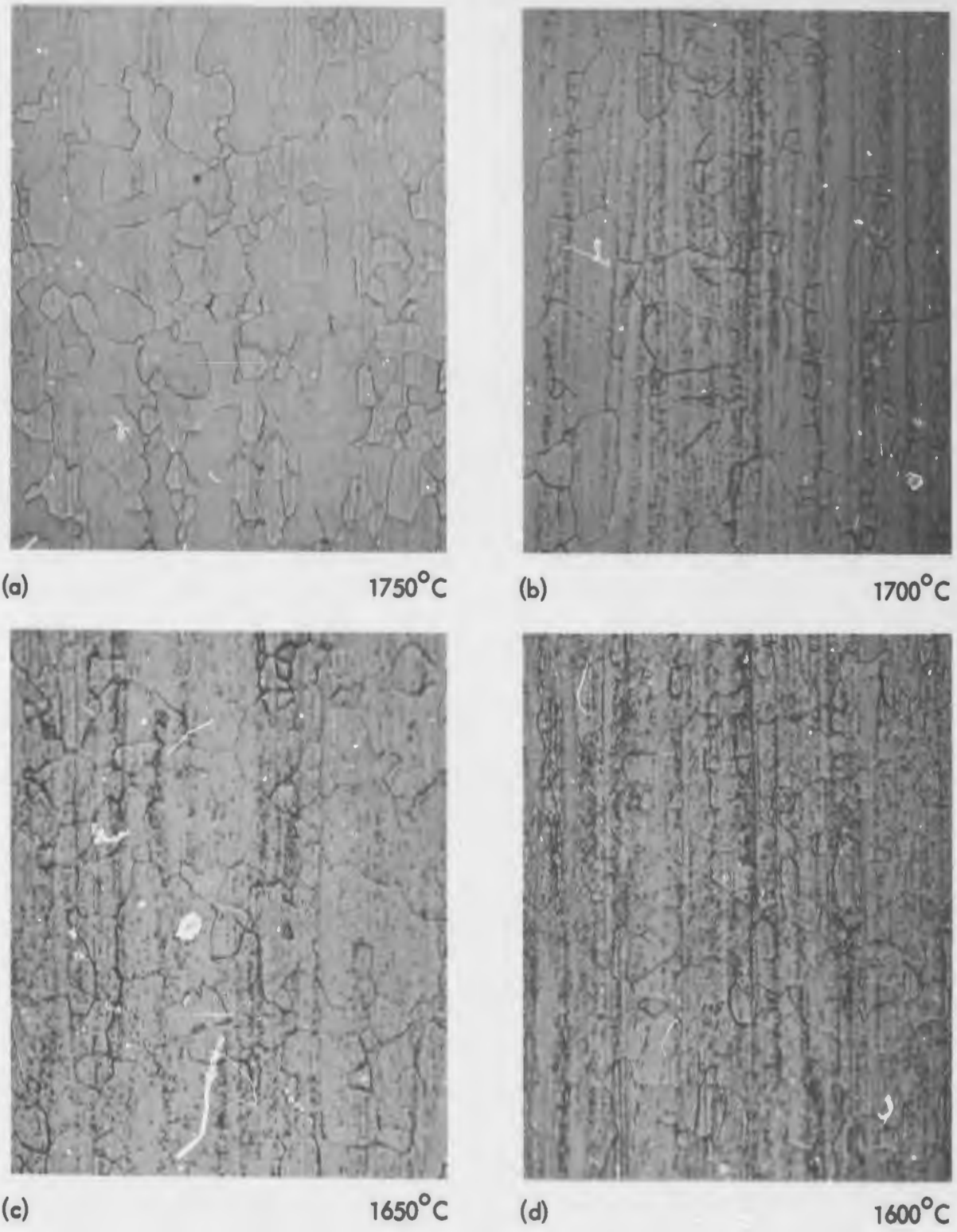

FIGURE 5 - Effect of Annealing on Microstructure of Cb-1 Processed by WANL Sequence. 1 Hour Anneals. 400X

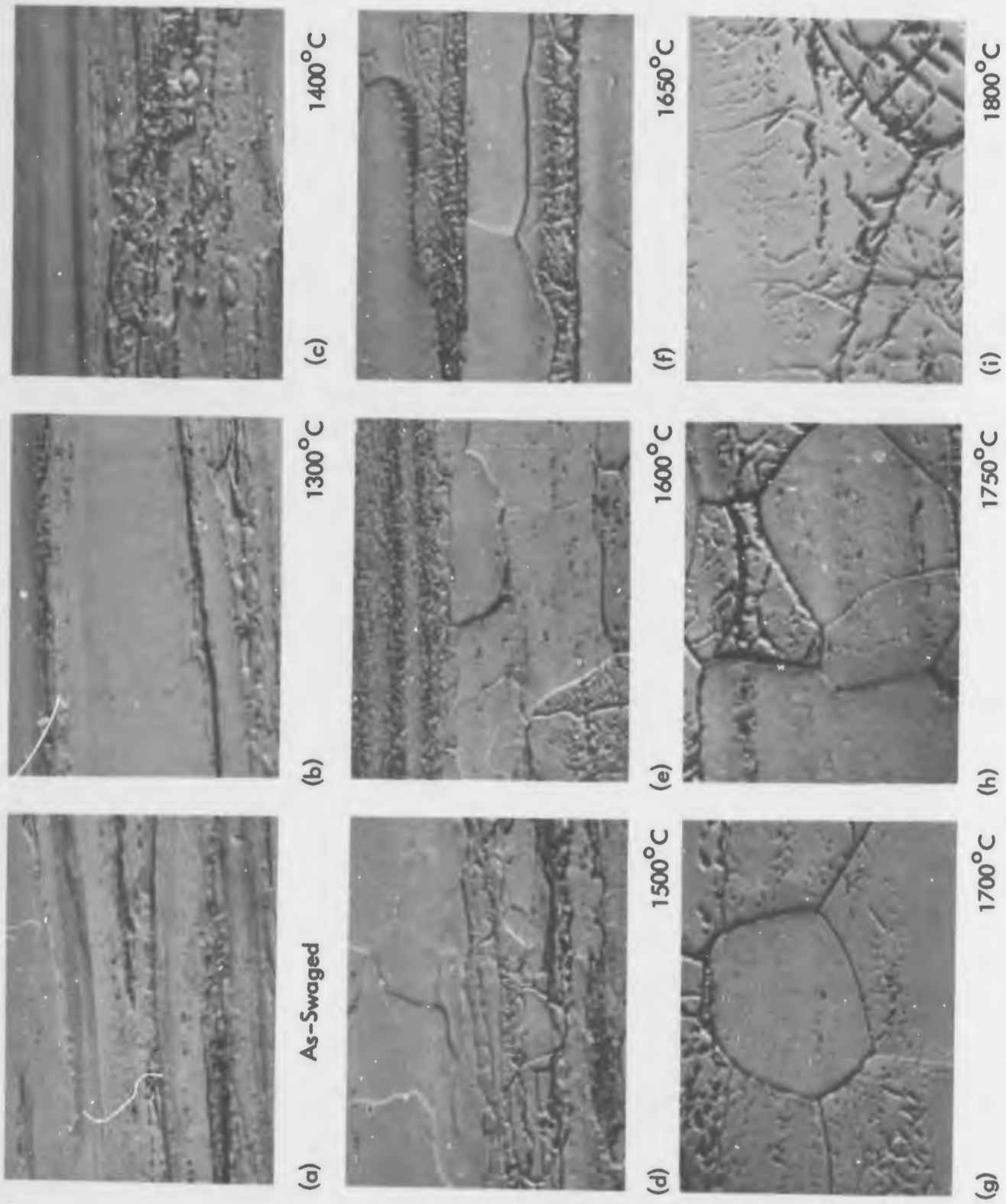

FIGURE 6 - Effect of Annealing on Microstructure of B-88 Processed by G. E. Sequence. 1 Hour Anneals. 1500X

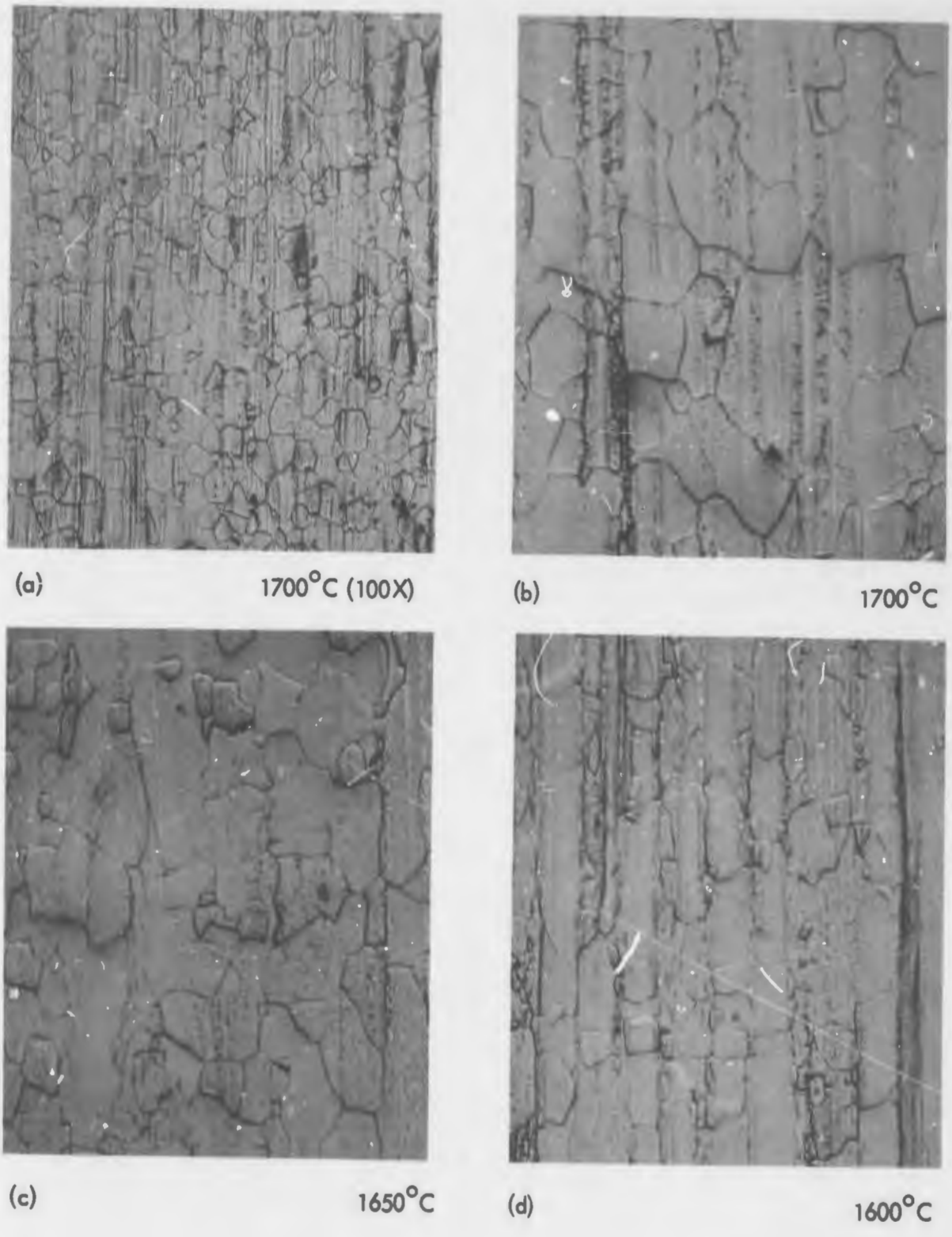

FIGURE 7 - Effect of Annealing on the Microstructure of B-88 Processed by G. E. Sequence. 1 Hour Anneals. 400X

The microstructure of B-88 processed by the G. E. sequence is shown in Figures 6 and 7. The gross microstructural features are quite similar to those observed for Cb-1 after the same final annealing treatment. The microstructure of B-88 processed by the WANL sequence (not shown) is fairly similar to that shown in Figure 7, except that the duplex structure shown in Figure 7d, consisting of elongated recrystallized grains (with an ASTM grain size of approximately 8) separated by bands of material with a precipitate stabilized substructure, is observed after final annealing at 1700°C. This structure provides the best combination of high temperature strength and low temperature ductility in B-88.

The mean grain diameter of B-88 and Cb-1, processed by both working schedules, is plotted as a function of 1 hour annealing temperature in Figure 8. This curve shows that a discontinuity occurs in the grain size versus annealing temperature plot at 1700°C for B-88 and about the same temperature for Cb-1. This temperature is the approximate carbon solvus for the B-88 alloy as determined in an earlier study,[1] indicating that the carbide precipitate is quite effective in inhibiting grain growth. The fact that grain size of Cb-1 also increases abruptly as the annealing temperature is raised above 1700°C strongly suggests that this is also the approximate carbon (or carbon plus nitrogen) solvus temperature for Cb-1. Again, B-88 and Cb-1 are quite similar in their recrystallization and grain growth characteristics.

Aging Studies

Begley et al[6,8] have shown that pronounced aging response can be achieved in columbium alloys by precipitation of hafnium and zirconium nitrides. It was anticipated that the nitrogen level of Cb-1 (315 ppm) would modify the aging behavior of Cb-1 compared to the low nitrogen (~50 ppm) B-88. A series of aging experiments were conducted on Cb-1 and B-88 to compore their response to thermal treatments. Samples were solution annealed 1 hour at 2000°C, helium quenched, and then aged 1 hour at temperatures ranging from 1000 to 2000°C. The room temperature hardness of B-88 and Cb-1 as a function of isochronal (1 hour) aging temperature is presented in Figure 9. B-88 showed little response to aging over the entire temperature range, confirming the results of previous work[2]. The Cb-1 alloy

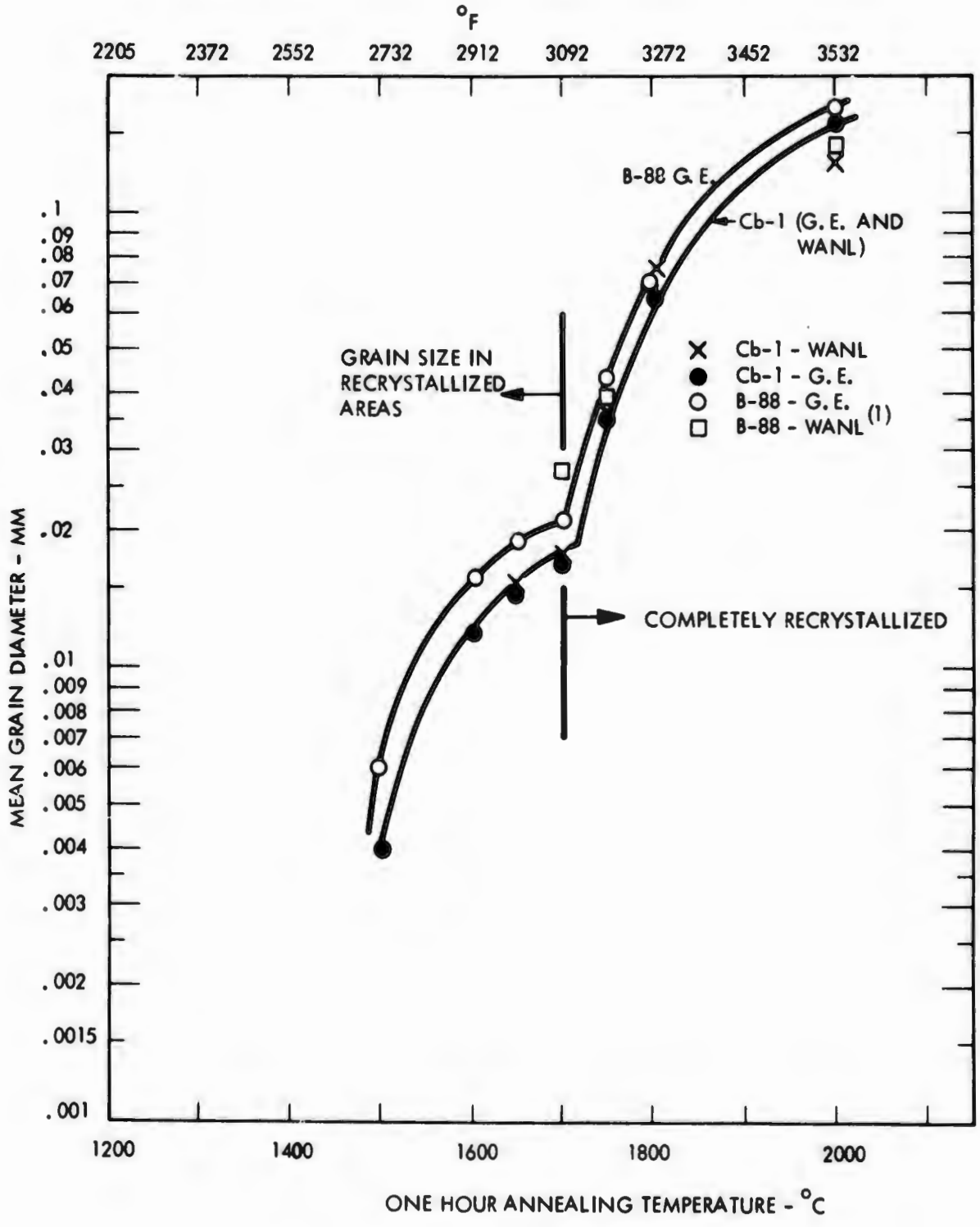

FIGURE 8 - Mean Grain Diameter of Cb-1 and B-88 as a Function of Annealing Temperature (1 Hour Anneals)

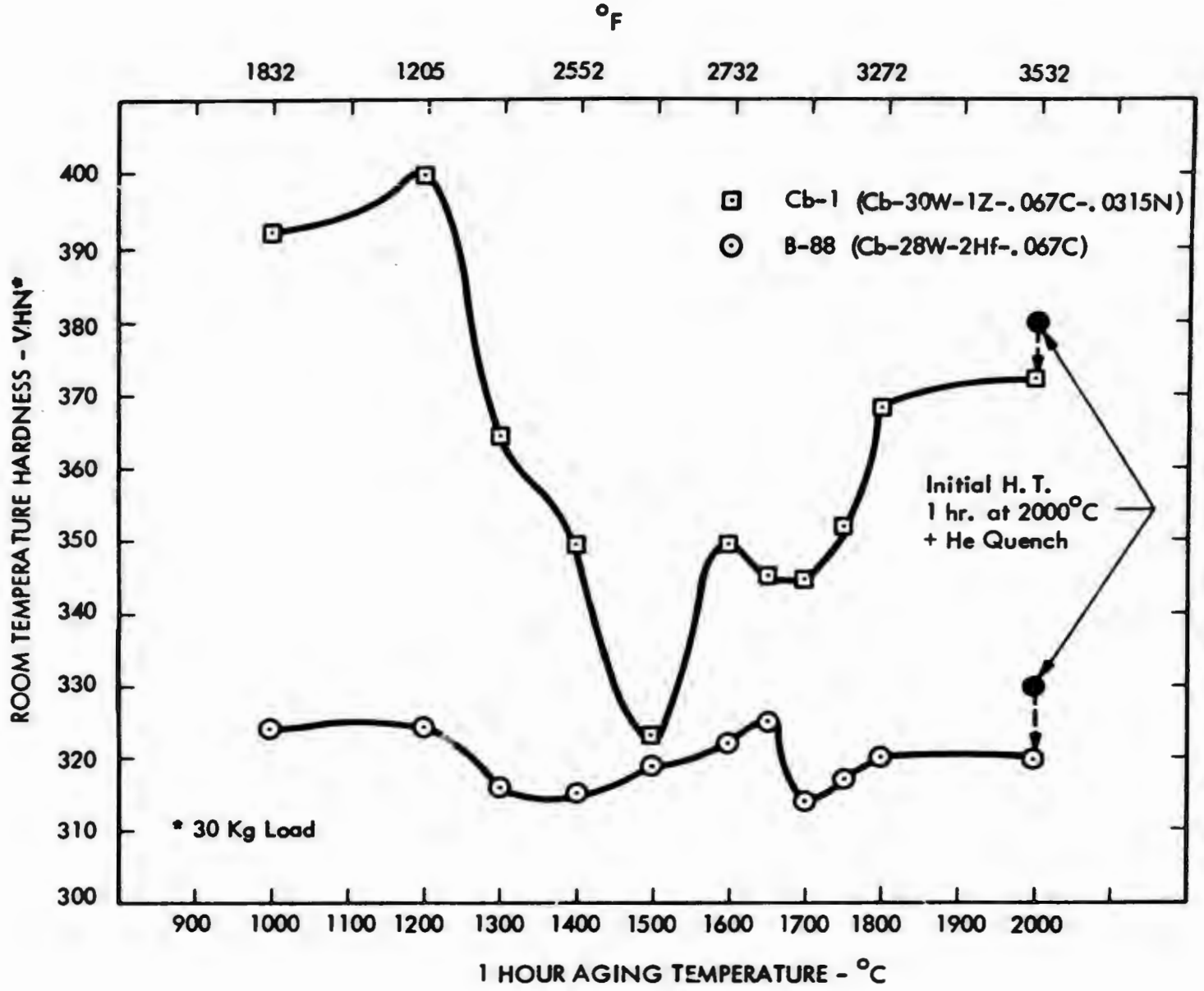

FIGURE 9 - Effect of Aging Temperature on the Hardness of Solution Annealed Cb-1 and B-88

exhibited significantly higher hardness than B-88 under virtually all conditions. The as-solution annealed hardness of Cb-1 was 380 VPN compared to 330 VPN for B-88. Aging Cb-1 at 1000 and 1200°C for 1 hour resulted in a hardness increase, followed by rapid softening as the aging temperature was increased to 1500°C. Aging at temperatures higher than 1500°C resulted in significantly higher hardness values compared to the 1500°C aging treatment which represents the fully overaged condition for this alloy.

Photomicrographs of Cb-1 and B-88 representing the solution annealed plus aged conditions are shown in Figures 10, 11, 12, and 13. The microstructures of B-88 show the typical thin platelets of the zeta carbide phase which forms on cooling after annealing above the carbon solvus. The zeta phase then transforms on aging at temperatures below 1700°C to the cubic $(Cb,Hf)C_{1-x}$ monocarbide. The microstructures of the solution annealed plus aged Cb-1 showed somewhat different microstructural features. In the as-solution annealed condition carbide platelets were observed similar to those found in B-88. A very small amount of fine general precipitation could be observed in random areas similar to that shown in Figure 10b. As the aging temperature was increased above 1200°C fine precipitates formed within the grain volumes, which were not resolveable by optical metallography as shown in Figures 12f, 13b, and 13d. After aging 1 hour at 1500°C, which corresponds to the minimum in hardness-aging temperature curve of Figure 9 , the precipitate within the grain volumes can be resolved optically. Increasing the aging temperature to 1600°C results in further precipitate growth. Electron micrographs (surface replicas) of Cb-1 in the solution-annealed and solution-annealed plus aged conditions are shown in Figure 14. In the solution annealed condition (annealed 2 hours at 2000°C and helium quenched) only the zeta carbide is precipitated in platelets within the grains and along the grain boundaries. Aging 1 hour at 1600°C (Figure 14b) shows that rectangular shaped precipitates have formed, primarily within the grain volumes. The precipitates on grain boundaries are discontinuous. The microstructure corresponding to the 1200°C aging peak is shown in Figure 14c. These photomicrographs show very fine precipitates within the matrix; as well as a few larger precipitates along grain boundaries and traces of the metastable zeta platelets.

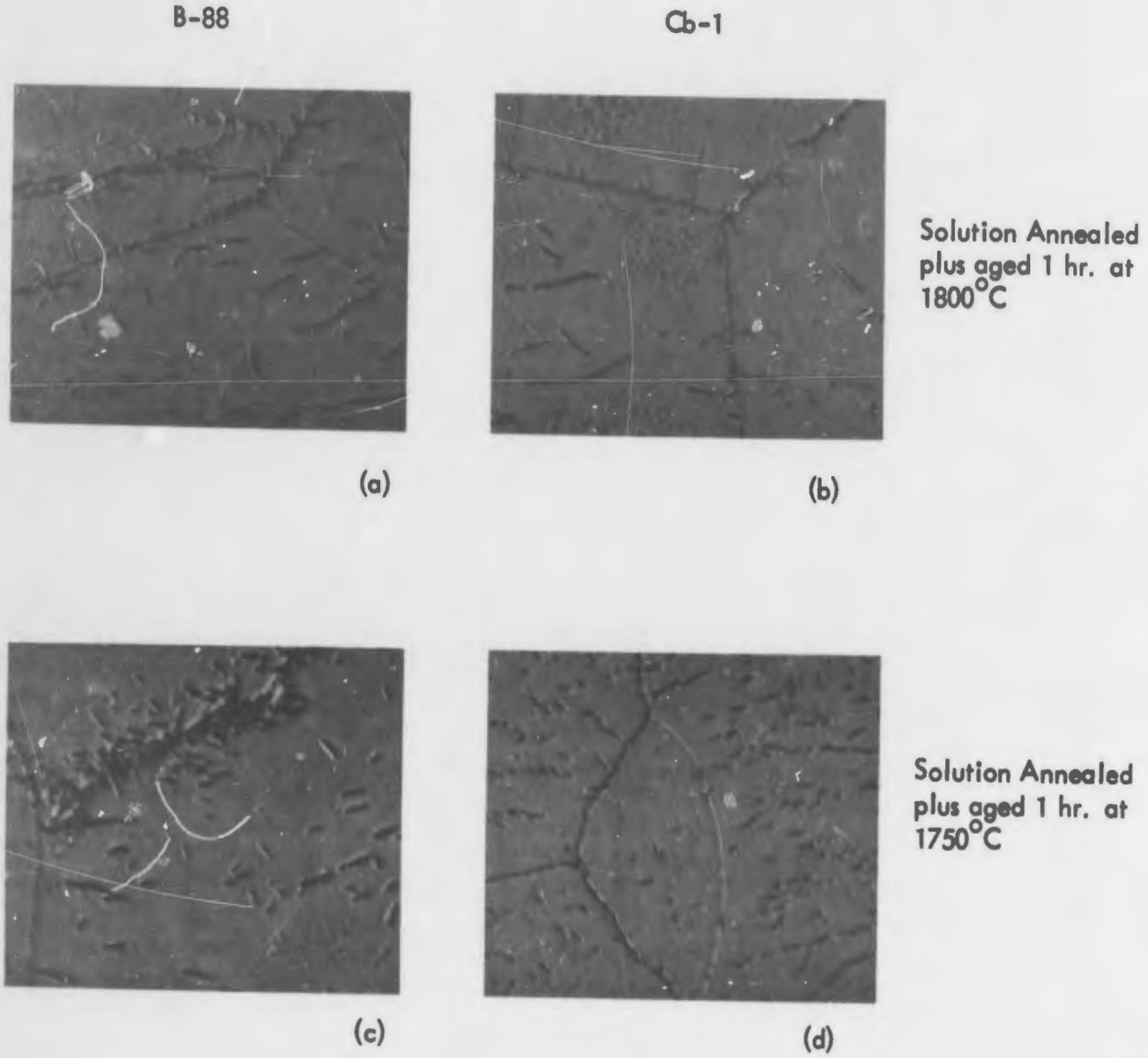

FIGURE 10 - Microstructure of B-88 (Cb-28W-2Hf-0.067C) and Cb-1 (Cb-30W-1Zr-0.06C-0.03N) Solution Annealed 1 Hr. at 2000°C and Aged 1500X

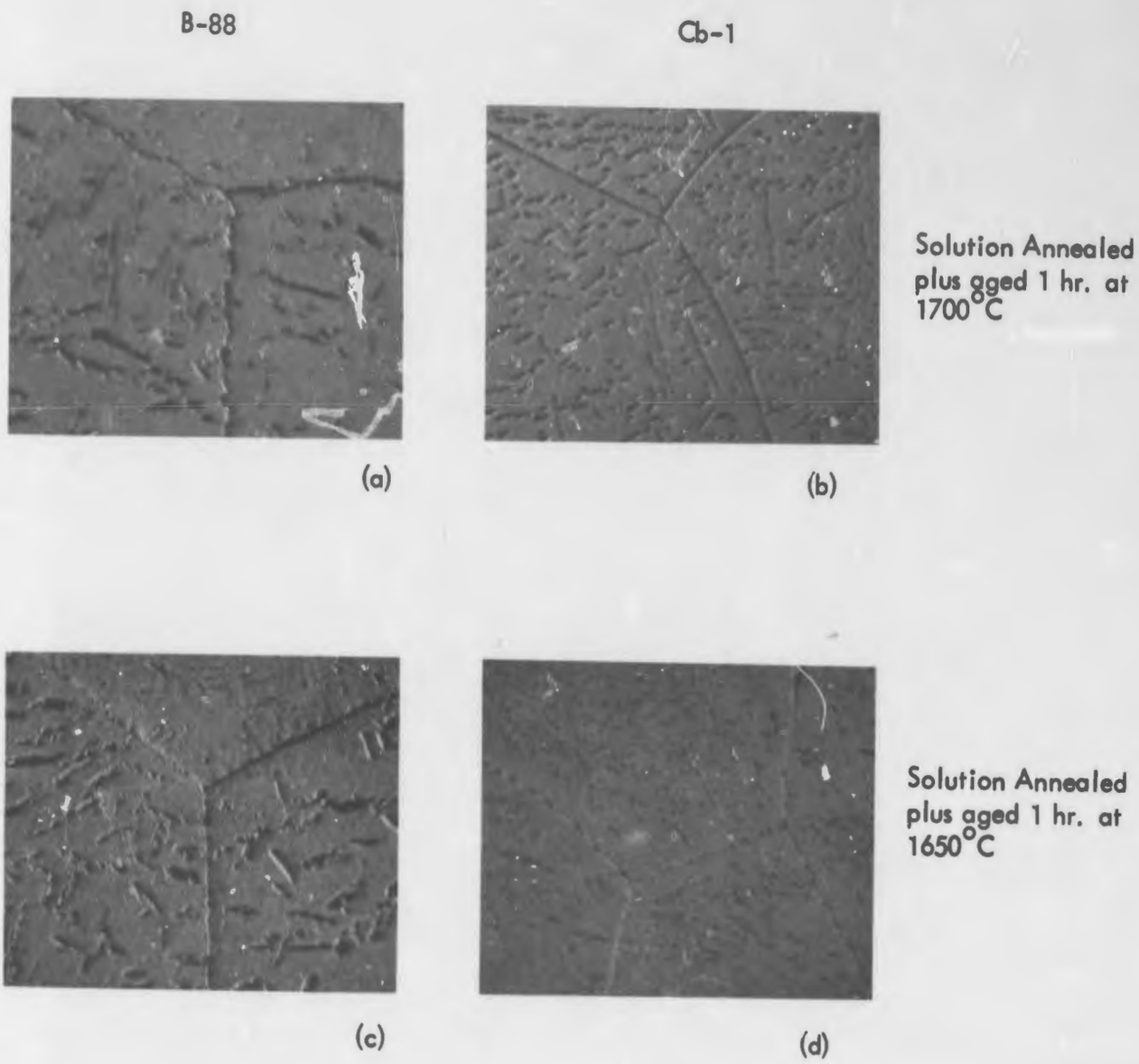

FIGURE 11 - Microstructure of B-88 (Cb-28W-2Hf-0.067C) and Cb-1 (Cb-30W-1Zr-0.06C-0.03N) Solution Annealed 1 Hr. at 2000°C and Aged 1500X

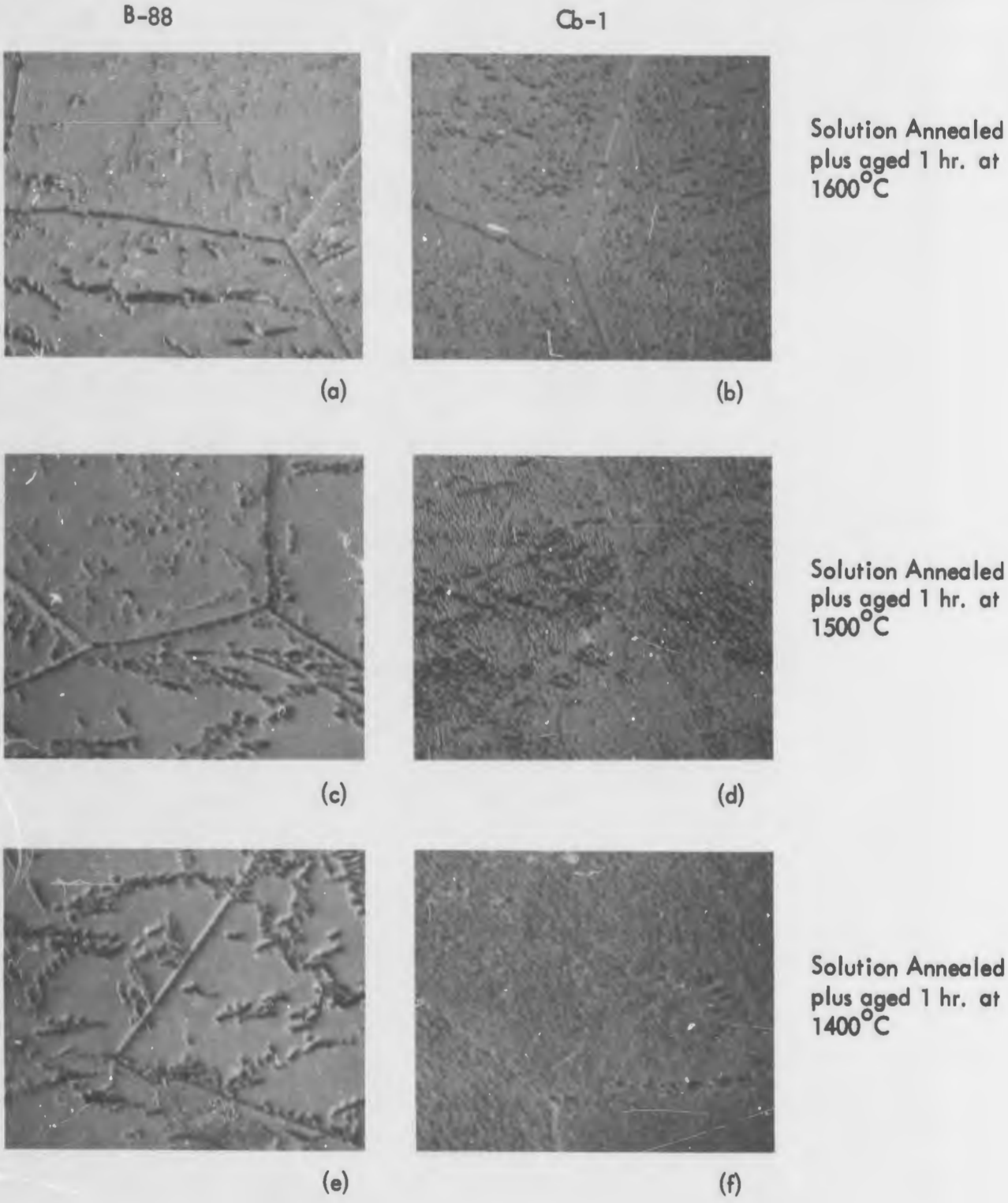

FIGURE 12 - Microstructure of B-88 (Cb-28W-2Hf-0.067C) and Cb-1 (Cb-30W-1Zr-0.06C-0.03N) Solution Annealed 1 Hr. at 2000°C and Aged 1500X

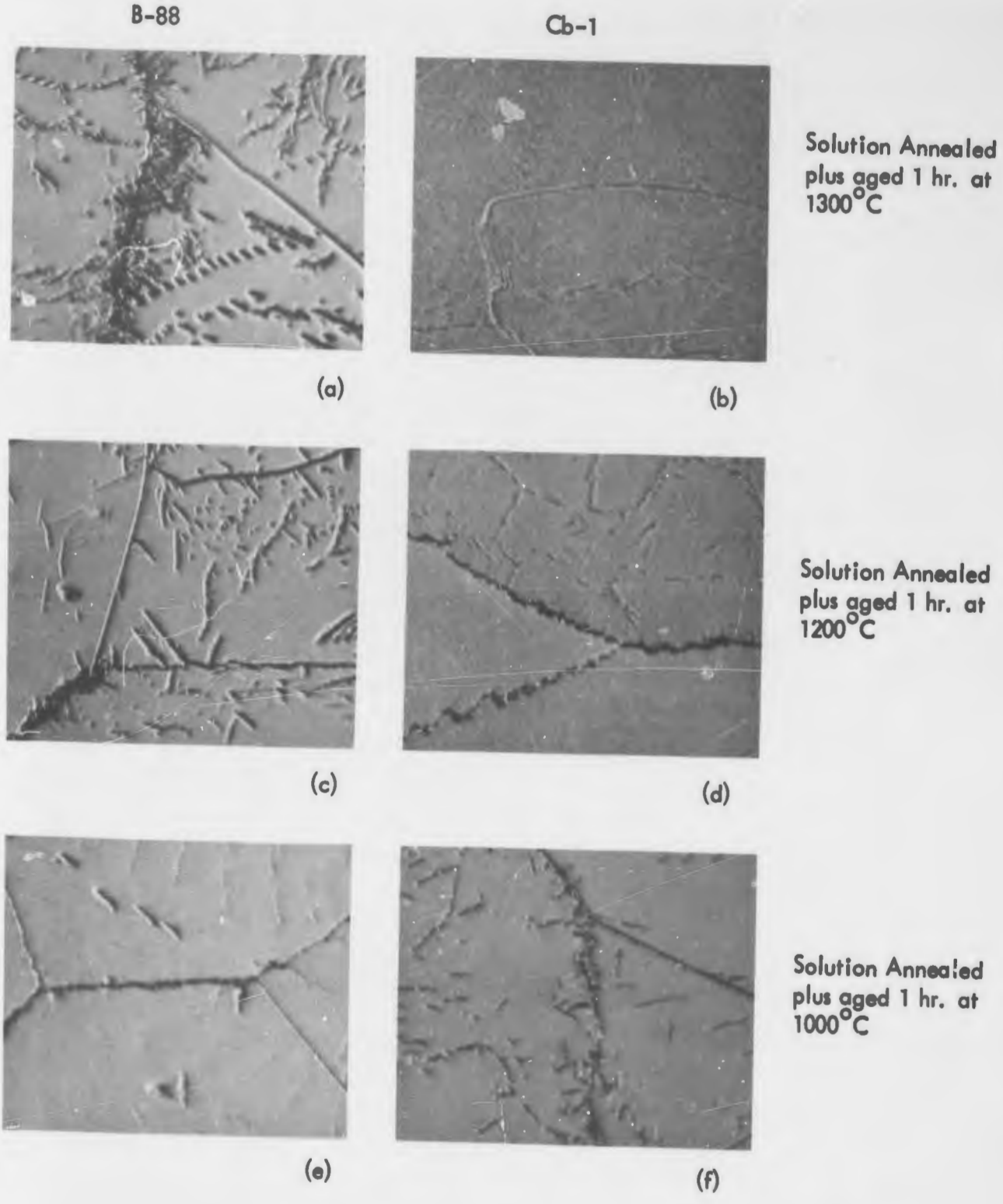

FIGURE 13 - Microstructures of B-88 (Cb-28W-2Hf-0.067C) and Cb-1 (Cb-30W-1Zr-0.06C-0.03N) Solution Annealed 1 Hr. at 2000°C and Aged 1500X

3000X 3000X 10,000X

(a) Annealed 1 Hr. at 2000°C

3000X 3000X 10,000X

(b) Annealed 1 Hr. at 2000°C plus 1 Hr. at 1600°C

FIGURE 14 - Electron Micrographs of Cb-1 Alloy

10,000X 10,000X 10,000X

(c) Annealed 1 Hr. at 2000°C plus 1 Hr. at 1200°F

FIGURE 14 (Continued) - Electron Micrographs of Cb-1 Alloy

Hardness data were obtained on Cb-1 and B-88 specimens which were annealed 1 hour at temperatures ranging from 1000 to 2000°C, following final swaging. The hardness data are shown in Figure 15. In this instance an aging peak was not observed in Cb-1 at 1200°C because overaging had occurred during the warm swaging process. However, a pronounced hardness increase was observed as the annealing temperature was increased above 1600°C arising from resolution of interstitials.

Phase Identification

Bulk extractions of the precipitates were obtained from the B-88 and Cb-1 alloys after each aging treatment by dissolving the samples in a bromine-methanol-tartaric acid solution and collecting the residue[2]. Extractions obtained from solution annealed and aged Cb-1 and B-88 were evaluated by Debye-Scherrer analysis. The extractions correspond to the microstructures shown in Figures 10 through 13. The resulting identification and lattice parameter data are given in Table 3. The phase relationships in Cb-1 alloys are similar to B-88. The zeta phase discussed during the previous study[2] was again observed in the Cb-1 alloy after cooling from above the interstitial solvus. The zeta phase was determined to be a metastable carbide type phase that transforms upon aging below the solvus to the NaCl type cubic phase (γ).

TABLE 3 - Identification and Lattice Parameter of Extracted Phases

Heat Treatment*	B-88	Cb-1
As Solutioned at 2000°C	Zeta (S)	Zeta (S)
Aged 1 hr. at 1800°C	Zeta (S)	Zeta (M)
Aged 1 hr. at 1750°C	Zeta(M)+γ,a_o=4.52	Zeta(M)+γ,a_o=4.598
Aged 1 hr. at 1700°C	Zeta(W)+γ,a_o=4.52	Zeta(W)+γ,a_o=4.604
Aged 1 hr. at 1650°C	γ^t, a_o=4.536	γ^t, a_o=4.609
Aged 1 hr. at 1600°C	γ^t, a_o=4.54	γ, a_o=4.614
Aged 1 hr. at 1500°C	γ^t, a_o=4.56	γ, a_o=4.614
Aged 1 hr. at 1400°C	γ^t, a_o=4.57	γ, a_o=4.609
Aged 1 hr. at 1300°C	γ^t, a_o=4.59	Zeta (VVW)
Aged 1 hr. at 1200°C	Zeta (S)	(Extraction not obtainable)
Aged 1 hr. at 1000°C	Zeta (S)	Zeta (S)

*All alloys solutioned 1 hr. at 2000°C before subsequent aging.
†Equilibrium values from previous study.[2]

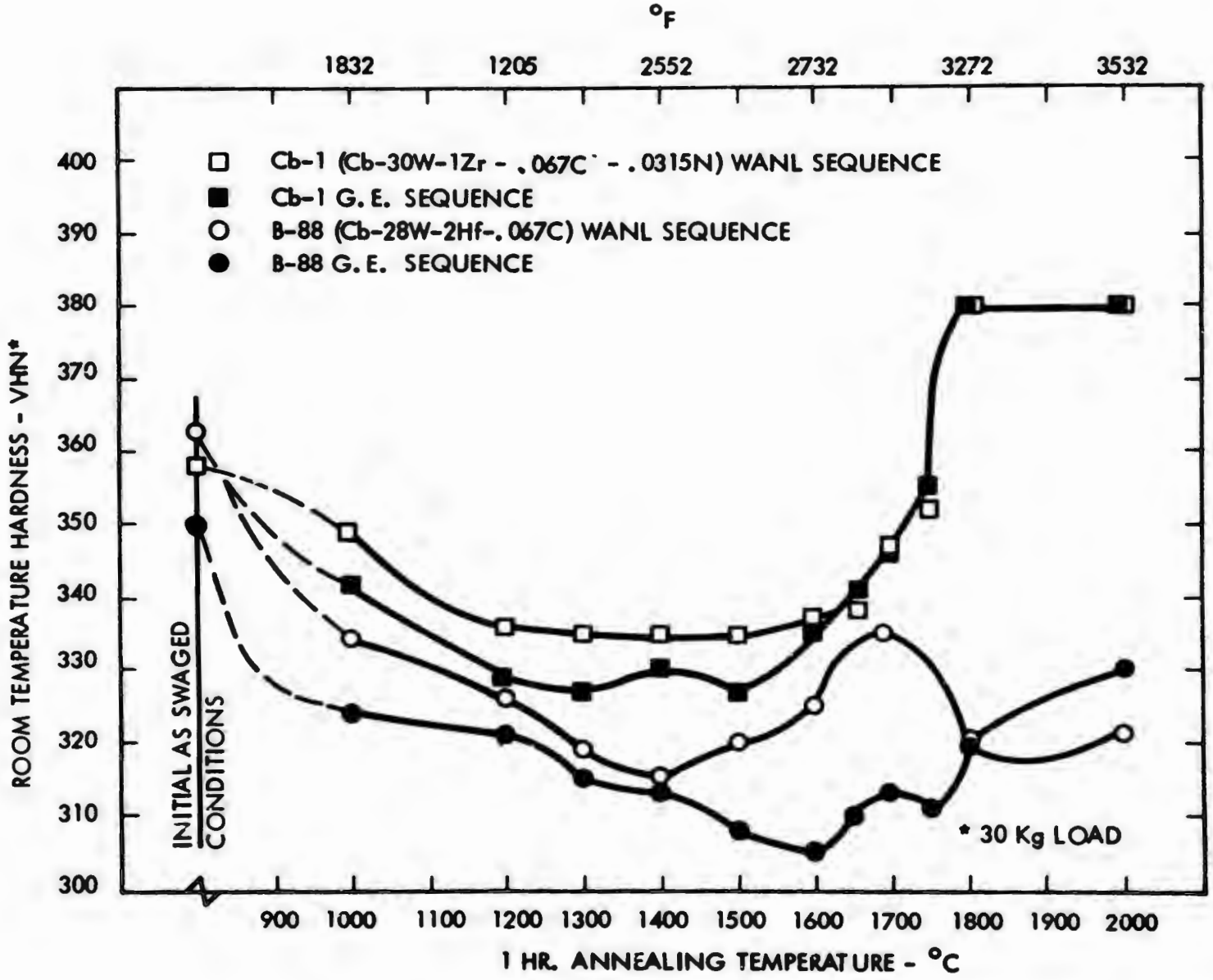

FIGURE 15 - Variation of Room Temperature Hardness of B-88 and Cb-1 with Processing and Heat Treatment

In Cb-1 the cubic phase has a slightly larger lattice parameter than the corresponding phase in B-88. The transformation of zeta to γ was very sluggish at lower temperatures as observed by Ostermann[7] and as shown by the weak patterns from the 1200°C and 1300°C aging treatments An extraction residue could not be obtained from the 1200°C aged Cb-1 specimens. The precipitates were either too fine to be retained during the extraction process[1] or a coherent phase precipitated during the aging treatment. The question of coherent precipitation during the aging process is not resolved at present. Aged specimens must be studied by transmission electron microscopy in order to answer this question.

Discussion of Thermal Treatment Results

The aging response of Cb-1 differs from that of B-88 in that a rather pronounced hardness peak is observed after aging solution annealed Cb-1 at temperatures of approximately 1100-1200°C. Aging at higher temperatures results in rapid softening, until a minimum in the hardness-aging temperature curve is achieved after a 1 hour anneal at 1500°C. Thereupon, increasing aging temperatures result in a generally progressive hardness increase. In contrast, B-88 shows little response to thermal treatment over the temperature range from 1000 to 2000°C.

Examination of the electron micrographs of Figure 14 shows that the observed hardness changes with thermal treatment in Cb-1 are reflected by the microstructural features. Aging solution annealed Cb-1 for 1 hour at 1200°C results in the formation of a very fine precipitate in the matrix, and subsequent growth of this matrix precipitate as the aging temperature is increased. Annealing at 2000°C results in the dissolution of this phase, with only the zeta carbide phase being observed in the microstructure of the solution annealed material. The aging response observed in Cb-1 is attributed to the precipitation of a nitride or a carbonitride phase. The aging response in Cb-1 is very similar to that observed in Cb-Zr-N, Cb-Hf-N, and Cb-W-Hf-N alloys.[6,8,9] In contrast, investigation of identical alloys where carbon is substituted for nitrogen does not provide the aging behavior observed in the nitrogen containing alloys. It thus seems apparent that nitrogen is necessary to provide the aging response observed in Cb-1. The lattice parameter data obtained on residues extracted from solution annealed and aged Cb-1 (Table 3) show that the cubic phase observed is most probably

ZrN or Zr(C,N). However, because of the very similar lattice parameters of ZrC and ZrN, and the substitution of Cb for Zr in the precipitate, unambiguous identification of the cubic phase is not possible by x-ray analysis alone.

Chang[3] also found aging response in Cb-1 similar to that described in this report, except that the hardness levels observed by Chang were considerably higher than those of this study. This may be attributed to the higher nitrogen level of Chang's material.

C. MECHANICAL PROPERTIES OF B-88 AND Cb-1

The mechanical properties of Cb-1 and B-88 were evaluated by means of creep-rupture tests at 1315°C (2400°F), and low temperature tensile tests. Marked differences in the high temperature properties of the two alloys would not be expected considering their similar compositions and generally equivalent processing sequences. However, Chang reported stress-relieved Cb-1 to be 14% stronger and recrystallized Cb-1 to be approximately 30% stronger (based upon stress to 100 hour rupture) than B-88 in its reference (optimum) condition. Consequently, each alloy was evaluated in the following conditions (See Figure 1).

1. G. E. processing sequence, recrystallized (1 hr. at 1700°C)
2. WANL processing sequence, recrystallized (1 hr. at 1700°C)
3. G. E. processing sequence, stress relieved (1 hr. at 1370°C)
4. WANL processing sequence, stress relieved (1 hr. at 1370°C)

Creep-Rupture Properties

Creep-rupture tests were conducted in Satec Model VC-100 stress-rupture units. These are 5-1 lever loaded machines with tantalum sheet heating elements capable of operation at temperatures up to 1650°C and pressures as low as 5×10^{-7} torr. The vacuum system is the oil diffusion pump type with a liquid nitrogen cold trap. Leak rates are less than 1.7×10^{-5} cc-atm/sec (<1 micron/hr.). The furnace is powered by a saturable core reactor and controlled with a Barber-Coleman MMC control unit to ± 2 C°, with temperature being measured

by Pt-Pt/Rh thermocouples. The temperature gradient over the 1-1/2 inch gage length is within $\pm 2^{\circ}C$. Strain is measured with a Satec extensometer in conjunction with a Wiedeman measuring system which resolves deflections as low as 0.040 over a 10 inch recorder range. The stress-rupture specimens are of the double shoulder type, having a 0.180 inch gage diameter and a 1.5 inch gage length.

The two alloys in the conditions listed above were creep-rupture tested at $2400^{\circ}F$ at stress levels of 30,000 psi and 27,500 psi. The resultant data are summarized in Table 4 and the rupture data are plotted in Figure 16. The following observations and conclusions can be drawn from the data.

1. The GE and WANL processing sequences evaluated have little effect on the creep rupture properties of recrystallized B-88 or Cb-1 (1 hr. at $1700^{\circ}C$).

2. Recrystallized (annealed 1 hr. at $1700^{\circ}C$) Cb-1 is slightly stronger than B-88 in the equivalent condition. However, the strength differential is very slight.

3. Both B-88 and Cb-1 are more creep resistant at $2400^{\circ}F$ in the stress-relieved condition when processed by the lower temperature WANL sequence. Cb-1 is somewhat stronger than B-88 when processed by the WANL sequence and tested in the stress-relieved condition.

4. The creep-rupture results from Cb-1 and B-88 in the stress-relieved condition show greater data scatter (as shown in Table 4)than the same alloys in the recrystallized conditions. This is probably due to non-homogeneous deformation during processing. These inhomogeneities become less important in recrystallized materials.

TABLE 4 - Creep Rupture Data

Specimen No.	Thermal-Mechanical History	Stress (psi)	Temperature (°C)	Temperature (°F)	Rupture Time (hrs.)	Minimum Creep Rate (%/hr.)	Transition Time (hrs.)	Deformation R. A. (%)	Deformation Elong.
88R*-GE-1	GE*+SR**	30,000	1315	2400	2.8	1.59	1.2	82.9	24.7
88R-GE-2	GE*+SR	27,500	1315	2400	3.1	1.30	1.26	75.8	22.0
88R-W-1	WANL***+SR	30,000	1315	2400	3.7	1.253	1.8	75.6	21.3
88R-W-3	WANL+SR	27,500	1315	2400	10.6	0.465	5.3	75.3	22.7
88R-GE-3	GE+R_X****	30,000	1315	2400	14.5	0.228	5.6	32.9	13.0
88R-GE-4	GE+R_X	27,500	1315	2400	32.6	0.058	7.0	32.7	13.3
88R-W-4	WANL+R_X	30,000	1315	2400	16.3	0.128	5.7	23.6	8.7
88R-W-6	WANL+R_X	27,500	1315	2400	27.2	0.078	11.3	25.7	7.3
92-GE-4	GE+SR	30,000	1315	2400	2.8	1.72	0.86	79.2	28.0
92-GE-5	GE+SR	27,500	1315	2400	6.3	0.886	2.25	75.3	34.0
92-W-1	WANL+SR	30,000	1315	2400	9.4	0.496	4.0	70.0	22.7
92-W-2	WANL+SR	27,500	1315	2400	14.9	0.290	5.8	68.8	26.0
92-GE-6	GE+R_X	30,000	1315	2400	18.2	0.170	7.8	42.3	19.3
92-GE-8	GE+R_X	27,000	1315	2400	35.6	0.060	11.7	39.0	17.3
92-W-3	WANL+R_X	30,000	1315	2400	31.7	0.062	11.0	37.2	20.0
92-W-6	WANL+R_X	27,000	1315	2400	41.0	0.0075	10.0	33.3	14.7

* GE processing sequence: Extruded + SR 1 hr/1510°C (2750°F)+ Swage 50% RA at 1510°C + Swage and additional 75% RA at 1370°C/2500°F

** SR = Stress Relieve Heat Treatment: 1 hr. at 1370°C/2500°F

*** WANL Processing Sequence: Extruded + Swaged at 1315°C/2400°F, 90% Red.

**** R_X = Recrystallization H. T. : 1 hr. at 1700°C/3092°F (also is Ref. H. T. for B-88)

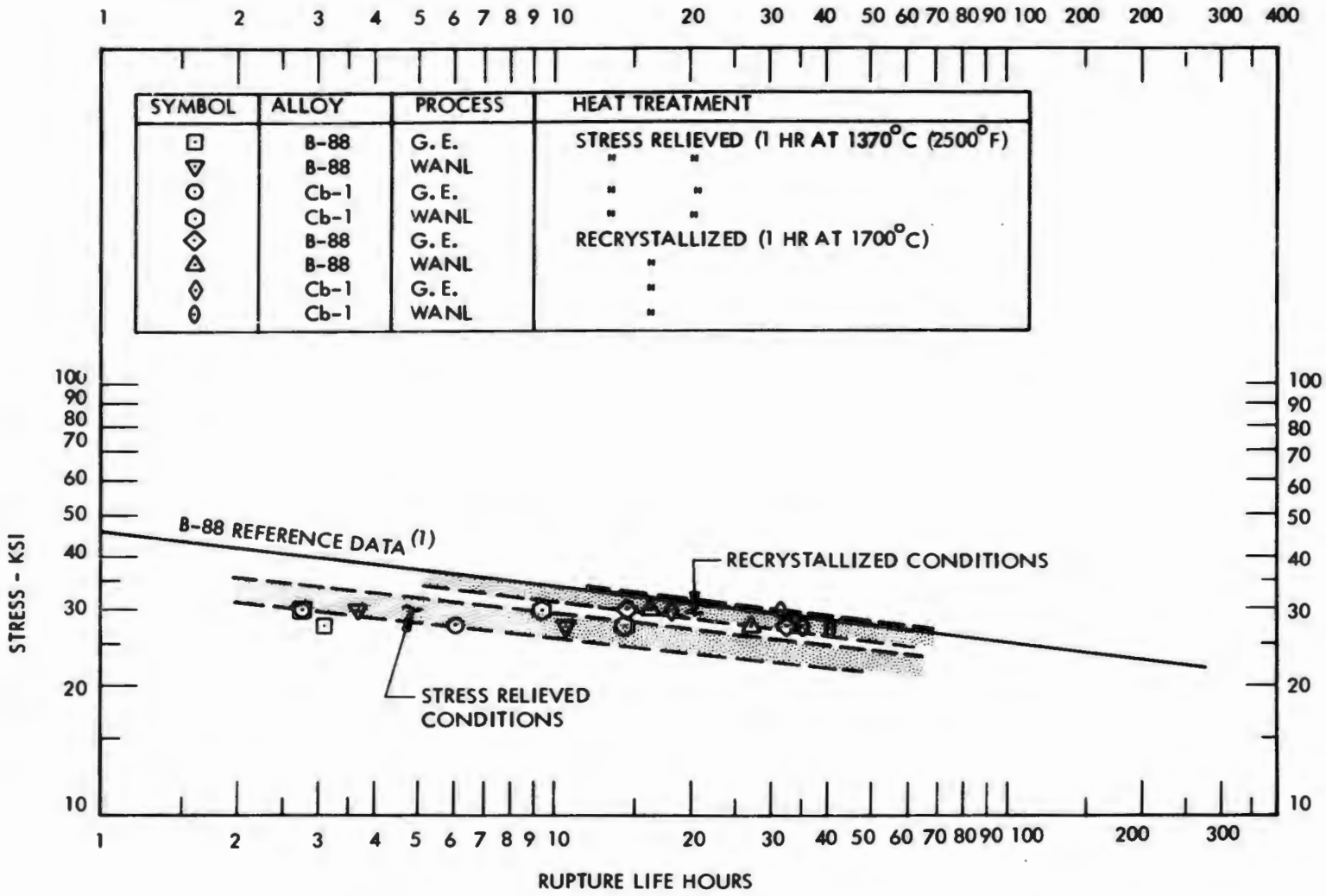

FIGURE 16 - Creep Rupture Properties of Cb-1 and B-88 at 1315°C (2400°F)

The initial Cb-1 creep-rupture data[3] are significantly higher than those determined in this investigation. Ascribing the difference to processing variations would seem to be definitely ruled out in view of the carefully controlled processing schedules followed in this study. A comparison of the chemical analyses of the two heats of Cb-1 is shown.

Cb-1 (Reference 4)

Cb-29.7W-0.83Zr-0.058C-0.044N-0.01O_2

Cb-1 (This Investigation)

Cb-29.9W-0.80Zr-0.066C-0.0315N-0.003O_2

B-88 (This Investigation)

Cb-27.1W-1.83Nf-0.071C-0.0048N-0.0039O_2

These data show the two heats of Cb-1 have virtually identical analyses except for somewhat higher nitrogen (130 ppm) and oxygen (70 ppm) in Chang's material. As shown previously, the presence of as little as 315 ppm nitrogen results in potent aging reactions in Cb-1. However, in view of the rapid overaging at temperatures above 1200°C, it does not appear likely that the difference in nitrogen content would have any significant effect on the 1315°C (2400°F) creep properties.* The minor difference in oxygen level would also have no influence on creep properties.

The difference in properties between the reported strength values for the two heats cannot be readily rationalized in terms of differences in either structure of chemistry. The variation in strength may result from differing test techniques. However, it may be more appropriate to consider the initial data to reflect the maximum properties possible with this class of alloy, and that the data presented in this report represents the range of heat to heat variation to be expected. The data taken together may constitute the range of obtainable properties, and the lower limit of this range may be utilized as a reasonably conservative design maximum.

---

*It is probable, however, that the nitrogen level would significantly affect lower temperature creep-rupture properties.

Low Temperature Tensile Properties

Low temperature tensile tests were conducted on Cb-1 and B-88 in the same thermal-mechanical conditions used for the creep-rupture study. The tensile tests were conducted in air at temperatures ranging from 600°F to 110°F (315°C to 79°C) to define the ductile-brittle transition temperature range. All tests were conducted on an Instron tensile machine at a strain rate of 0.05 min^{-1}. The specimens used were of the single shoulder loaded type with a gage length of 1 inch and a gage diameter of 0.18 inch.

The tensile data summarized in Table 5 are plotted in Figures 17 and 18. The results of the low temperature tests may be summarized as follows:

1. Cb-1 is stronger than B-88 at low temperatures (condition for condition).
2. The DBTT for B-88 is 80 to 100°F lower than that of Cb-1.
3. The DBTT for B-88 and Cb-1 in the stress relieved condition is 50 to 100°F lower than for the same two alloys in the recrystallized (1 hr. at 1700°C) condition.
4. The prior fabrication sequence does not have an obvious effect on the DBTT of B-88 and Cb-1.
5. Both alloys were slightly stronger when processed by the WANL sequence. This slight strength advantage was observed in both the stress relieved and recrystallized conditions.

The mechanical property comparison showed Cb-1 to be very slightly stronger than B-88 in terms of both 1315°C (2400°F) creep-rupture strength and low temperature tensile properties. The slight strength advantage of Cb-1 is gained at some sacrifice in ductile-brittle transition temperature and fabricability. These differences appear to reflect the slightly higher solute level of Cb-1.

TABLE 5 - Low Temperature Tensile Data for Cb-1 and B-88

Alloy and Condition Code	Test Temperature (°C)	Test Temperature (°F)	0.2% Y.S. (ksi)	U.T.S. (ksi)	Elongation (%) Uniform	Elongation (%) Total	Reduction in Area (%)
Cb-1-W-R_X*	27	80	--	136.6	0	0	0
	149	300	119.6	129.3	15.0	20.4	28.6
Cb-1-W-SR	-29	-20	143.3	147.4	1.5	1.9	2.5
	27	80	131.8	139.0	3.3	3.5	**
	149	300	112.4	130.9	14.6	25.8	58.9
B-88-W-R_X***	-79	-110	146.6	151.0	--	1.0	1.0
	27	80	119.3	137.3	--	11.3	8.8
	93	200	102.0	107.0	--	16.7	24.2
	316	600	80.0	98.0	--	19.3	58.2
B-88-W-SR	-29	-20	134.7	136.0	0.7	0.8	1.1
	27	80	123.0	133.1	6.2	6.1	**
	149	300	103.0	121.2	12.7	25.6	68.6
Cb-1-GE-R_X	27	80	--	86.3	0	0	0
	93	200	123.0	131.5	14.8	18.6	21.6
	149	300	112.2	120.9	14.9	21.8	38.8
Cb-1-GE-SR	-29	-20	142.1	142.1	1.1	1.6	0.9
	27	80	125.6	131.3	4.3	4.2	**
	149	300	108.6	121.9	15.1	27.6	70.8
B-88-GE-R_X	-29	-20	--	123.2	0	0	0
	27	80	117.1	124.4	8.8	8.8	8.8
	149	300	99.2	106.4	9.6	18.0	29.0
B-88-GE-SR	-29	-20	132.6	146.4	16.2	15.9	**
	27	80	124.8	134.2	12.1	11.6	**
	149	300	100.5	110.9	15.1	28.8	73.1

* Condition Code: B-88 = alloy composition Cb-28W-2Hf-0.067C
Cb-1 = alloy composition Cb-30W-1Zr-0.067C-0.03N
W = WANL processing sequence
GE = General Electric processing sequence
SR = stress relieved (1 hr. at 1370°C)
R_X = recrystallized (1 hr. at 1700°C)

** Fillet break

*** Evaluated during previous program (Reference 1)

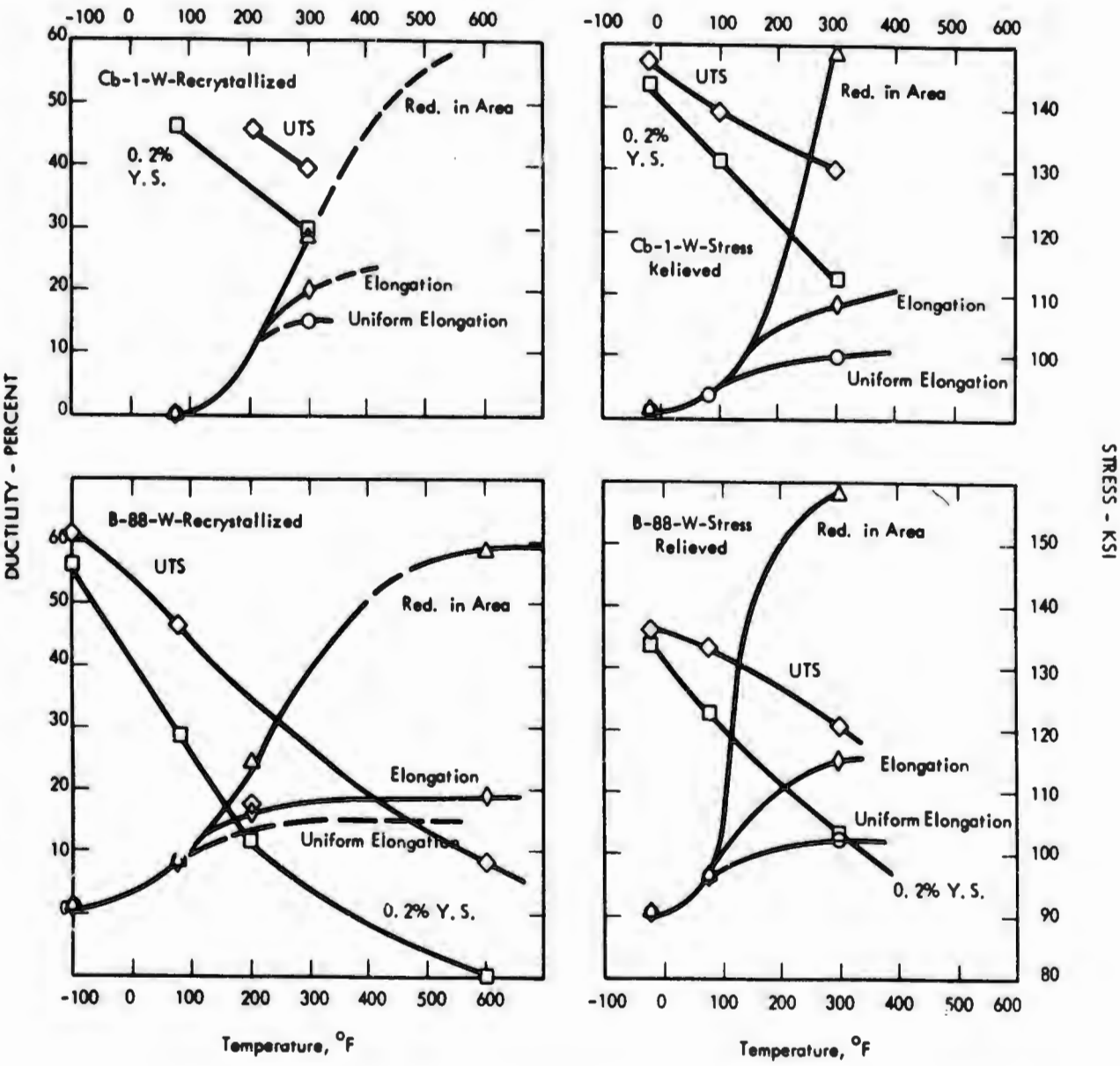

FIGURE 17 - Low Temperature Tensile Properties of Recrystallized and Stress Relieved Cb-1 and B-88 Processed by the WANL Fabrication Sequence

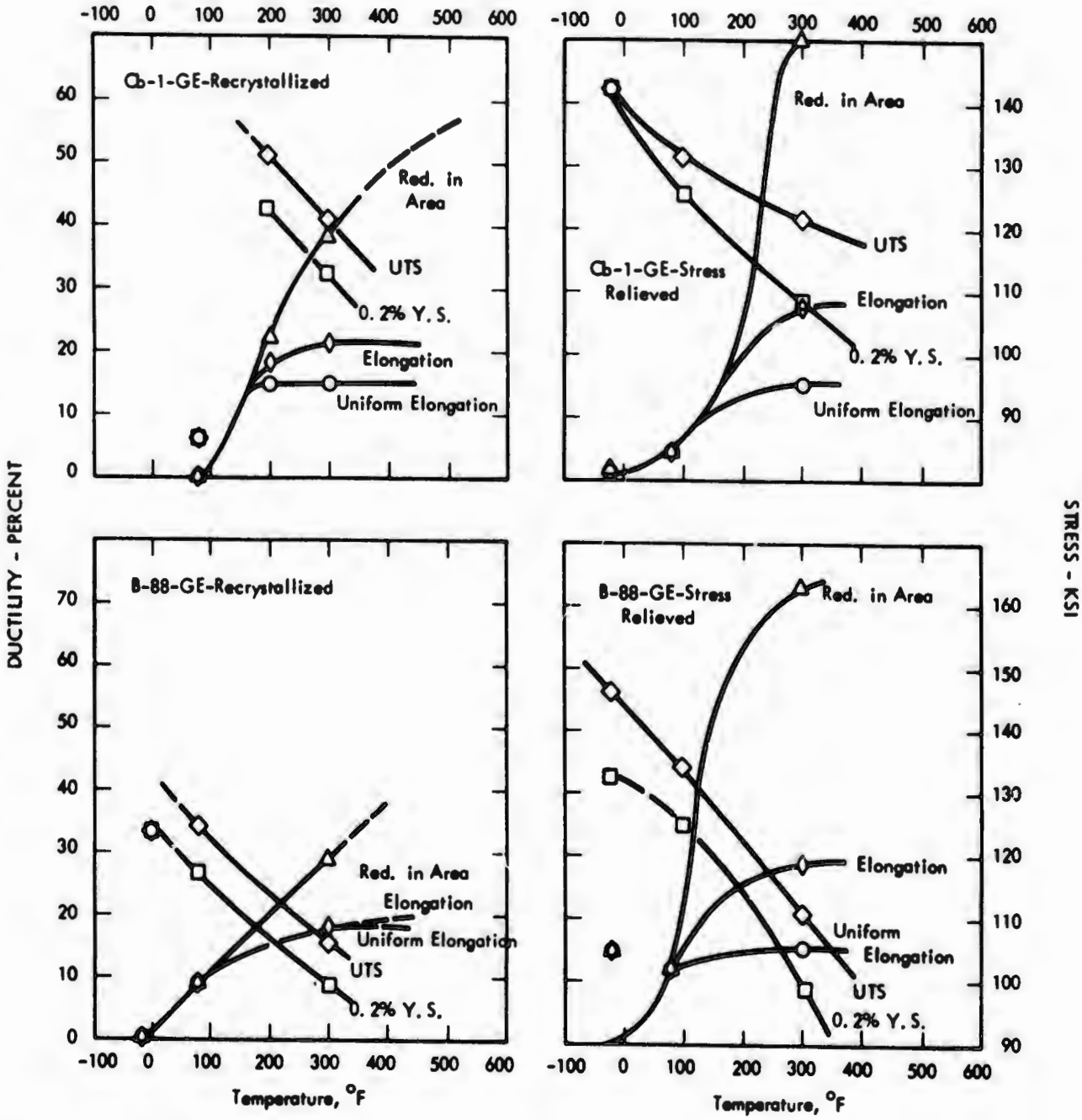

FIGURE 18 - Low Temperature Tensile Properties of Recrystallized and Stress Relieved Cb-1 and B-88 Processed by the GE Fabrication Sequence

III. STRAIN HARDENING AND RECOVERY STUDIES

The development of columbium alloys for gas turbine applications has emphasized the improvement of creep properties. As a result, alloy compositions and thermal-mechanical processing sequences have generally been selected to provide an optimum combination of creep resistance and low temperature ductility. For B-88 (Cb-28W-2Hf-0.067C) and similar high strength columbium alloys, the optimized thermal treatment to provide the best combination of high temperature strength and low temperature ductility results in a relatively fine grained, recrystallized structure. However, this structure provides relatively low intermediate temperature (1200-1600°F) yield strength values, on the order of 50,000 psi for B-88. A high yield strength in this intermediate temperature range is critical to avoid plastic deformation in the root area of a turbine blade. Yield strength values of over 70,000 psi are required in most turbine designs in this temperature range.

Columbium alloys of the B-88 type strain harden rapidly at low and intermediate temperatures. It is thus possible to preferentially work harden the root section* of an otherwise creep optimized turbine blade during the last portion of the blade fabrication sequence. However, selection of such a fabrication sequence for a columbium alloy must take into consideration the protective coating thermal cycle. Strain hardening will be rapidly recovered at the temperature commonly utilized for applying protective coating to columbium alloys.

The objective of this phase of the investigation was to determine the work hardening characteristics of a high strength columbium alloy and the kinetics of the recovery process(es). The alloy selected for this phase of the investigation was Cb-22W-2Hf-0.06C (designated B-99) which is identical to B-88 except for the slightly lower tungsten content. This composition was selected because of its better low temperature ductility, which provides more

---

* Extensive work hardening the air foil section of the blade would result in serious degradation of high temperature creep properties.

flexibility in the selection of processing sequences. While the high temperature creep strength is lower than that of B-88, the strength properties are still very attractive.

A. MATERIAL PROCESSING

The Cb-22W-2Hf-0.06C alloy (heat VAM-97) was double vacuum arc melted to produce a 2.7 inch diameter ingot. The columbium was obtained in the form of columbium - 10 w/o tungsten alloy bar available from another Air Force program. The material in the as-received condition contained numerous surface cracks which were deeply oxidized. The bars were heavily etched and then analyzed for tungsten, carbon, oxygen and nitrogen. The analysis showed 8.6 w/o W, 215 ppm oxygen, 47 ppm carbon and 97 ppm nitrogen. Representative samples for chemical analysis were difficult to obtain because of the localized nature of the surface contamination. Although this material was somewhat higher in interstitial content than what is normally considered acceptable at this laboratory, it was decided not to reject the Cb-10W bars because a considerable amount of the surface contamination would be removed by additional etching and by milling surface flats for electrode fabrication. Since carbon was to be added to the electrode assembly the relatively high oxygen level was not considered critical. The first melt electrodes were fabricated by milling 3/4 inch flats on opposite sides of the 1-1/4 inch diameter Cb-10W bars. The electrode assembly for heat VAM-97 is shown in Figure 19. Additional tungsten and hafnium was added as thin strip, and carbon as graphite cloth wrapped in columbium foil. The electrode assembly was welded in a vacuum purged weld chamber back filled with high purity helium.

The first melt electrodes were vacuum arc melted into a 2 inch diameter water cooled copper mold. A second melt electrode was fabricated by welding the first melt ingot together and to a columbium adapter. The resultant electrodes were melted into a 2.7 inch diameter mold. The resultant ingot was 10.9 inches long, 2.63 inches in diameter, and weighed 21 pounds. The ingot was machined to 2.55 inch diameter, cut in half and fitted into molybdenum extrusion cans.

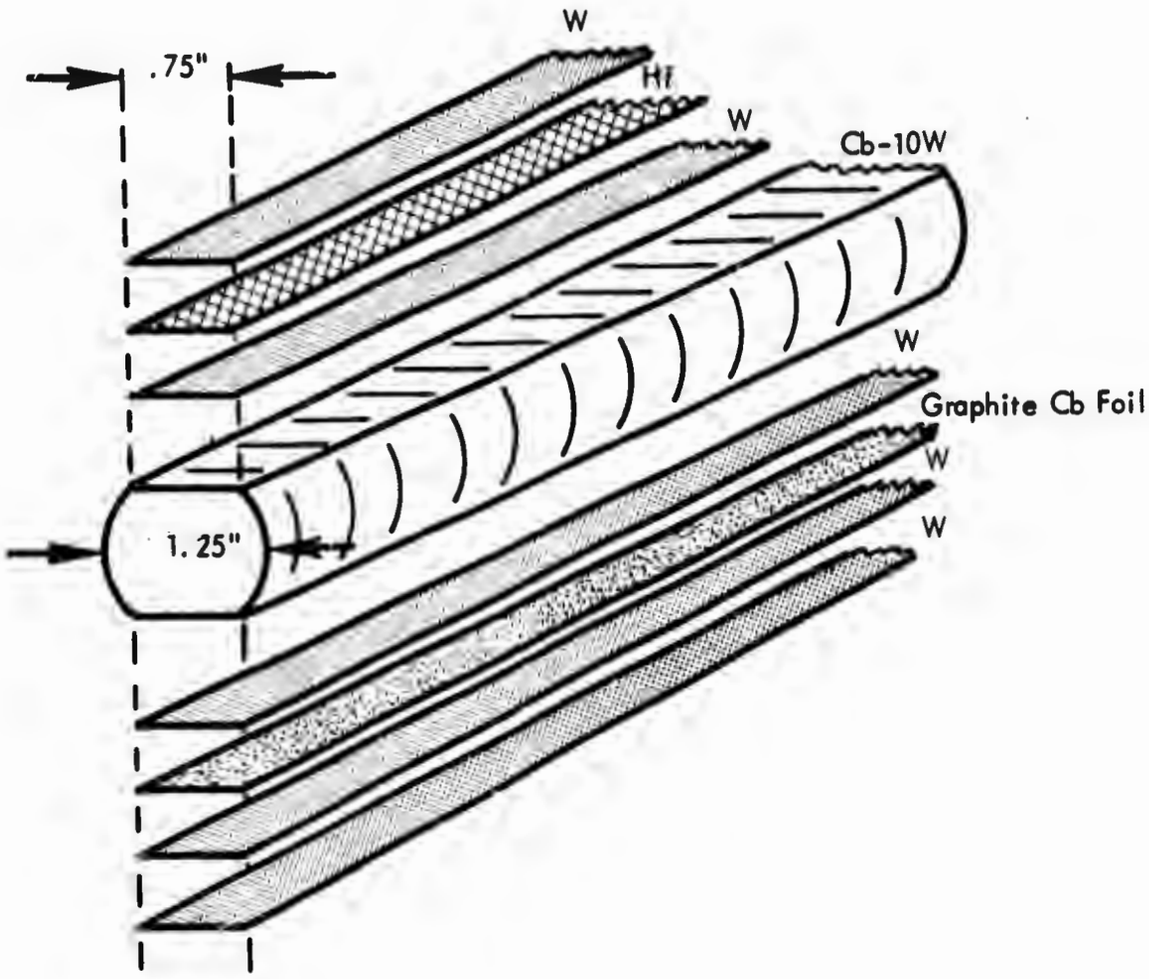

FIGURE 19 - First Melt Electrode Arrangement for Heat No. VAM-97
(Cb-22W-2Hf-0.067C)

Chemical analyses obtained on the as-melted ingot as listed in Table 6. Agreement with the nominal composition was excellent. Approximately 70 ppm of carbon was lost during melting, presumably due to the presence of excess oxygen in the base alloy stock resulting in carbon removal as CO during melting.

TABLE 6 - Chemical Analysis of VAM-97

Location	Nominal Composition (w/o)	Composition (w/o)				
		W	Hf	C	N	O
	Cb-22W-2Hf-0.067C					
Ingot Top	---	22.1	1.9	0.059	0.0069	0.0047
Ingot Bottom	---	22.0	1.9	0.061	0.0069	0.0038

Two billets of the Cb-22W-2Hf-0.06C alloy were extruded at the AFML Extrusion Facility at Wright-Patterson Air Force Base. The extrusion were similar to those described previously in this report for B-88 and Cb-1, with the exception that MgO was used as the parting compound between the billet and the molybdenum extrusion can. The MgO caused some reacrion with either the molybdenum or columbium oxides and caused localized zones of poor surface. However, little material was lost due to the reaction. Most of the surface defects were removed after approximately 0.020 inch was removed from the surfaces of the extrusions by centerless grinding. The remaining defects were removed by a small amount of surface conditioning. The extrusion parameters are listed in Table 7.

Secondary Working

The extruded bars were reduced from 1.1 inch diameter to 0.72 inch diameter by swaging at 1200°C. The material was then locally conditioned and centerless ground to 0.70 inch diameter. Swaging of a portion of the B-99 bar for the initial portion of

TABLE 7 - Extrusion Data for VAM-97

	Cb-22W-2Hf-0.67C	
Extrusion Parameter	Ingot Bottom	Ingot Top
Extrusion No.	2779	2778
Ingot Wt.	9.6 lbs.	9.4 lbs.
Length	5.38 in.	5.3 in.
Dia.	2.55 in.	2.55 in.
Billet Wt.	14.3 lbs.	14.2 lbs.
Length	6.0 in.	6.0 in.
Dia.	2.95 in.	2.95 in.
Billet Heating (Induction)	22 min.	23 min.
Time at Temp.	5 min.	5 min.
Temperature	3200°F	3200°F
Ram Speed Maximum	2.5 ips	2.25 ips
Minimum	2.0 ips	1.75 ips
Load Maximum (Breakthrough)	90 ksi	103 ksi
Load Minimum (Running)	86 ksi	92 ksi
Extrusion Constant (Total)	58.1 ksi	56.5 ksi
Reduction Ratio	4.4:1	5.1:1

Lubricant
Billet: DC7740
Container: MoS_2
Die: MoS_2

Container
Size: 3.072 in.
Temp.: 800°C
Die: 90°
ZrO_2 Faced 800°F Preheat
Jacket: Molybdenum

the work hardening and recovery study continued at 1300°C until the bars had been reduced in diameter to the predetermined size for cold working. The varying diameter bars were surface conditioned by centerless grinding, cleaned, etched, and annealed 1 hour at 1700°C. The bars were then swaged at 800°C to final specimen stock size (0.44 inch diameter) equivalent to cold reductions of 35%, 20% and 15%. The processing sequence for this material is outlined in Figure 20.

The microstructures of the Cb-22W-2Hf-0.06C alloy after various amounts of cold reduction are shown in Figures 21, 22 and 23. These photomicrographs show grain elongation to increase with increasing deformation, as expected. Deformation bands were observed in the material worked 35% (Figure 21). These bands appear to originate at triple points (Figure 21b) and also occurred as slip on intersecting systems (Figure 21c). A carbide decorated substructure was also observed as shown in the photomicrographs of the 20% cold worked material, Figures 22b and 22c. This structure has been observed in B-88 after annealing at 1700°C[2] and therefore cannot be definitely attributed to the cold deformation. However, extensive substructure development would be expected in the cold worked plus heat treated condition.

The material swaged at 800°C (1470°F) following a 1700°C anneal displayed numerous radial cracks. The cracking problem may be in part attributed to the presence of a brittle surface oxide layer developed at the working temperature. Results of studies on B-88 described later in this report indicate that higher cold working temperatures (~1000°C) can result in about the same general working levels with little incidence of cracking. Despite the cracking problem sufficient material was obtained for the initial studies.

B. STRAIN HARDENING

Preliminary evaluation of strain hardening effects were carried out on both the B-88 and B-99 alloys. The purpose of these tests was to demonstrate the potential of work

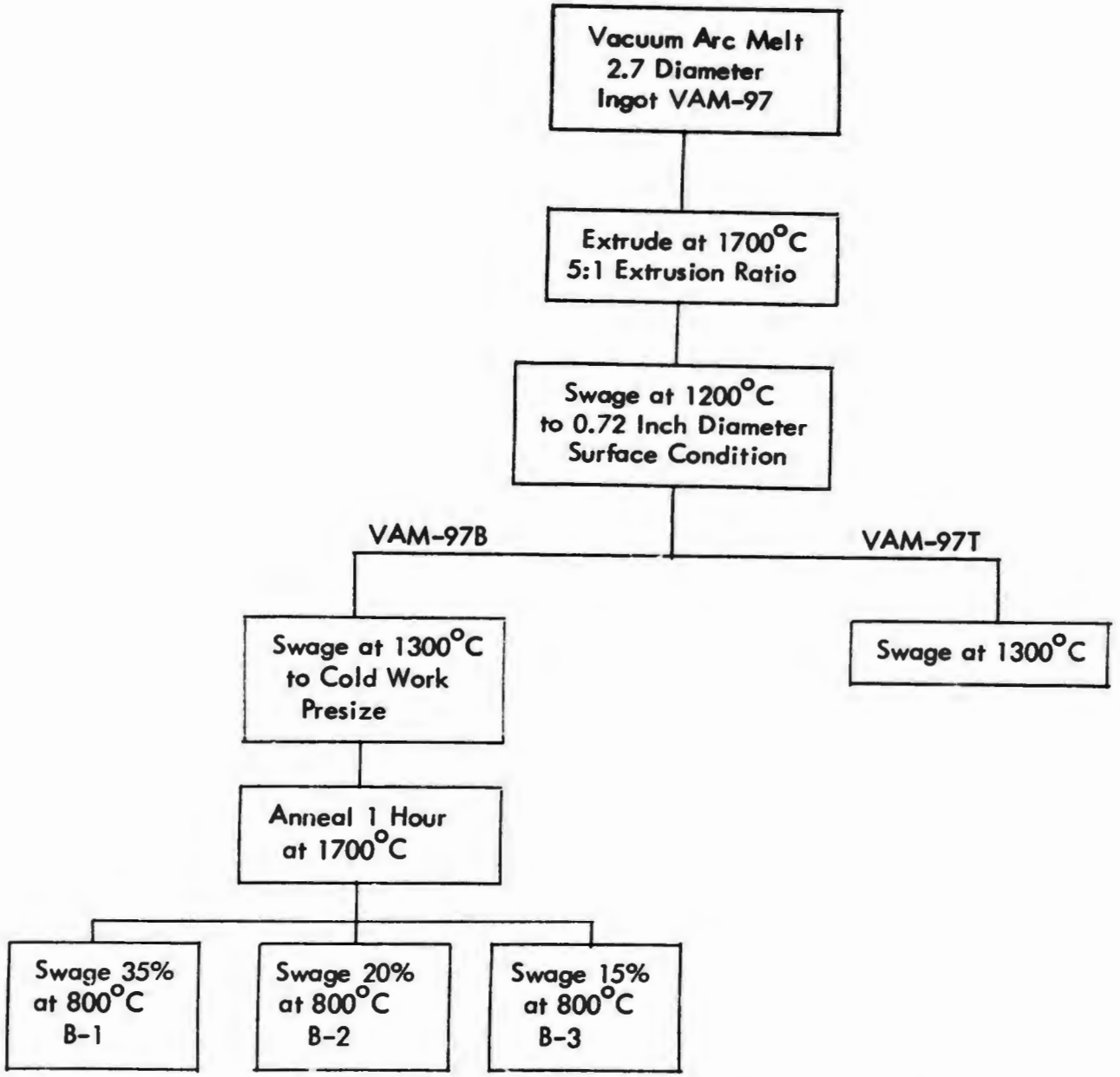

FIGURE 20 - Fabrication Schedule for VAM-97 (Cb-22W-2Hf-0.06C)

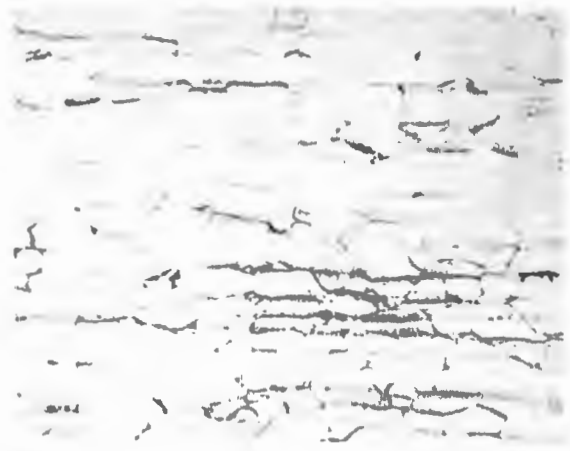

(a) 100X

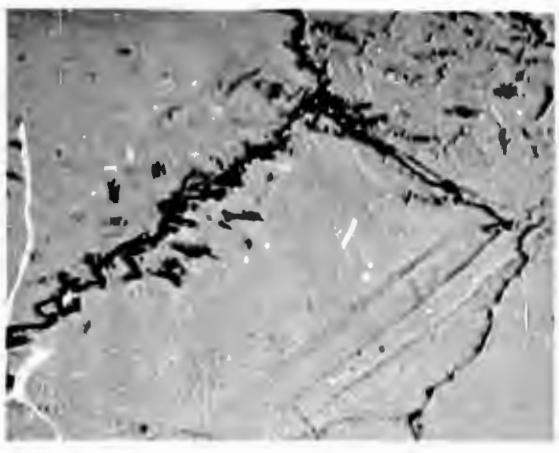

(b) 1500X

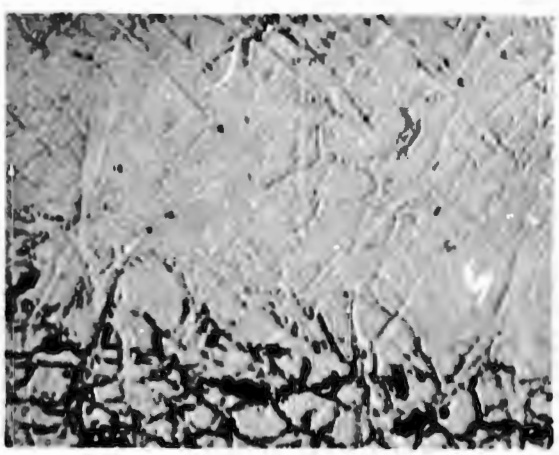

(c) 1500X

As-Swaged + 1 Hr. at 1700°C + 35% Cold Work

FIGURE 21 - Microstructure of VAM-97 (Cb-22W-2Hf-0.06C) Annealed at 1700°C Plus 35% Cold Reduction at 800°C

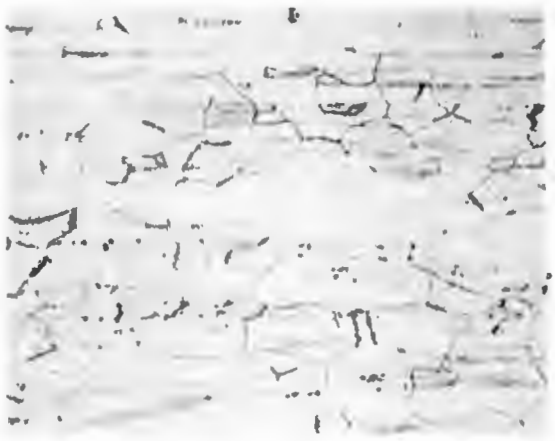

(a) 100X

(b) 1500X

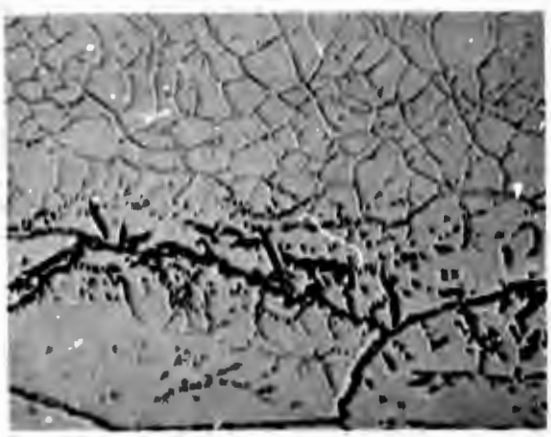

(c) 1500X

As-Swaged + 1 Hr. at 1700°C + 20% Cold Work

FIGURE 22 - Microstructure of VAM-97 (Cb-22W-2Hf-0.06C) Annealed at 1700°C Plus 20% Cold Reduction at 800°C

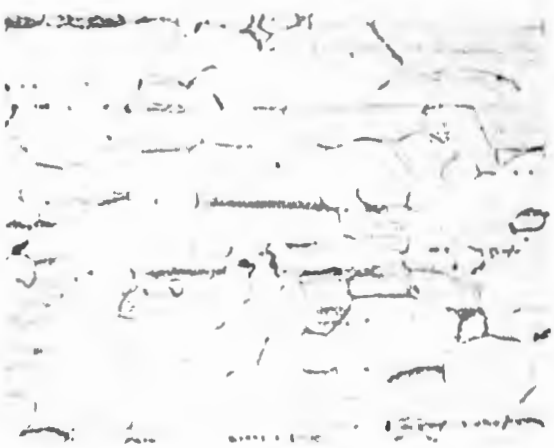

(a) 100X

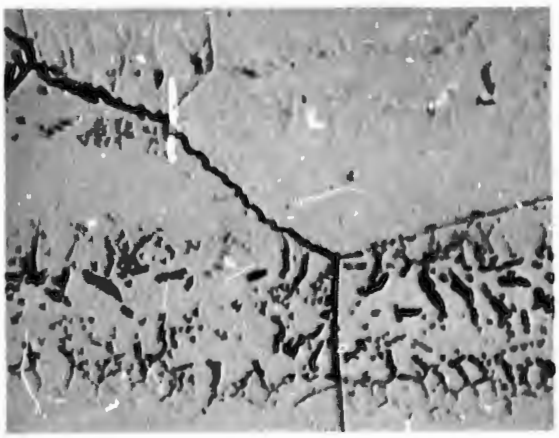

(b) 1500X

As-Swaged + 1 Hr. at 1700°C + 15% Cold Work

FIGURE 23 - Microstructure of VAM-97 (Cb-22W -2Hf-0.06C) Annealed at 1700°C Plus 15% Cold Reduction at 800°C

hardening for increasing intermediate temperature yield strength, and to bracket the appropriate temperature range for warm working and the required amount of deformation.

Tensile tests were conducted on specimens machined from bars of the Cb-22W-2Hf-0.06C alloy (B-99) which had been swaged to 15, 20 and 35% reduction at 800°C. Tensile tests were carried out in vacuum at 760°C (1400°F) with the test pressure being maintained below 5×10^{-6} torr. The strain rate was 0.05 in/in/min. The tensile data are plotted as a function of percent prior cold work in Figure 24, and the tensile results are tabulated in Table 8.

As shown in Figure 24, the 0.2% yield strength of B-99 was 42,000 psi at 760°C (1400°F). However, the yield strength was increased to 101,000 psi with 15% cold reduction by swaging (at 800°C). The yield strength increased moderately with further reduction. These results clearly demonstrated that relatively small reductions could more than double the yield strength in the intermediate temperature range.

To explore the effect of deformation temperature on strain hardening, three B-88 specimens were evaluated. All were initially in the reference condition (as-swaged plus annealed 1 hour at 1700°C). The testing conditions are outlined as follows:

T-6 Specimen was prestrained 9.5% (true plastic strain) at 300°F in air and then retested in vacuum at 1400°F. The strain rate was 0.05 in/in/min.

T-5 Specimen was prestrained 11% (true plastic strain) at 1800°F in vacuum and retested at 1400°F in vacuum at a strain rate of 0.05 in/in/min.

T-10 Specimen was tensile tested at 1400°F to fracture, again using a strain rate of 0.05 in/in/min.

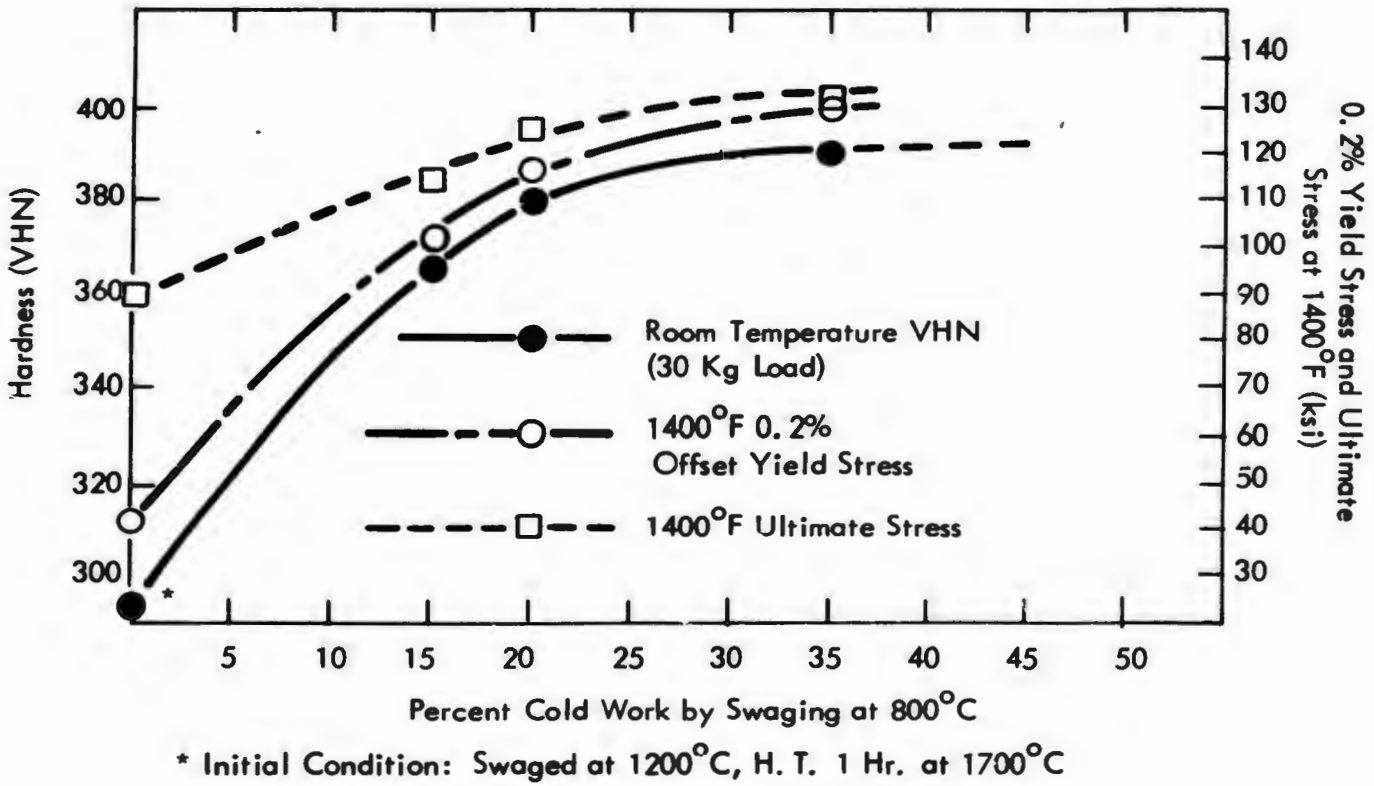

FIGURE 24- Variation of Strength of VAM-97 with Cold Work

TABLE 8 - Tensile Properties of VAM-97 (Cb-22W-2Hf-0.06C) at 1400°F (760°C) as a Function of Prior Reductio

	Percent Cold Work at 800°C (1470°F)			
	0%	15%	20%	35%
0.2% Offset Yield Stress (psi)	42,000	101,300	117,200	130,900
Ultimate Tensile Stress (psi)	90,000*	114,400	124,200	131,700
Uniform Strain (%)	11.0*	5.05	3.8	0.61
Elongation (%)	--	9.0	8.0	4.0
Reduction in Area (%)	--	40.2	42.0	37.1

NOTES:

1. Strain rate: 0.05 in/in/min
2. Tests conducted in vacuum $<5 \times 10^{-6}$ torr.

* Data taken from pre-straining portion of recovery test. Specimen was prestrained = 11% at 1400°F

The true stress-true strain curve of specimen T-6 is shown in Figure 25. This specimen displayed a yield point during straining at 300°C, with a lower yield stress of 96,000 psi. The yield point drop was approximately 2000 psi. The true stress-true strain curve extrapolated beyond the lower yield intersects the elastic loading curve at a stress level of 89,000 psi. The flow stress after 9.5% plastic strain was 117,000 psi, at which point the specimen was unloaded. Upon subsequent reloading at 1400°F plastic flow occurred when the stress reached 96,000 psi. The true stress-true strain curve at 1400°F for the prestrained specimen was characterized by a very high strain hardening rate up to the point of ultimate load (corresponding to a true stress of 117,500 psi) followed by serrated flow (Portevin-Le Chatelier effect) beyond this point.

The true stress-true strain curve for specimen T-5, prestrained to 11% true plastic strain at 1800°F and retested at 1400°F is shown in Figure 26. Yielding occurred at 49,000 psi but no yield point was observed. The strain hardening rate was more rapid than during the 300°F prestrain of specimen T-6. The flow stress increased to 100,000 psi at a true plastic strain of 11%, whereupon the specimen was unloaded. Upon retesting at 1400°F the specimen yielded at 99,000 psi but immediately displayed serrated flow which continued up to fracture. The initial amplitude of the serrated flow was $\pm$ 3000 psi but continuously decreased to fracture.

The plastic portions of the true stress-true strain curves obtained for specimens T-5 and T-6 are given in Figure 27. The plastic portion of a specimen (T-10) tested to fracture at 1400°F is also shown in Figure 27 for comparison. The two prestrained specimens and the reference specimen all displayed at 1400°F flow stress of approximately 100,000 psi after a total of approximately 10% true plastic strain.

These preliminary experiments showed that prestraining can be accomplished over a wide temperature range. The strain hardening rate of B-88 is quite high at all the temperatures investigated, the highest being achieved at 1400°F. Very similar behavior would be

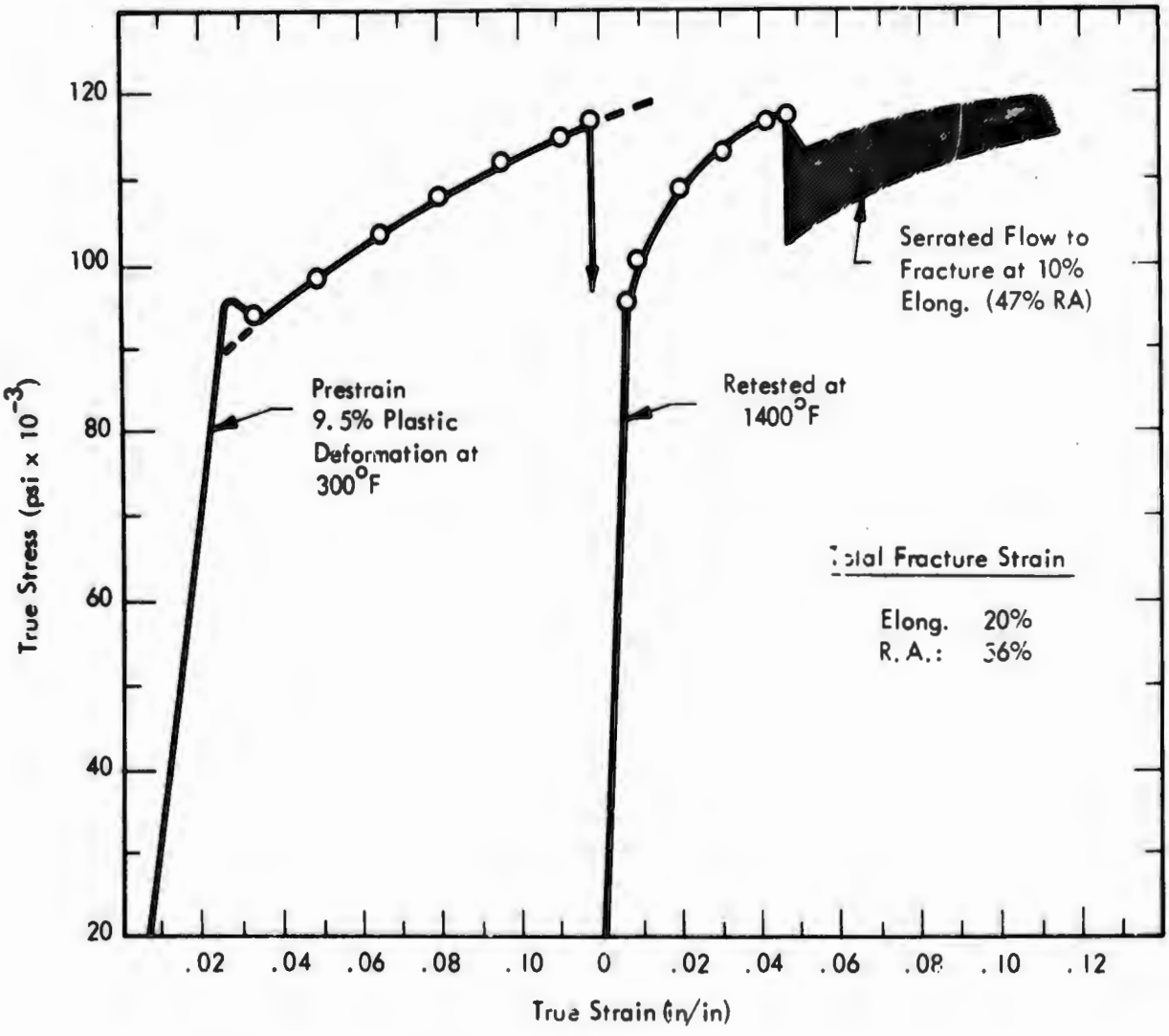

FIGURE 25 - True Stress-True Strain Curves of B-88 Specimen T-6, Heated 1 Hr. at 1700°C, Prestrained to 9.5% (Plastic) at 300°F, Retested at 1400°F

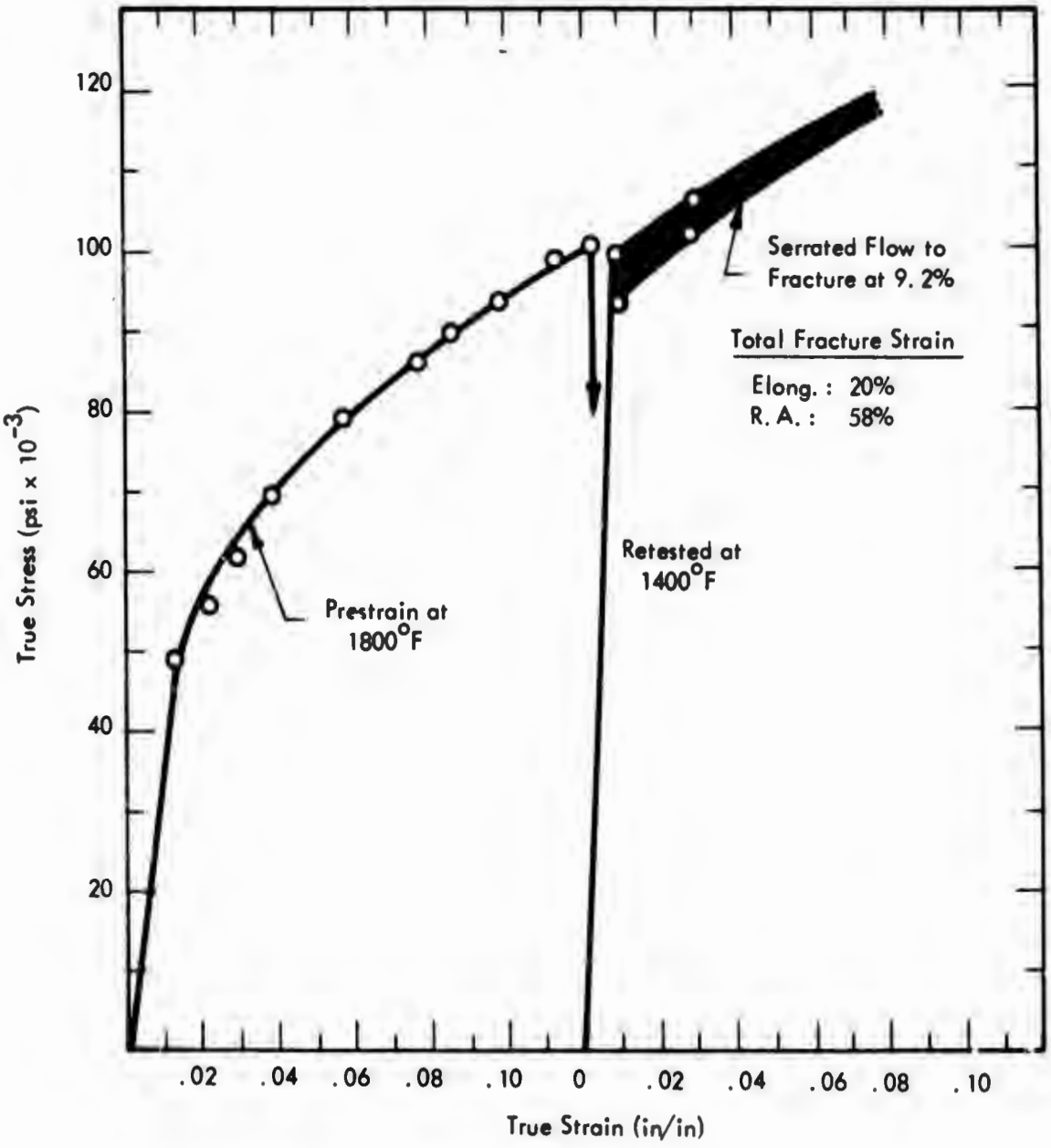

FIGURE 26 - True Stress-True Strain Curves of B-88 Specimen T-5, Heated 1 Hr. at 1700°C, Prestrained to .11 (Plastic) at 1800°F, Retested at 1400°F

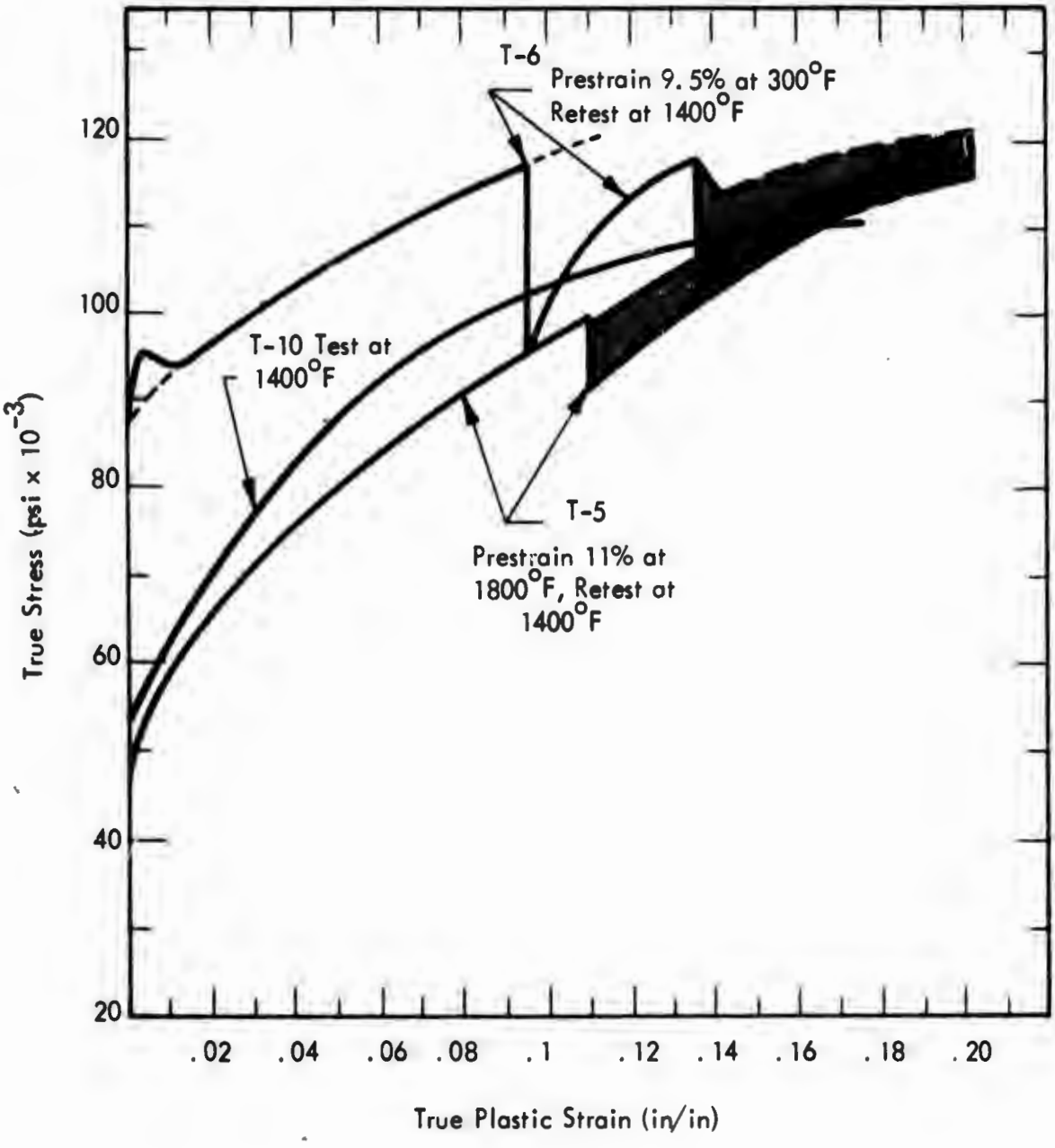

FIGURE 27 - Work Hardening Characteristics of B-88 at 300°F, 1400°F, and 1800°F

expected with the Cb-22W-2Hf-0.06C alloy (B-99). These results indicate that considerable latitude is possible in developing processing sequences which will provide the increment in intermediate temperature yield strength which is required. Although the state of stress and the strain rate used in the initial tensile studies are quite different than those encountered during rolling, swaging, or forging, the work hardening behavior should generally be similar irrespective of the type of deformation.

C. RECOVERY STUDIES

The data presented in the previous section show that B-99 may be strain hardened to increase the yield strength from approximately 50,000 psi to greater than 130,000 psi (at 1400°F). If this strength increment is to be utilized the characteristics of the recovery process(es) should be well defined. This phase of the investigation was initiated to determine the characteristics of yield strength recovery at 760°C (1400°F) as a function of thermal treatments bracketing the range of probable coating and fabrication temperatures.

Experimental Procedure

Tensile specimens having a 1 inch gage length and a 0.1 inch gage diameter were machined from as-swaged VAM-97 bar. All the specimens were annealed 1 hour at 1800°C at pressures below 5×10^{-6} torr. This heat treatment produced a mean grain diameter of 0.02 mm.

The specimens were prestrained 9 to 10% (true) in tension at 760°C (1400°F) in an Instron machine fitted with a Brew Model 1064 vacuum furnace. Pressure was maintained below 5×10^{-6} during the testing. A constant strain rate of 0.05 in/in/min was selected. The material characteristically yielded at 45,000 psi to 52,000 psi and work hardened to about 100,000 psi. The specimens were cooled to room temperature and measured prior to the recovery and retesting portions of the test.

The parameter (1-R) was used in evaluating the recovery characteristics. This parameter can be described as the residual strain hardening where R is the actual recovery. Recovery R is defined as:

$$R = \frac{\sigma_m - \sigma_2}{\sigma_m - \sigma_y} \; ; \text{ and } 1-R = \frac{\sigma_2 - \sigma_y}{\sigma_m - \sigma_y}$$

These values are defined in Figure 28. R varies from 0 where there has been no reduction in yield strength to 1.0 when the work hardening increment has been completely removed through annealing. Conversely, the residual strain hardening parameter (1-R) varies from 1.0 to 0.

A prestrain of approximately 9% true was selected in order to avoid necking but still obtain adequate work hardening. The specimens were removed from the testing machine after each prestrain and were carefully measured and examined for possible necking.

Specimens that were to be annealed short times (3 minutes to 3 hours) were reloaded in the vacuum tensile testing furnace and heated in vacuum for the desired times and temperatures after first stabilizing the temperature at 1400°F for one to two minutes. Thirty seconds to one minute were required to increase temperature to the desired level from 1400°F. A 1/3 atmosphere helium was bled into the chamber the instant the power was cut at the end of the recovery treatment. This enabled cooling rates on the order of 1200 °F/min. during cooling from the recovery treatment to 1400°F, the testing temperature.

Long time recovery treatments (3 to 100 hours) were performed in a 424 Brew vacuum furnace at a pressure of less than 1×10^{-6} torr. The specimens were wrapped in tantalum foil to avoid contamination. The heating and cooling procedures were exactly the same as in the vacuum tensile testing furnace described above. In both cases, the temperature was monitored by Pt - Pt 13% Rh thermocouples strapped directly to the specimens.

Experimental Results

The experimental data are summarized in Table 9. Figures 29 and 30 show the true stress-true strain curves for B-99 from the various pre-strain and post-recovery anneal re-strains at 2000°F and 2600°F. The specimens recovered at 2000°F show a low rate of work hardening upon retesting as compared to the more recovered specimens tested at 2600°F.

The fractional residual strain hardening parameters were calculated for each recovery test and are plotted vs. time for the 1095, 1260 and 1425°C (2000, 2300 and 2600°F) isotherms in Figure 31. These curves show a peak in each of the isotherms investigated. These peaks are interpreted as aging reactions. If we assume the aging reactions are thermally activated, then,

$$\text{rate} \propto \frac{1}{t} = A \exp(-Q/RT)$$

when A is a constant, t is time to form the aging peak, R and T have the usual meaning and Q is the apparant activation energy for the aging reaction. A plot of ln t vs. $1/T^{\circ}K$ results in a Q of 10 Kcal. This value is almost 1/3 of the activation energy for carbon diffusion in columbium, but is close to the expected value for carbon diffusion along dislocations.

The fractional residual strain hardening data (1-R) are plotted versus ln t for the three isotherms in Figure 32. The data becomes unreliable at short times at the higher temperatures because of the uncertainty in time due to heat up and cool down from the recovery temperature. When using the methods of Tichner and Bever[10] and Michalak and Paxton[11], an activation energy of 85,000 $\pm$ 10,000 Kcal was obtained over the temperature range 2000° - 2600°F. This value is useful in describing the recovery behavior and in prediction but is of limited fundamental use because the recovery curves are obscured by the aging reaction.

TABLE 9. Summary of Experimental Data, Recovery Study (VAM-97)

Specimen* No.	Pre-Anneal Data			Post Recovery Anneal Data			
	.2% y s σ_y (ksi)	Pre-Strain ϵ_m (in/in)	Work Hardening σ_m (ksi)	Temp. (°F)	Time (min)	Post Test .2% ys (ksi)	1-R
97-27	52.6	.092	95.1	2600	3	76.8	.570
97-16	54.2	.102	100.0	2600	6	71.8	.384
97-19	47.0	.103	98.4	2600	12	67.1	.391
97-33	52.9	.093	91.5	2600	18	64.1	.291
97-17	47.1	.100	98.7	2600	24	64.4	.335
97-26	54.8	.092	98.2	2600	30	61.7	.159
97-32	54.5	.094	99.0	2600	60	58.3	.086
97-18	50.6	.101	98.9	2600	120	57.1	.135
97-21	53.3	.091	93.5	2300	6	82.4	.724
97-34	48.4	.094	95.4	2300	18	82.2	.720
97-41	52.8	.090	94.0	2300	36	78.5	.621
97-20	50.0	.102	98.8	2300	60	73.6	.483
97-40	52.2	.088	91.7	2300	180	69.1	.427
97-42	53.5	.030	94.7	2300	360	62.0	.206
97-22	52.8	.092	97.0	2300	600	59.5	.151
97-44	49.5	.088	97.0	2000	18	91.9	.892
97-23	55.0	.088	97.1	2000	60	89.5	.821
97-29	51.0	.091	98.7	2000	180	91.9	.858
97-24	53.1	.087	98.7	2000	600	89.1	.789
97-30	49.4	.092	97.8	2000	1800	77.4	.578
97-25	54.8	.091	98.1	2000	6000	69.0	.328

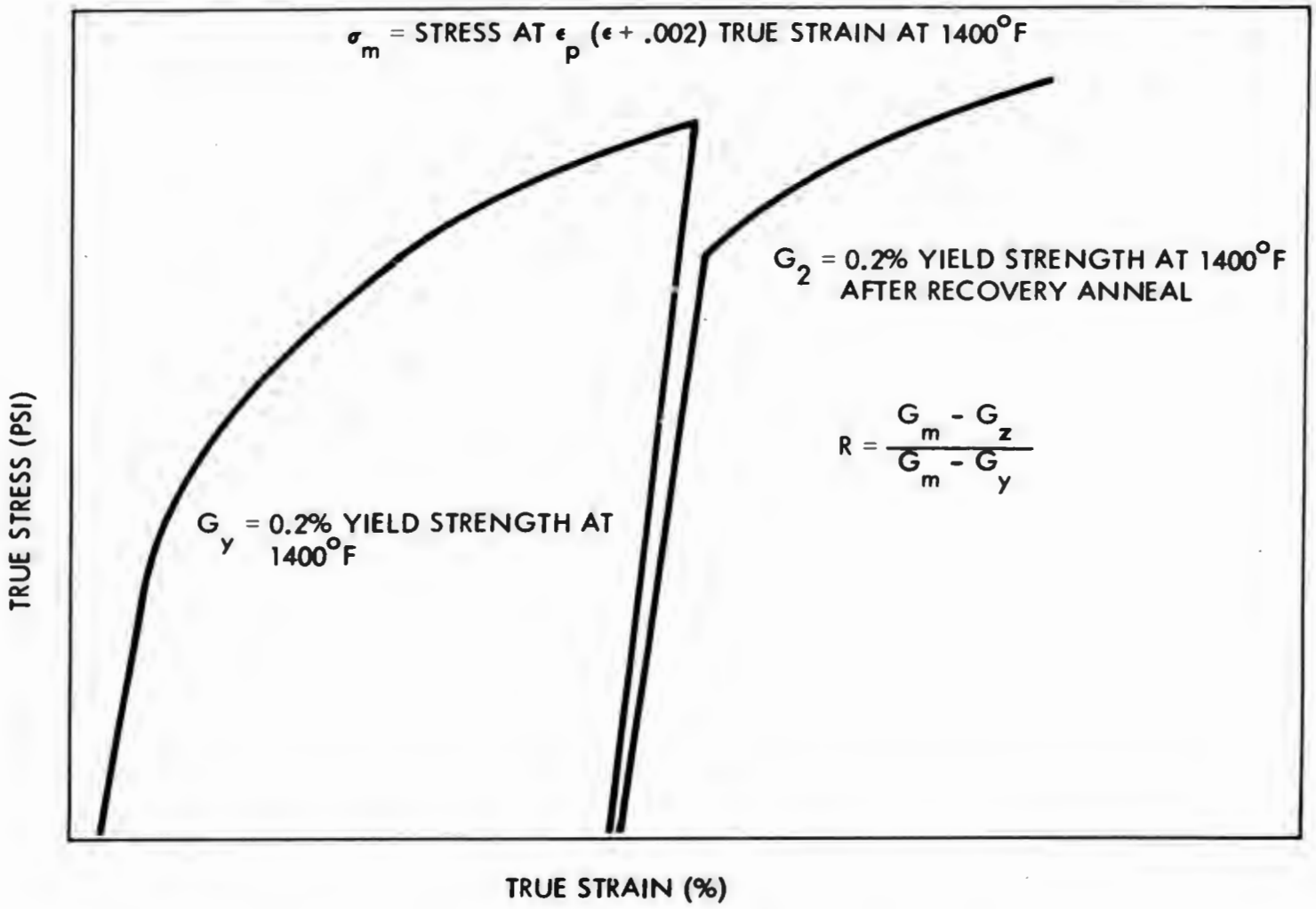

FIGURE 28 - Graphical Definition of Recovery Parameters

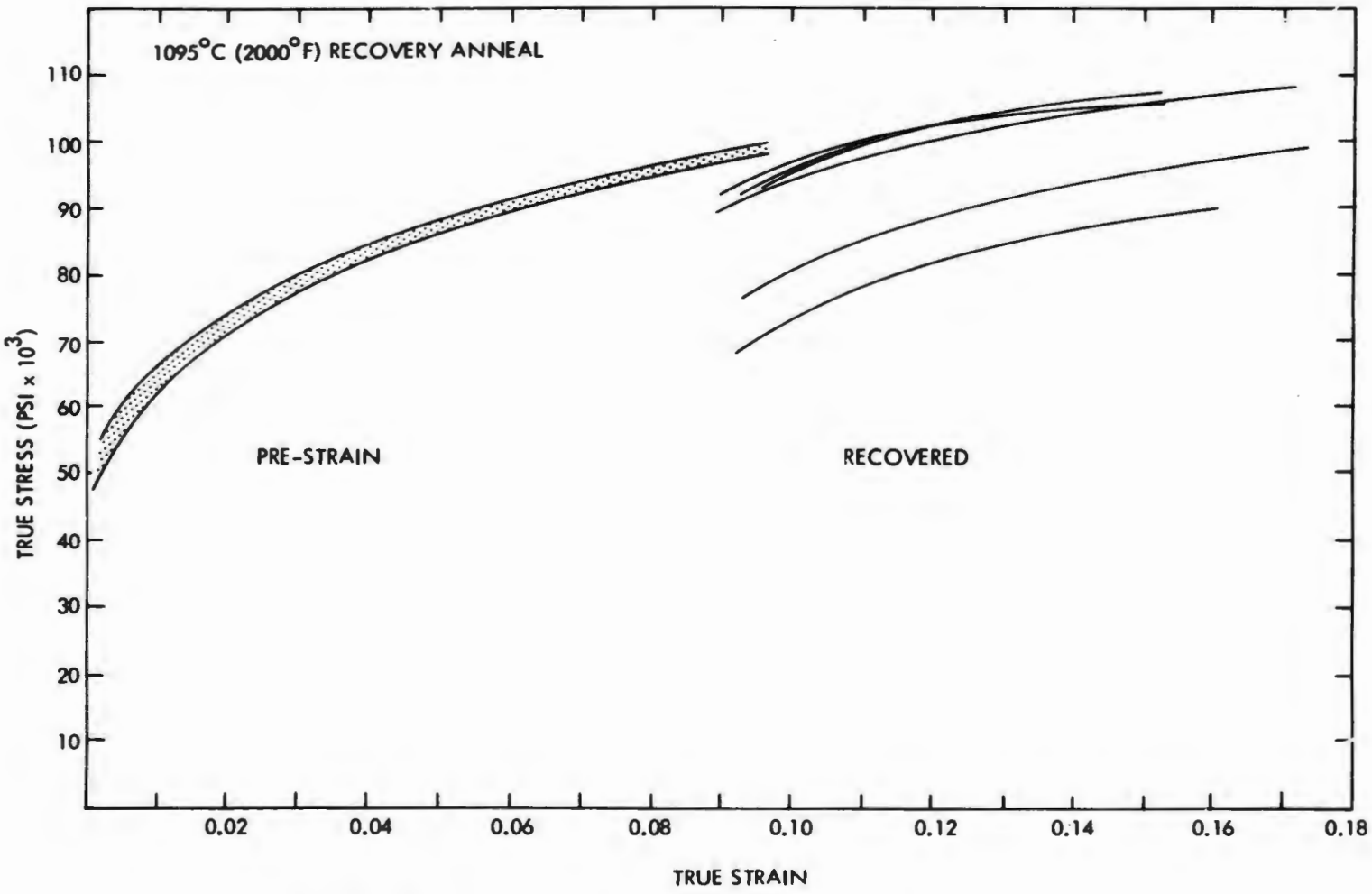

FIGURE 29 - True Stress-True Strain Curves for VAM-97

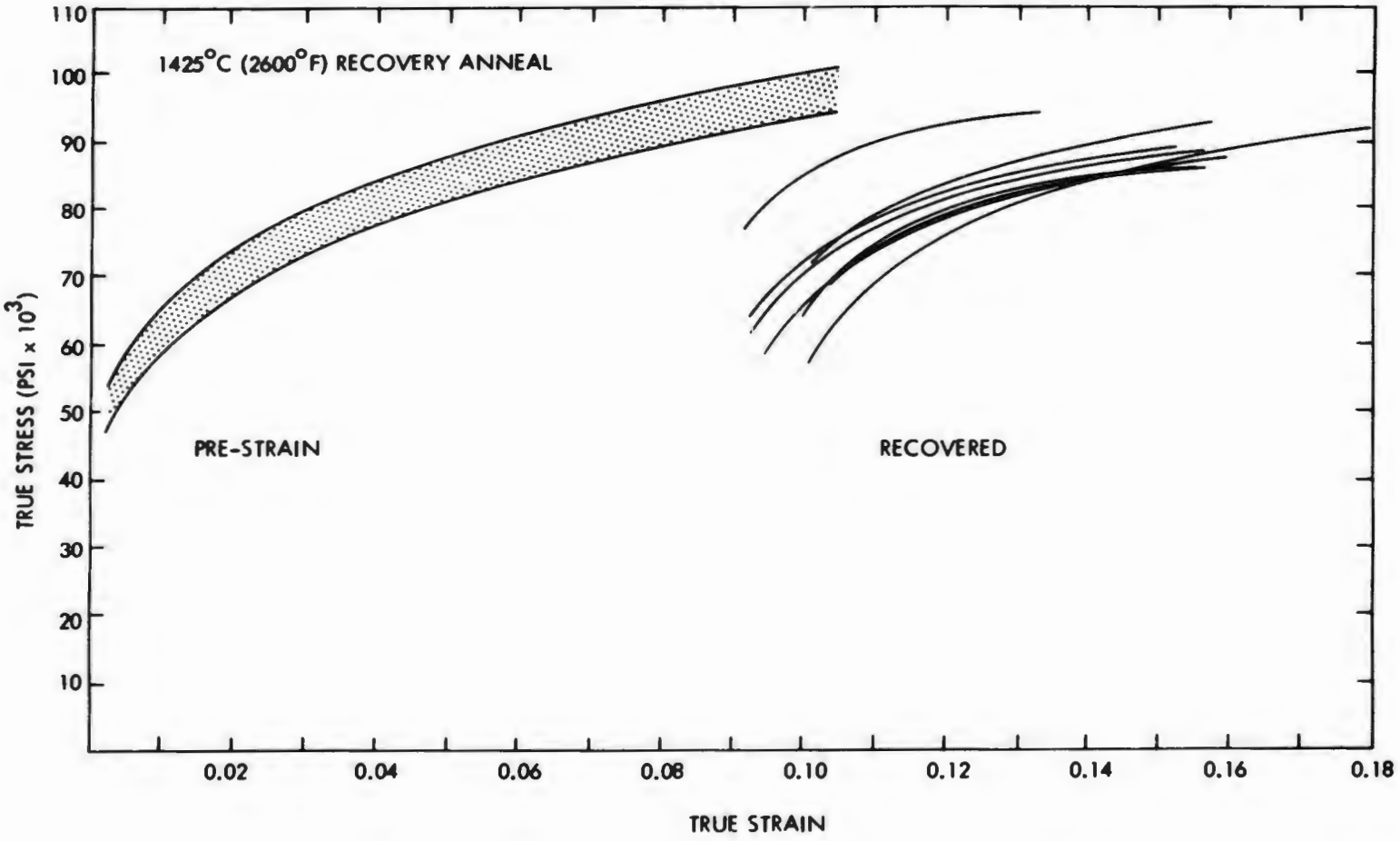

FIGURE 30 - True Stress-True Strain Curves for VAM-97

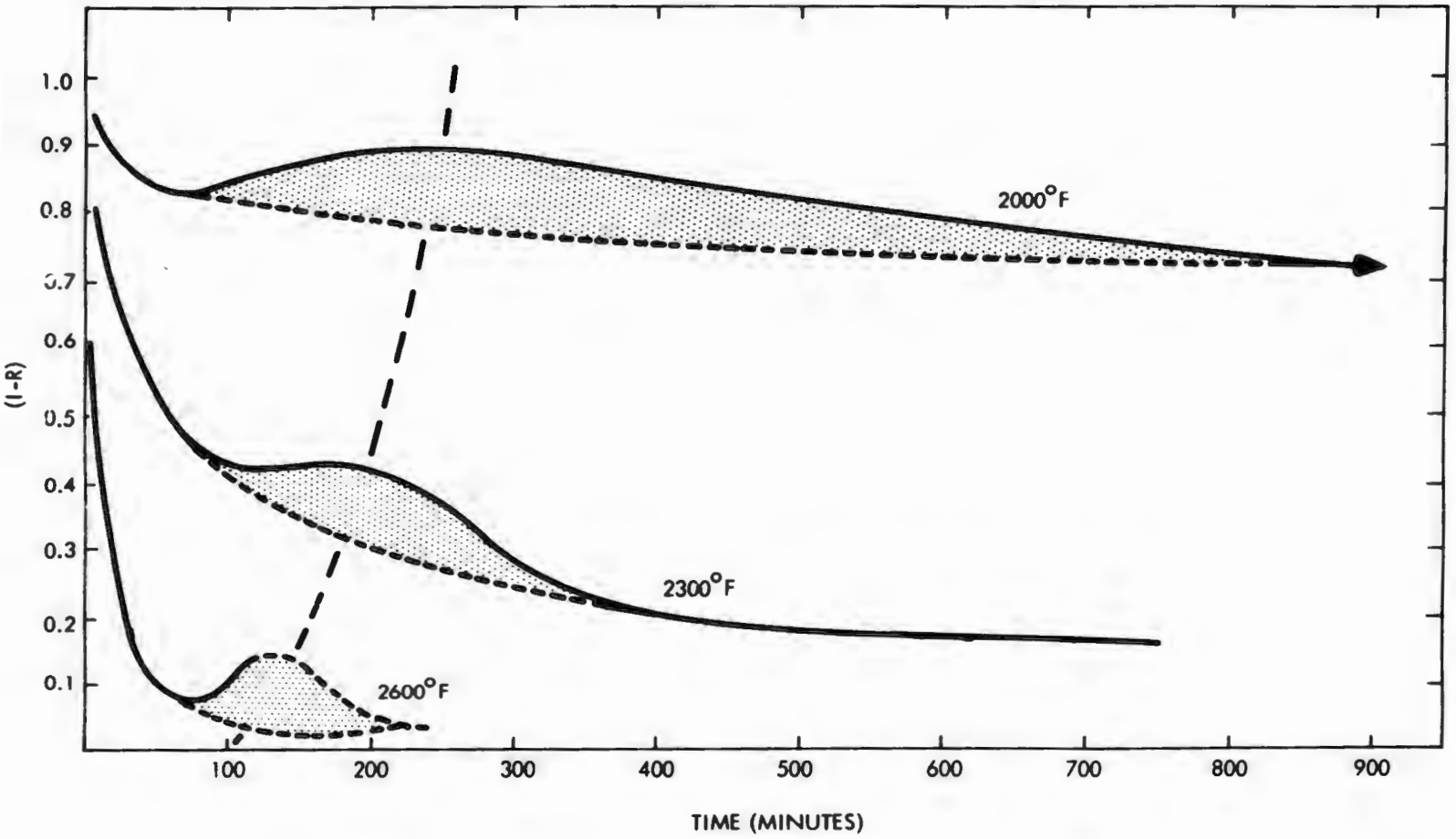

FIGURE 31 - Residual Strain Hardening Parameter (I-R) as a Function of Time

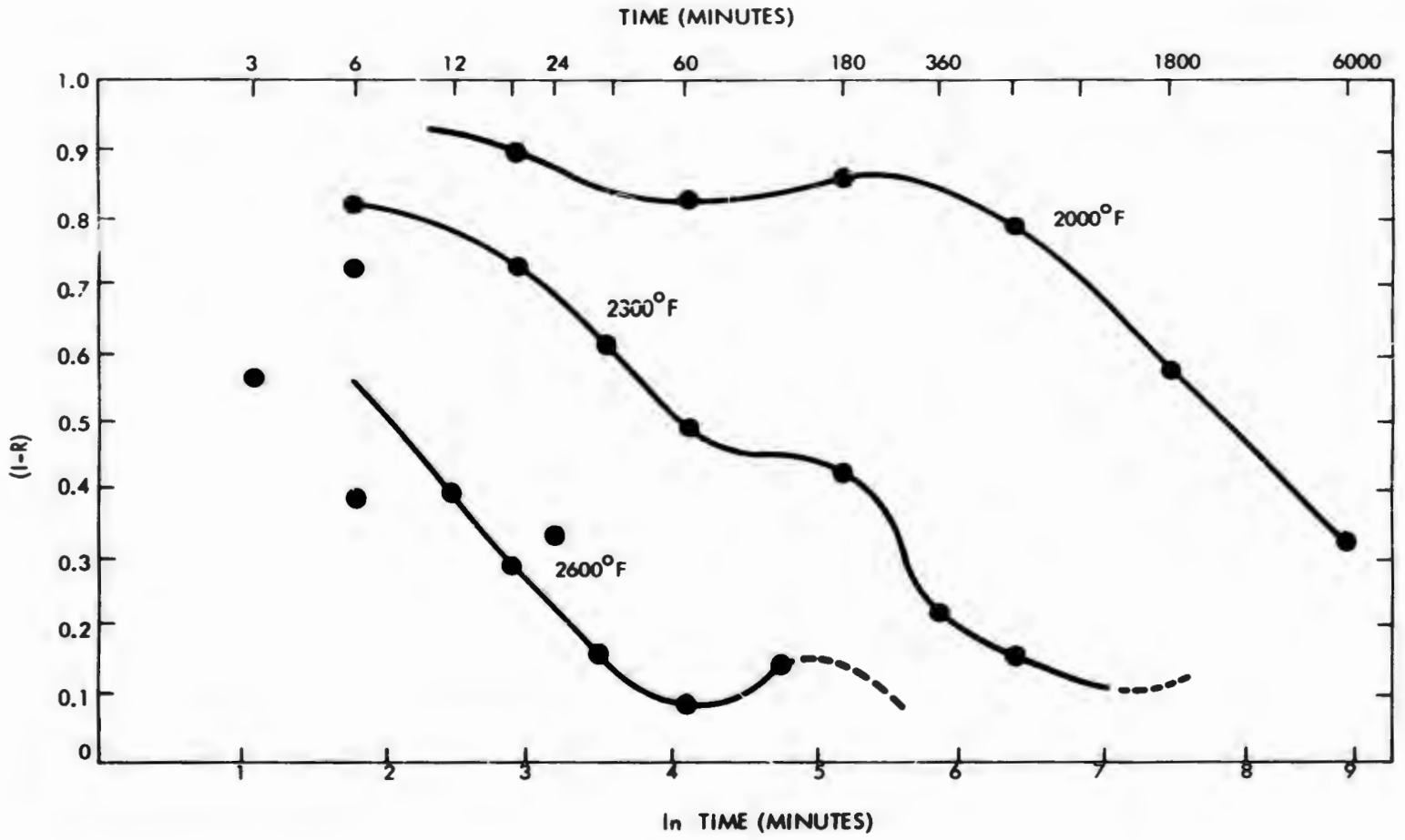

FIGURE 32 - Residual Strain Hardening Parameter as a Function of ln Time

Figure 32 also shows that the material recovers by greater than 50% within the first 6 minutes at 2600°F. Since data is difficult to obtain during this crucial initial period due to transient time during cooling and heating, the 2600°F isotherm is incomplete and certainly less reliable than the 2300°F and 2000°F isotherms.

The recovery parameter (1-R) is shown as a function of (ln) recovery time and recovery temperature in Figure 33. This curve can serve as the basis of the design of the thermal mechanical processing sequence. For example, if the work hardening increment is 50,000 psi and it is desired to retain 20,000 psi or 40% (1-R = 0.4) then only 12 minutes thermal exposure at 2600°F or 120 minutes at 2300°F can be tolerated, assuming 10% cold work initially.

D. MECHANICAL PROPERTY EVALUATION

Tensile and creep rupture data were obtained on the Cb-22W-2Hf-0.06C alloy during a previous program[1]. However, these initial tests were rather limited, hence additional creep-rupture and low temperature tensile tests were conducted during the current program to confirm and extend the results of the earlier investigation.

Creep-Rupture Properties

Creep-rupture specimens, having a 0.180 inch gage diameter and a 1.5 inch gage length, were machined from swaged VAM-97 rod. The specimens were annealed 1 hour at 1800°C prior to test to provide a recrystallized structure identical to that used for the recovery studies. The creep testing procedure was the same as that described previously in Section I.C of this report. A SATEC clamp-on extensometer was used to measure creep deformation. The creep-rupture results obtained at 1095, 1205 and 1315°C (2000, 2200 and 2400°F) are shown in Figure 34 and the creep data are summarized in Table 10. The stress dependence of the secondary creep rate is illustrated in Figure 35. Also included in these figures are the initial data obtained during a previous program[1]. The earlier results were

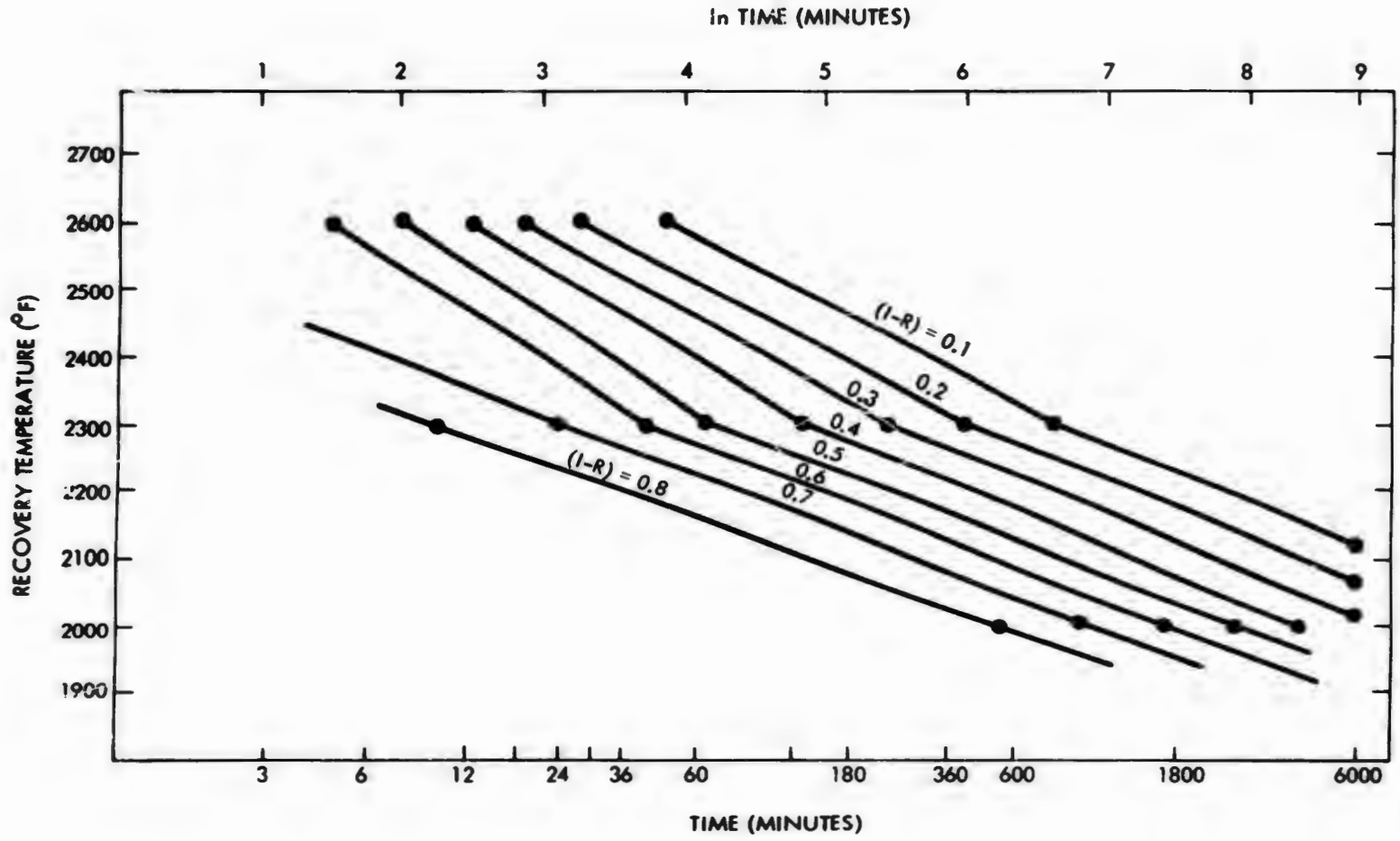

FIGURE 33 - Residual Strain Hardening (1-R) as a Function of Recovery Time and Temperature (VAM-97)

TABLE 10 - Creep-Rupture Data for VAM-97 (Cb-22W-Hf-0.06C)

Specimen No.	Test Temperature (°C)	(°F)	Stress (psi)	Rupture Time (hrs.)	Minimum Creep Rate (%/hr.)	Transition Time (hrs.)	Red. in Area (%)	Elong. (%)	Prior Treatment
VAM-97-5	1095	2000	60,000	11.7	0.156	9.4	30.5	14.7	Annealed 1 hour at 1800°C
VAM-97-6	1095	2000	50,000	49.5	0.028	33.5	32.5	13.3	Annealed 1 hour at 1800°C
VAM-97-1	1205	2200	45,000	2.5	0.727	1.9	25.4	9.3	Annealed 1 hour at 1800°C
VAM-97-2	1205	2200	40,000	7.5	0.211	5.0	25.3	9.3	Annealed 1 hour at 1800°C
VAM-97-3	1205	2200	35,000	18.8	0.090	11.9	25.3	10.7	Annealed 1 hour at 1800°C
VAM-97-4	1205	2200	30,000	58.8	0.025	30.5	24.8	10.7	Annealed 1 hour at 1800°C
VAM-97-12	1205	2200	30,000	68.5	0.026	40.5	13.2	7.3	Prestrained 9% at 870°C (1600°F) prior to test
VAM-97-9	1315	2400	30,000	3.0	0.904	1.5	28.9	16.0	Annealed 1 hour at 1800°C
VAM-97-8	1315	2400	25,000	23.3	0.185	9.6	35.1	18.7	Annealed 1 hour at 1800°C
VAM-97-7	1315	2400	20,000	143.3	0.027	28.0	59.8	34.6	Annealed 1 hour at 1800°C

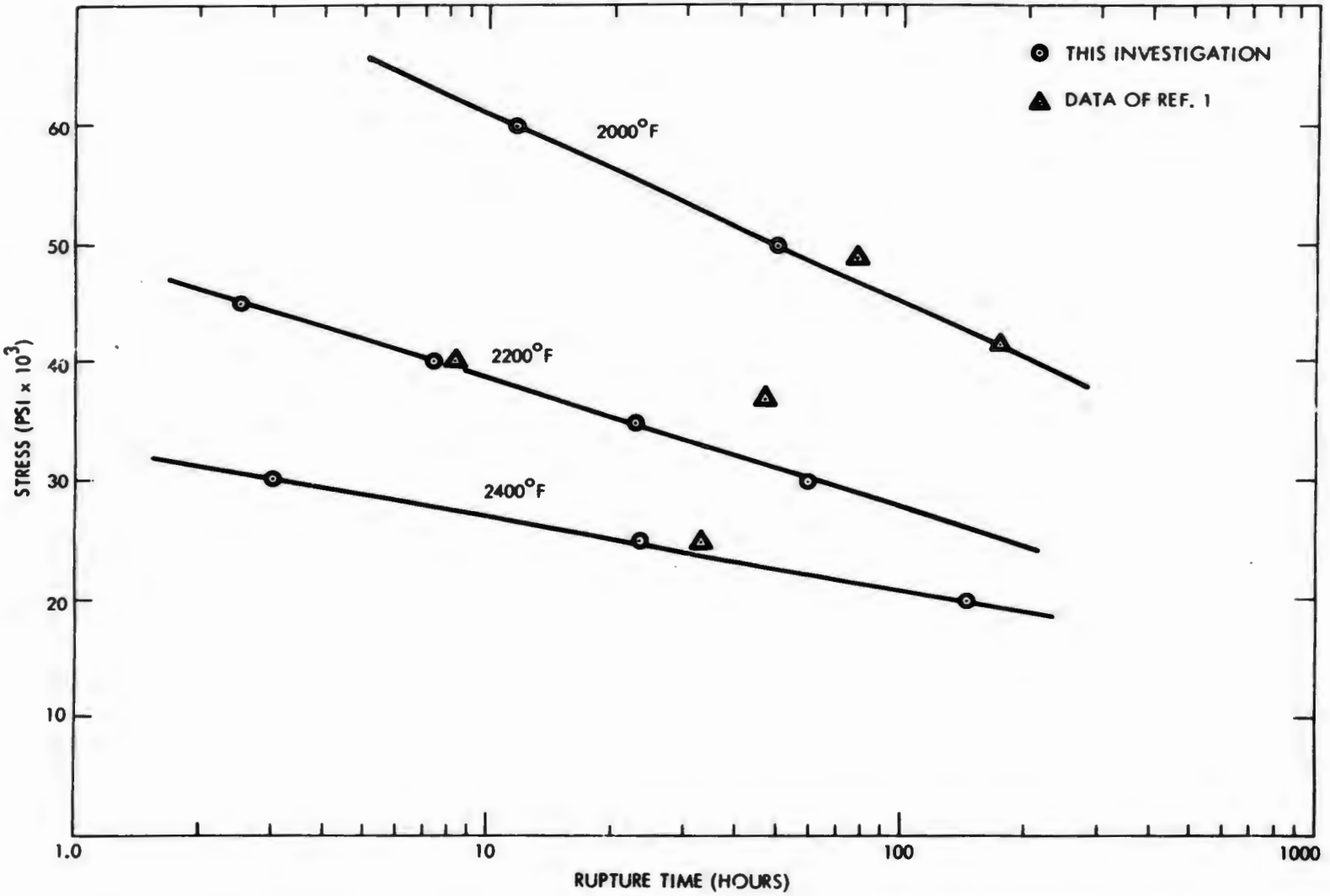

FIGURE 34 - Creep Rupture Properties of Cb-22W-2Hf-0.06C Alloy (VAM-97)

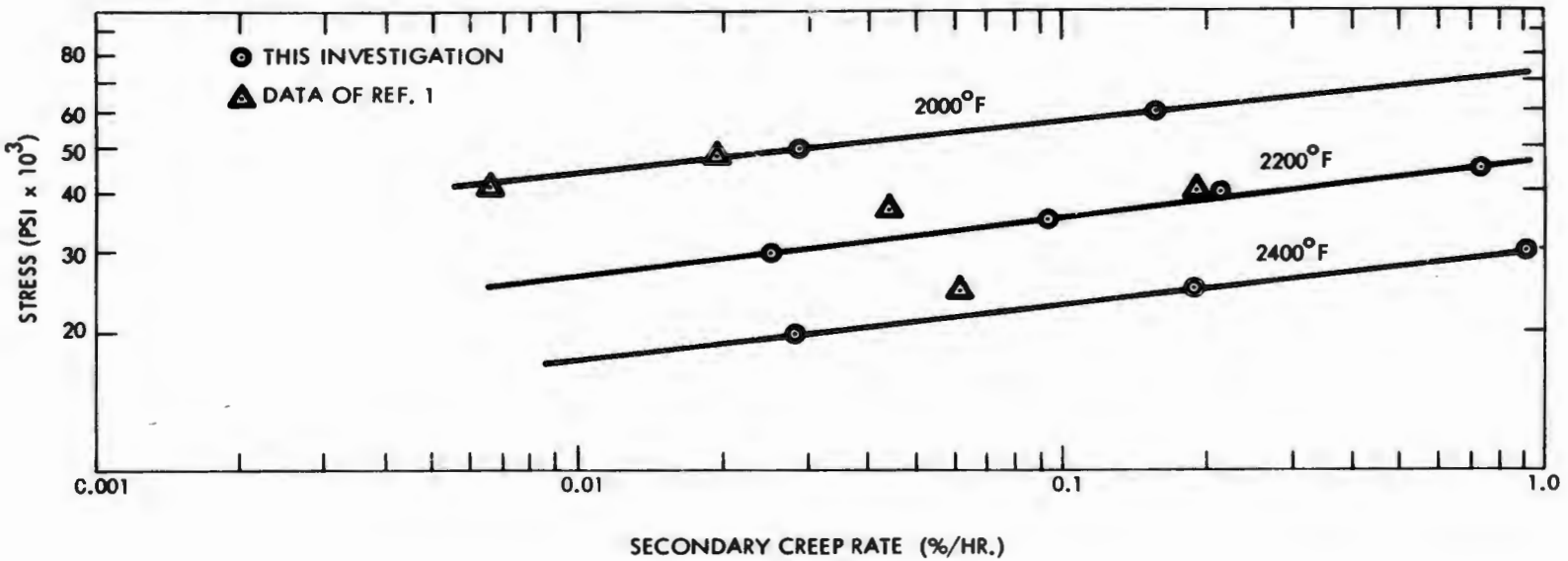

FIGURE 35 - Effect of Stress on the Secondary Creep Rate of the Cb-22W-2Hf-0.06C Alloy (VAM-97)

obtained on material annealed 2 hours at 2000°C prior to test which provided a grain size of approximately 0.2 mm, as compared to the 0.02 mm grain size of the material used in the present study. Despite the difference in pre-test thermal treatment, the agreement between the two sets of data is remarkably good. The only exception is the test conducted at 2200°F and 37,000 psi during the previous investigation. Unfortunately, this one test point indicated an erronously high 2200°F, 100 hour rupture strength for the Cb-22W-2Hf-0.06 composition. The current results indicate that the 100 hour rupture strength of B-99 at 2200°F is 28,000 psi, rather than 35,000 psi which was indicated by the limited results of the earlier study.

To evaluate the effect of intermediate temperature pre-strain on creep rupture behavior, one recrystallized (1 hour at 1800°C) VAM-97 specimen was strained 9.3% in a vacuum tensile unit at 870°C (1600°F). This specimen was then creep tested at 1205°C (2200°F) and 30,000 psi in a SATEC vacuum creep unit. The resulting creep curve is compared to that obtained for a specimen which was not pre-strained in Figure 36. The pre-strained specimen had a somewhat longer rupture life and a slightly lower rupture elongation than the non-pre-strained specimen. The secondary creep rates were virtually identical. However, the major effect of pre-straining was to reduce the primary creep strain by approximately a factor of three. This is quite significant since the relatively large amount of primary creep exhibited by columbium alloys is a matter of considerable concern in turbine applications. The data of Figure 36 indicate that small amounts of strain following a solution anneal can improve creep-rupture properties. More extensive studies are required to determine if this improvement can be realized over a wide range of temperature and stress conditions, and if it can be maintained after protective coating application thermal cycles. Earlier studies[1,2] had shown that wrought-stress relieved structures had considerably poorer creep properties than those of solution annealed material. These observations were confirmed by the results on B-88 and Cb-1 discussed in Section I of this report. However, all of the previous work was done with material which had received high (>50%) reductions prior to test. It appears that small amounts of strain following the final anneal do not degrade creep properties as do larger reductions.

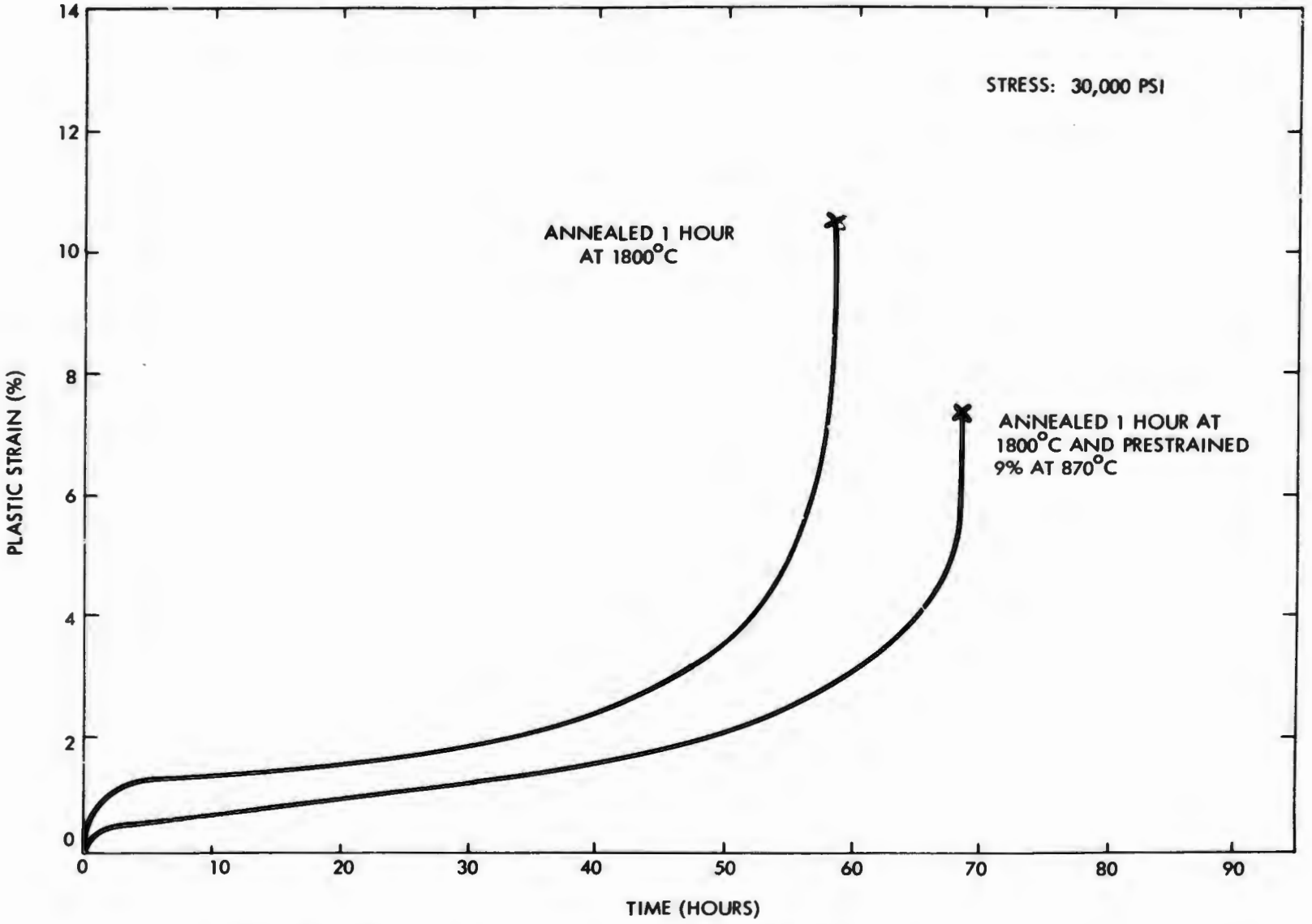

FIGURE 36-Effect of Prestrain on the 1205°C (2200°F) Creep Properties of Cb-22W-2Hf-0.06C Alloy (VAM-97)

Low Temperature Tensile Properties

Room temperature tensile tests were carried out on VAM-97 in the following conditions:

- Annealed 1 hour at 1700°C
- Annealed 1 hour at 1700°C + swaged 20% at 800°C
- Annealed 1 hour at 1800°C

The tensile results are tabulated in Table 11. The specimen annealed 1 hour at 1700°C (following extrusion and swaging at 1300°C) had 10% elongation. The reduction in area was only 8.7%, indicating that the ductile-brittle transition temperature for material in this condition is close to room temperature. The specimen cold swaged (at 800°C) following the 1700°C anneal had no room temperature ductility. Annealing 1 hour at 1800°C provided 19% elongation and 20% reduction in area. The high temperature annealed condition thus provides excellent room temperature ductility for a high strength alloy.

TABLE 11 - Room Temperature Tensile Properties of VAM-97 (Cb-22W-2Hf-0.06C)

Specimen No.	0.2% Offset Yield Strength (psi)	Ultimate Strength (psi)	Elongation (%)		Red. in Area (%)	Prior Treatment
			Uniform	Total		
VAM-97-13	93,400	116,800	9.6	9.6	8.7	Annealed 1 hour at 1700°C
VAM-97-B2-2	---	93,100*	0.0	0.0	0.0	Annealed 1 hour at 1700°C + 20% reduction at 800°C
VAM-97-14	90,300	112,900	15.4	19.5	20.0	Annealed 1 hour at 1800°C

* True fracture stress

Comparison of B-88 and B-99 Properties

The creep-rupture data for the Cb-22W-2Hf-0.06C alloy (B-99) are compared with the results obtained on B-88 in the Larsen-Miller plot of Figure 37. The two alloys are compared in similar, but not identical, structural conditions. Both alloys were given a final anneal above the carbon solvus, but the 1800°C anneal for the B-99 provided a fully recrystallized structure. The final anneal used for B-88 (1 hour at 1700°C) produced an almost completely recrystallized structure of somewhat finer grain size.[2] The data of Figure 37 show that B-88 is superior in strength at all temperatures. The density compensated 100 hour rupture strength values for the two alloys are summarized in Table 12. B-88 is clearly superior to B-99 even on a strength/density basis despite the fact that the alloys only differ to the extent of the 6 w/o higher tungsten level of B-88. This difference is greater than would be expected from solid solution strengthening assuming a linear dependence of creep strength with composition (which is probably somewhat over optimistic at this concentration range). It appears likely that the slightly higher tungsten level of B-88 not only contributes to strength in terms of its effect on the elastic modulus and diffusivity of the matrix[12] but also influences structure or structural stability. Compensating for the lower strength of B-99 is its superior low temperature ductility and somewhat better processing characteristics.

TABLE 12 - Comparison of the Creep-Rupture Properties of B-88 and B-99

Temperature (°C)	Temperature (°F)	B-88* 100 hour rupture str. (psi)	B-88* Stress/Density** (inches)	B-99 100 hour rupture str. (psi)	B-99 Stress/Density (inches)
1095	2000	56,000	150,000	45,000	126,000
1205	2200	36,000	96,500	28,000	78,600
1315	2400	25,500	68,500	21,000	59,000

* From Reference 2

** Density of B-88 - 0.373 lbs/in^3
Density of B-99 - 0.352 lbs/in^3

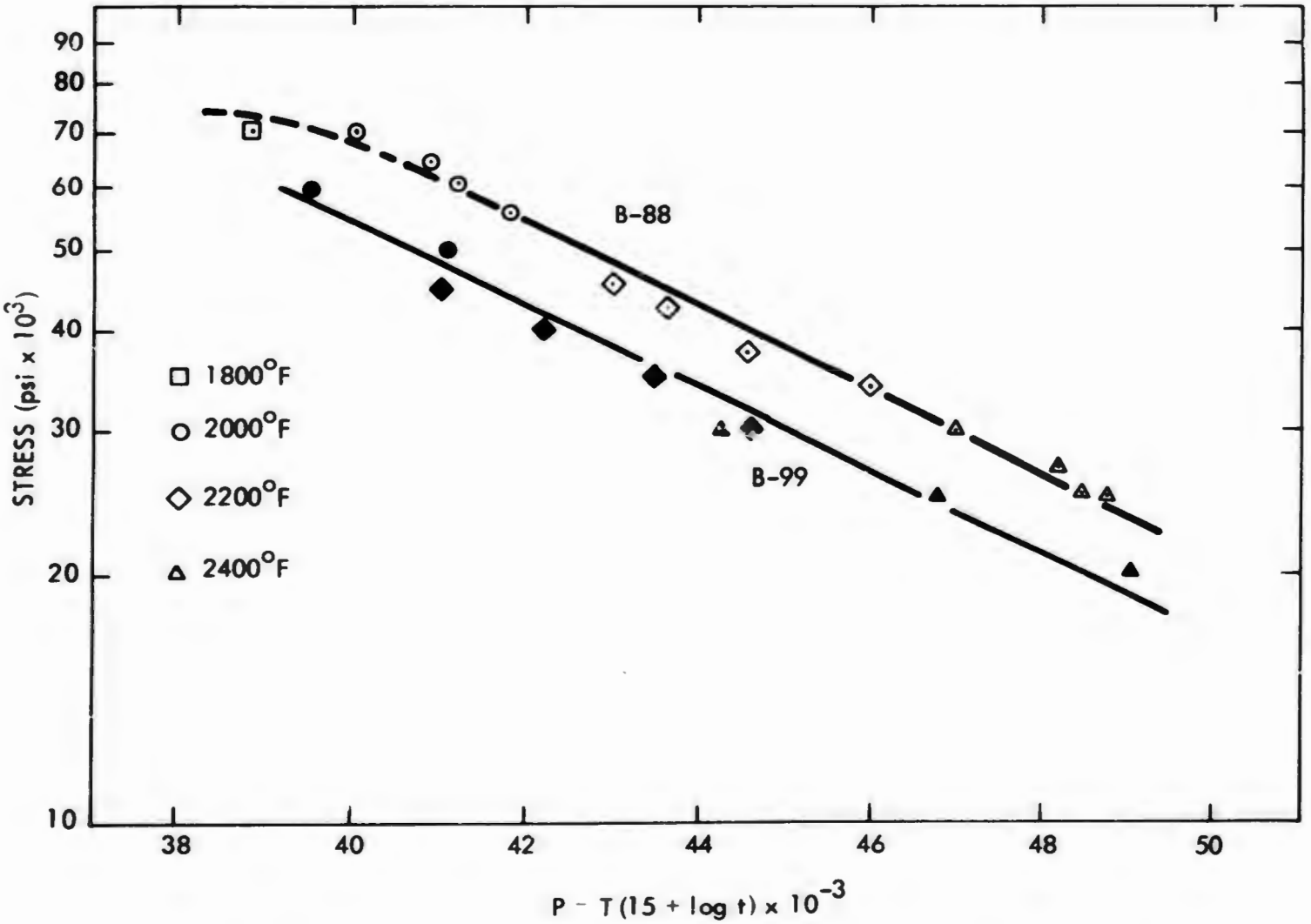

FIGURE 37 - Larson-Miller Plot of Creep Rupture Strength of B-88 and B-99

IV. AGING RESPONSE OF A Cb-W-Hf-C-N ALLOY

The second approach to the problem of increasing intermediate temperature (1200 - 1600°F) yield strength in creep resistant columbium alloys was to explore the potential of precipitation hardening. Earlier studies by Begley, Godshall and Stickler[6] had shown pronounced aging response in a Cb-Hf-N alloy arising from the precipitation of a fine HfN phase. Similar aging response was also observed in Cb-Zr-N and Cb-W-Hf-N alloys[13,14] containing 700 to 1500 ppm nitrogen. Similar hardening of tantalum alloys arising from the precipitation of HfN and ZrN has been reported by Buckman and Goodspeed.[15]

Chang[3] reported aging response in the Cb-1 alloy (Cb-30W-1Zr-0.06C) which contained a nitrogen impurity level of 440 ppm. Chang's data showed a significant hardness peak in material which had been solution annealed and aged 1 hour at 1095°C (2000°F). This aging response was confirmed in the course of the present investigation, as described in Section I of this report. The current study showed that as little as 315 ppm nitrogen added to the Cb-1 alloy produces pronounced aging effects that cannot be attributed to carbon alone.

Although the precipitation hardening behavior of columbium alloys containing nitrogen in combination with a reactive element has been known for some time, relatively little work has been done to exploit alloys of this type because the nitride precipitate overages rapidly at temperatures above approximately 1000°C. Thus the potential of nitride precipitation strengthening for high temperature creep resistant alloys appeared to be limited unless overaging kinetics could be significantly altered.

The objective of this portion of the current investigation was to further explore nitride (or carbonitride) precipitation effects to determine if improvements in intermediate temperature yield strength could be realized by this approach.

A. MATERIAL PROCESSING

A Cb-22W-2Hf-0.05C-0.04N alloy (heat VAM-98) was prepared in the same manner as that used for the nitrogen free B-99 alloy described in Section IIIA of this report. Nitrogen was added to the electrode as nitrided columbium sheet. A 10.2 inch long ingot 2.63 inches in diameter and weighing 19.7 lbs. was prepared by double vacuum arc melting. Chemical analysis data for the as-cast ingot is listed in Table 13. The base material (Cb-10W) used to prepare the electrode contained 95 ppm nitrogen. In addition, the equivalent of 670 ppm was added to the electrode as nitrided columbium sheet which is 35% in excess of the desired nominal composition. The final chemical analysis of Table 13 shows that about 440 ppm nitrogen was retained where 500 ppm was the target composition indicating a significant nitrogen loss during melting which must be compensated for in the initial electrode. An additional nitrogen analysis was performed on as-extruded material to evaluate the possibility of nitrogen loss during high temperature processing. The data of Table 13 show good agreement between as-cast and as-extruded material.

The as-cast ingot was machined to 2.55 inch diameter; cut in half and fitted into molybdenum extrusion jackets. The billets were extruded at 3200°F and a 5:1 extrusion ratio. The extrusion data are summarized in Table 14. The extrusions were conditioned and then swaged to 0.70 inch diameter at 1200°C. Although the resultant material was sound, the alloy worked with considerable difficulty. The swaged bar was centerless ground and then annealed 1 hour at 1500°C. The bar was then swaged to final size (0.44 inch diameter) at 1300°C.

TABLE 13 - Chemical Analyses of VAM-98

Heat No.	Nominal Composition	Composition (w/o)				
		W	Hf	C	N	O
VAM-98	Cb-22W-2Hf-0.05C-0.05N					
Ingot Top		21.4	1.9	0.046	0.049	0.0079
Ingot Bottom		20.3	1.7	0.052	0.040	0.0060
Extrusion						
Bottom (Tail Section)					0.047	
Top (Tail Section)					0.040	

TABLE 14 - Extrusion Data for VAM-98

Extrusion Parameter	Cb-22W-2Hf-0.05C-0.05N	
	Ingot Bottom	Ingot Top
Extrusion No.	2777	2776
Ingot Wt.	9.0 lbs.	9.16 lbs.
Length	5.0 in.	5.0 in.
Dia.	2.55 in.	2.55 in.
Billet Wt.	14.2 lbs.	14.2 lbs.
Length	6.0 in.	6.0 in.
Dia.	2.95 in.	2.95 in.
Billet Heating (Induction)	23 min.	23 min.
Time at Temp.	5 min.	5 min.
Temperature	3200°F	3200°F
Ram Speed Maximum	2.5 ips	5.0 ips
Minimum	2.0 ips	4.5 ips
Load Maximum (Breakthrough)	99 ksi	113 ksi
Load Minimum (Running)	88 ksi	90 ksi
Extrusion Constant (Total)	55.4 ksi	55.1 ksi
Reduction Ratio	4.9:1	5.1:1

Lubricant
Billet: DC7740
Container: MoS_2
Die: MoS_2

Container
Size: 3.072 in.
Temp.: 800°C
Die: 90°
ZrO_2 Faced 800°F Preheat
Jacket: Molybdenum

B. RESPONSE TO THERMAL TREATMENT

To determine the response of the nitrogen containing alloy (VAM-98) to thermal treatment, specimens were given a series of isochronal and isothermal anneals and changes in structure were followed by hardness measurements and metallographic examination.

Isochronal Annealing Studies

As-swaged sections of the alloy bar were conditioned and then given a series of 1 hour anneals at temperatures ranging from 1400 to 2000°C. Hardness data as a function of annealing temperature are shown in Figure 38. The hardness varied from a minimum of 270 VPN at 1400°C to 320 VPN after annealing 1 hour at 1800°C. The peak in hardness after annealing at 1800°C indicates that the carbon and nitrogen solvus had been exceeded. The hardness decreased slightly after annealing at temperatures greater than 1800°C. This indicated that some nitrogen may have been lost during the higher temperature anneals. In the as-swaged condition VAM-98 contained 400 ppm nitrogen. An analysis of a specimen after heating 1 hour at 2000°C in a dynamic vacuum of 5×10^{-6} torr showed a decrease to 310 ppm nitrogen, indicating that extended annealing at high temperatures in vacuo can result in serious nitrogen depletion. This observation is consistent with the data of Inouye[16] who predicts a nitrogen partial pressure of approximately 5×10^{-9} torr over Cb-1%Zr at 2000°C.

The microstructures associated with the hardness data of Figure 38 are shown in Figure 39. Some grain boundary migration was observed after a 1 hour exposure at 1500°C (Figure 39b). Partial recrystallization and substructure formation begins at 1600°C as shown in Figure 39c. The microstructure shown in Figure 39d for VAM-98 annealed 1 hour at 1700°C is very similar to the structure developed in B-88 (Cb-28W-2Hf-0.067C) and B-99 (Cb-22W-2Hf-0.06C) after the same thermal-mechanical treatment. A heat treatment of 1 hour at 1800°C and above results in complete equiaxed recrystallization with large zeta carbide platelets uniformly distributed throughout the matrix.

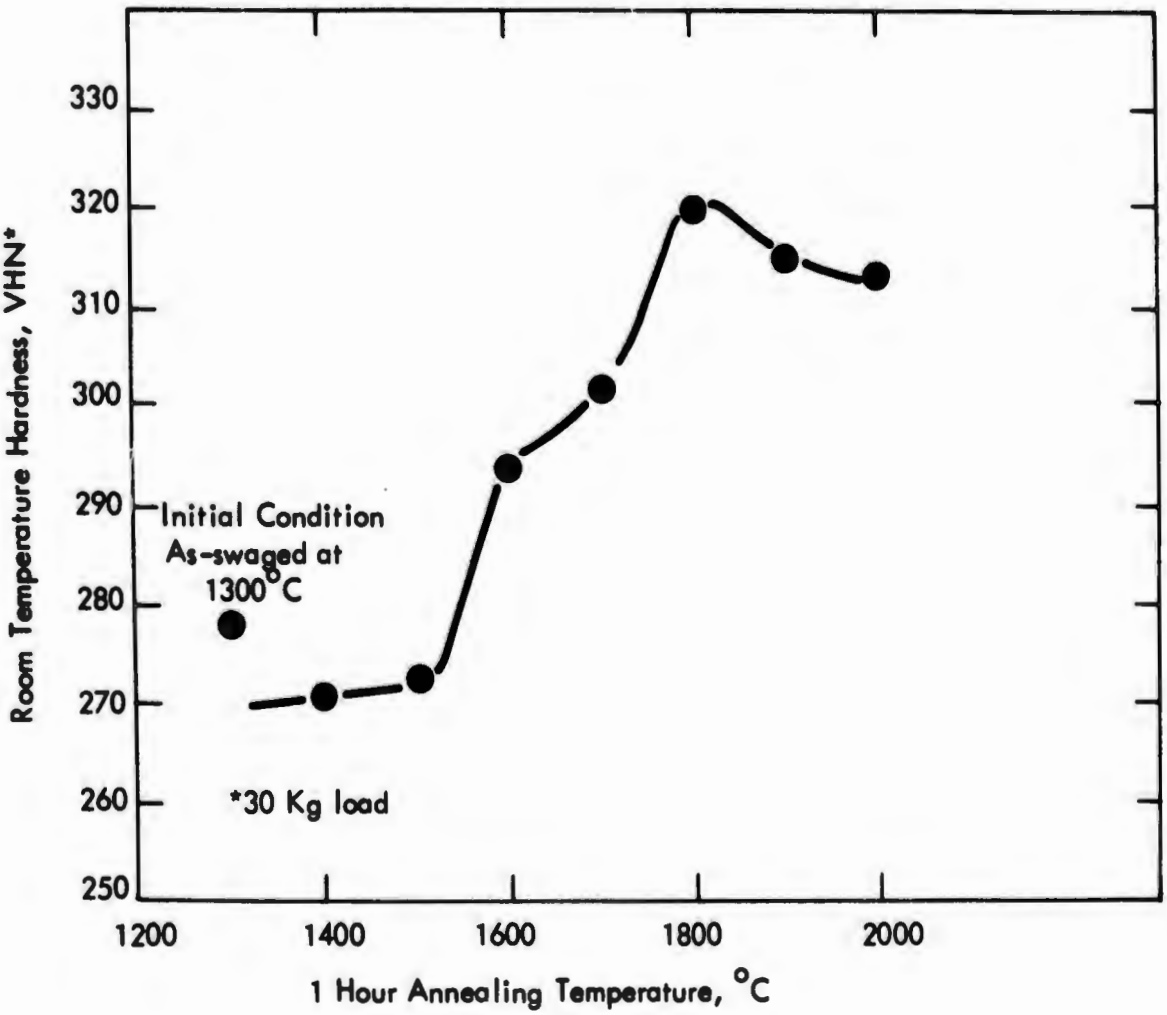

FIGURE 38 - Effect of 1 Hour Annealing Temperature on the Hardness of VAM-98 (Cb-22W-2Hf-0.05C-0.04N)

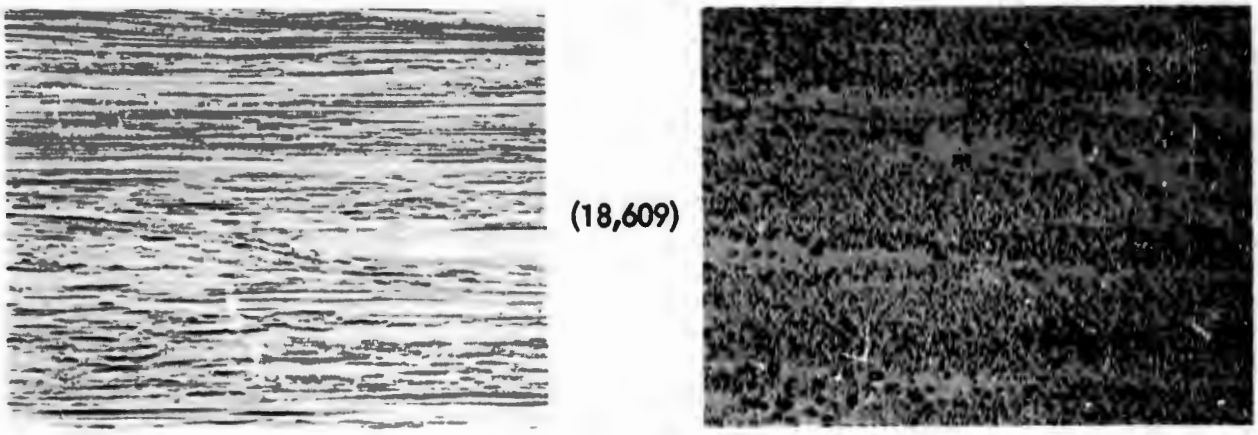

(18,609)

(a) 1500X

1 Hr. at 1400°C

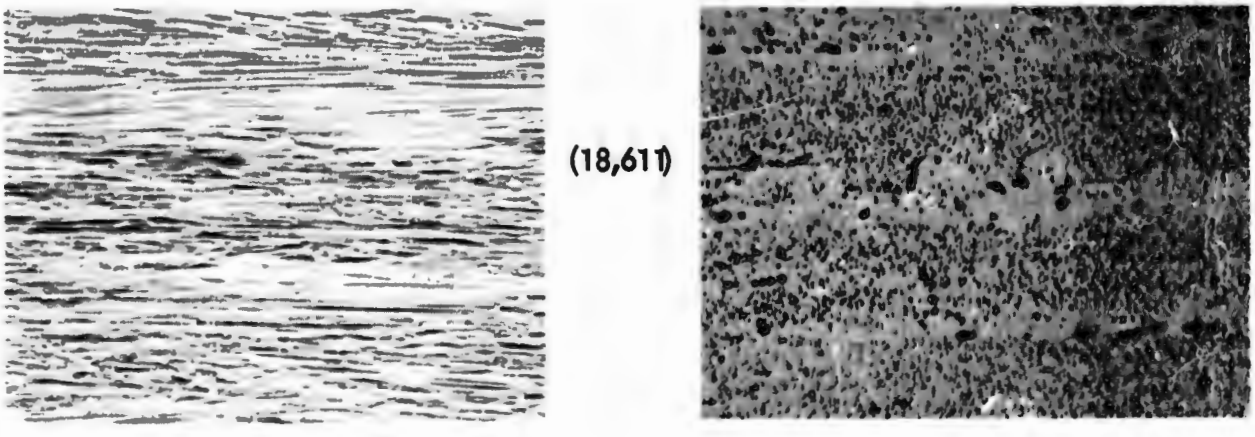

(18,611)

(b) 1500X

1 Hr. at 1500°C

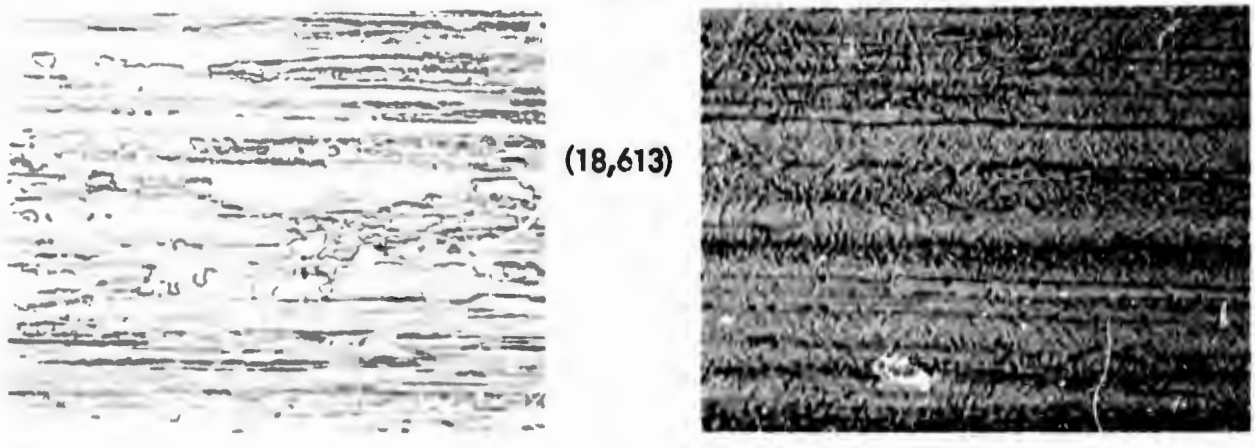

(18,613)

(c) 1500X

1 Hr. at 1600°C

FIGURE 39 - Microstructure of VAM-98 (Cb-22W-2Hf-0.05C-0.04N) As-Swaged at 1300°C Plus 1 Hour Heat Treatments at Indicated Temperature

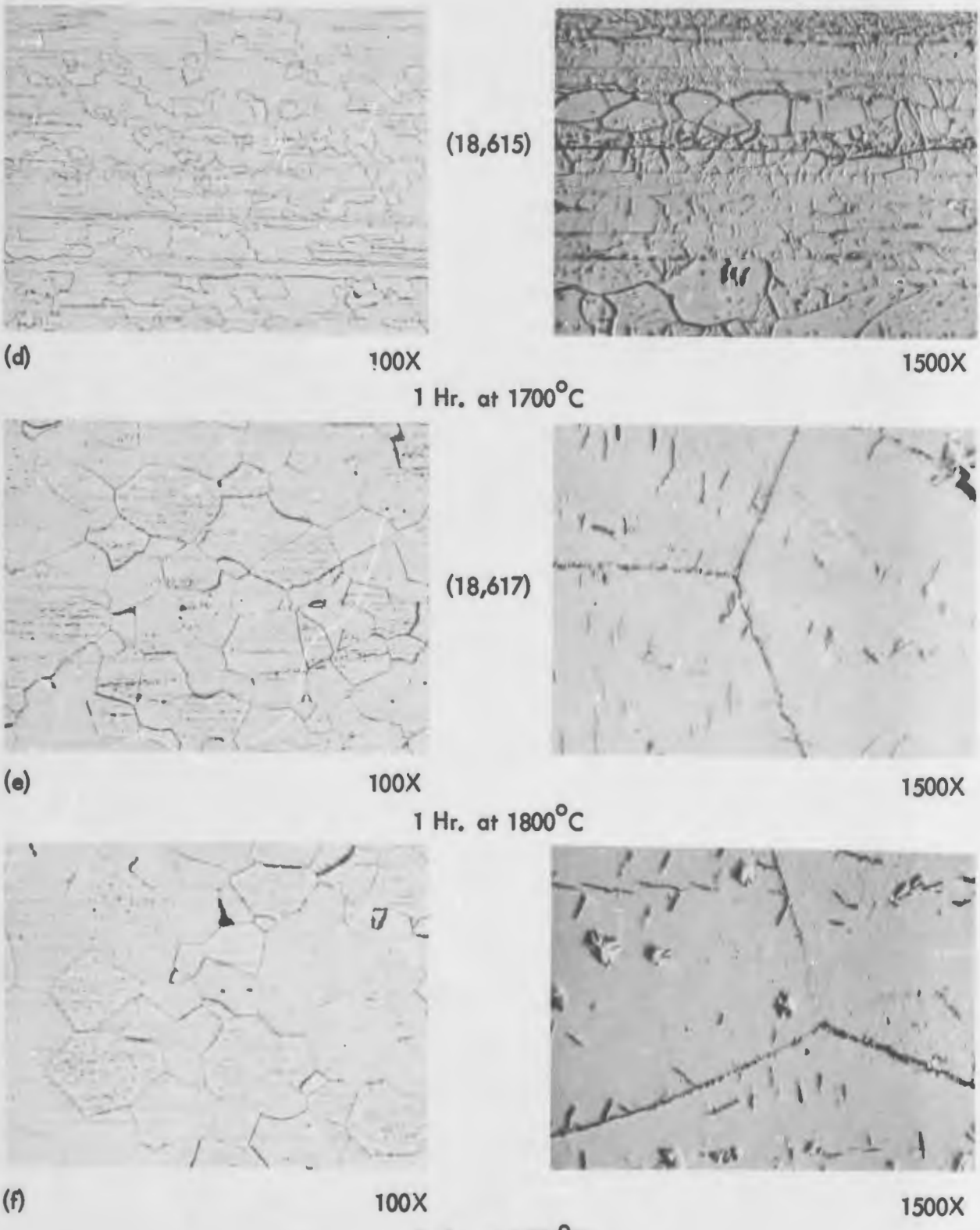

(d) 100X (18,615) 1500X

1 Hr. at 1700°C

(e) 100X (18,617) 1500X

1 Hr. at 1800°C

(f) 100X 1500X

1 Hr. at 1900°C

FIGURE 39 (Continued) - Microstructure of VAM-98 (Cb-22W-2Hf-0.05C-0.04N) As-Swaged at 1300°C Plus 1 Hr. at Indicated Temperature

A preliminary aging study was conducted on the Cb-22W-2Hf-0.05C-0.04N alloy in the solution annealed condition (1 hour at 2000°C + He cooled). To increase the cooling rate following the solution anneal high purity helium was admitted to the furnace chamber.

One hour aging treatments were conducted on the solution annealed material over the temperature range 800°C to 1700°C. The hardness data are plotted in Figure 40. A hardness minimum of 280 VHN was observed at 1500°C and an aging peak of 325 VHN occurred at 1100°C. Photomicrographs of the solutioned and solutioned plus aged specimen are shown in Figure 41. The as-solution annealed structure, Figure 41a, is similar to the material described in Figure 39f. Aging at 1700°C produces no real change in precipitate morphology (Figure 41b). The 1 hour at 1600°C age (Figure 41c) results in a breakup in the zeta platelets present in the as-solutioned material and a uniform dispersion of apparently equiaxed precipitates. The microstructure associated with the 1500°C anneal is shown in Figure 41d. The material shows progressively finer precipitation of the nitrides or carbonitrides within the matrix as the temperature is lowered from 1400°C to 1200°C (Figures 41e through 41g). The optical microstructure at the 1100°C aging peak and at lower aging temperatures (Figures 41h and 41i) are nearly identical in appearance to the as-solution annealed specimen (Figure 41a).

Previous studies[14] indicated that cooling rates from the solution heat treat conditions may have an important effect on the aging response of nitrogen containing columbium alloys. This was verified by an experiment in which the VAM-98 alloy was solutioned 1 hour at 1800°C and quenched. The specimen was suspended in an evacuated quartz capsule and induction heated. After solutioning, the capsule was broken and the specimen was quenched in a water bath. Although cooling was rapid, some zeta precipitation occurred during cooling as shown in Figure 42a. The specimens of the quenched material were given conventional 1 hour ages at temperatures ranging from 900 to 1400°C. Resulting hardness values are compared to the conventionally solutioned material (solutioned plus He cooled) in Figure 40. The general hardness level of water quenched plus aged material is significantly

higher than the conventionally annealed material. Some of the difference may result from the 90 ppm nitrogen loss in the 2000°C solution heat treatment of the conventional material (lower curve) discussed earlier. The as-solution annealed hardness data are summarized below.

Condition	VHN(30 Kg Load)
As-swaged + 1 Hour at 2000°C + He Cooled	313
As-swaged + 1 Hour at 1800°C + He Cooled	334
As-swaged + 1 Hour at 1800°C + Water Quench	366

A hardness difference of 20 VHN may be accounted for by loss of nitrogen when comparing 1800°C to 2000°C solutioning temperatures. However, the 32 VHN increment of the specimen water quenched from the 1800°C solutioning temperature over the slower He cooled specimen can be considered to be due to interstitials and possibly to vacancies retained in solid solution during quenching.

Microstructures associated with the hardness data from the water quenched plus aged material are shown in Figures 42a through 42i. The structures are similar to those shown in Figure 41 for the He cooled material with the exception that a finely dispersed phase was observed in the matrix of the 1000°C aged specimen (Figure 42). The kinetics of precipitation may be sufficiently rapid in the water quenched material to allow the finely dispersed precipitates to form at lower temperatures.

Isothermal Aging Studies

To provide a more complete description of the aging response of the Cb-22W-2Hf-0.05C-0.04N alloy isothermal aging studies were carried out over the temperature range from 1000 to 1500°C. Sections of as-swaged rod, 0.4 inch in diameter were cut into 1/8 inch thick discs and solution annealed 1 hour at 1800°C. Approximately 1/3 atmosphere of high

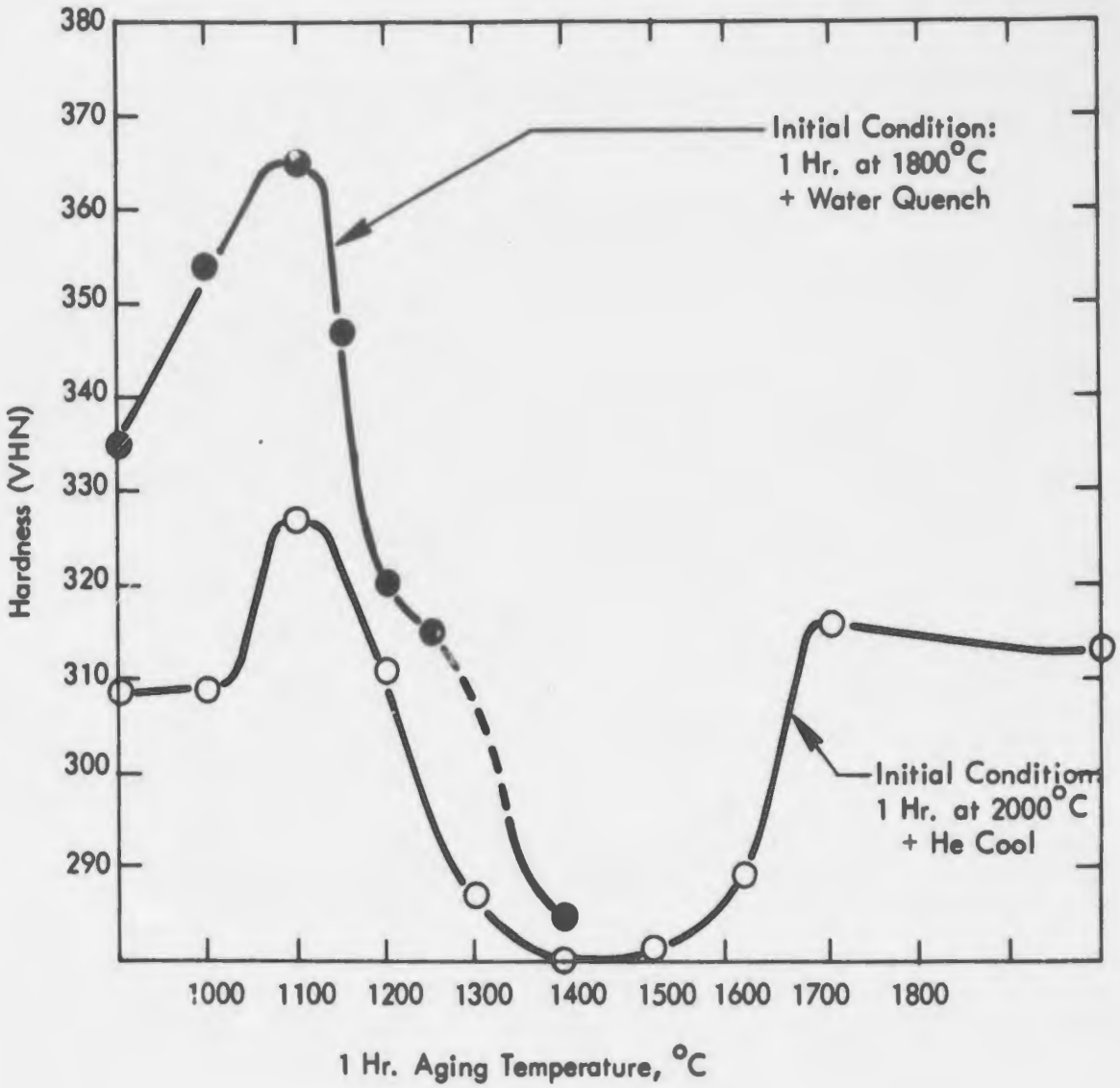

FIGURE 40 - Effect of Aging Temperature on the Room Temperature Hardness of VAM-98 (Cb-22W-2Hf-0.05C-0.04N) in the Solution Heat Treated Condition

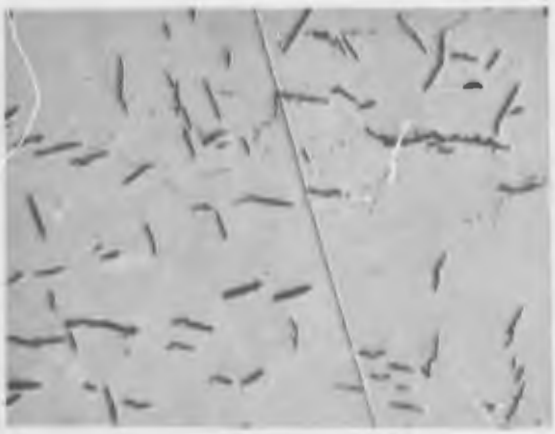

(a) (18,700)
As Solution Heat Treated at 2000°C

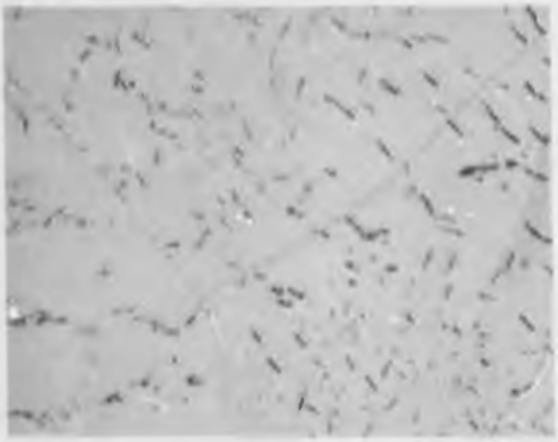

(b) (18,702)
Solution Heat Treated + 1 Hr. at 1700°C

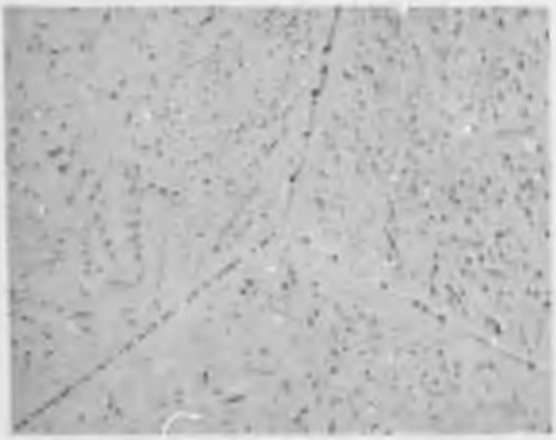

(c) (18,703)
Solution Heat Treated + 1 Hr. at 1600°C

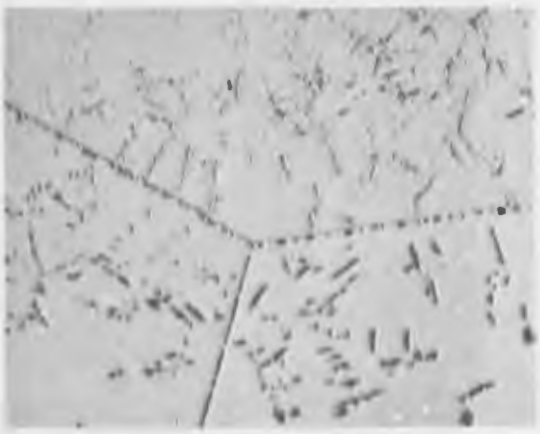

(d) (18,704)
Solution Heat Treated + 1 Hr. at 1500°C

(e) (18,705)
Solution Heat Treated + 1 Hr. at 1400°C

(f) (18,707)
Solution Heat Treated + 1 Hr. at 1300°C

FIGURE 41 - Microstructure of VAM-98 (Cb-22W-2Hf-0.05C-0.04N) Solution Annealed 1 Hour at 2000°C, then Aged 1 Hour at Indicated Temperature

(g) (18,708)

Solution Heat Treated + 1 Hr. at 1200°C

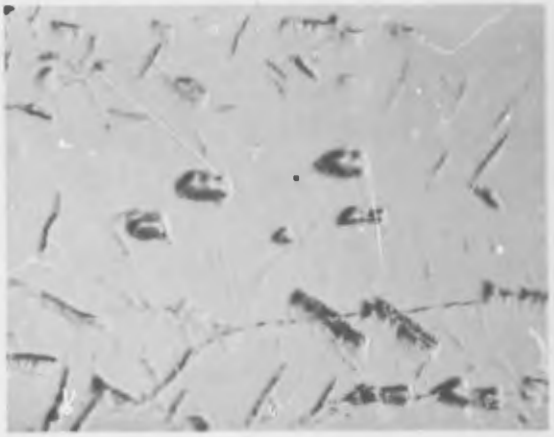

(h) (18,709)

Solution Heat Treated + 1 Hr. at 1100°C

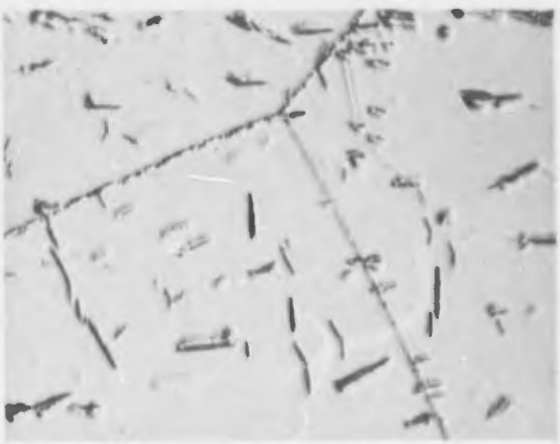

(i) (16,710)

Solution Heat Treated + 1 Hr. at 1000°C

FIGURE 41 (continued) - Microstructure of VAM-98 (Cb-22W-2Hf-0.05C-0.04N) Solution Annealed 1 Hour at 2000°C plus Aged at Indicated Temperature 1500X

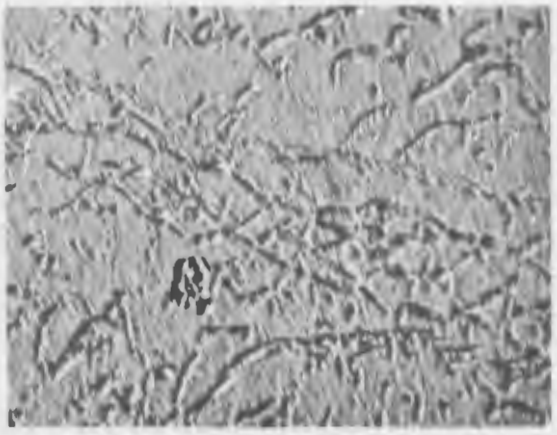

(a) (18,829)

Solution Heat Treated 1 Hr. at 1800°C + Water Quench

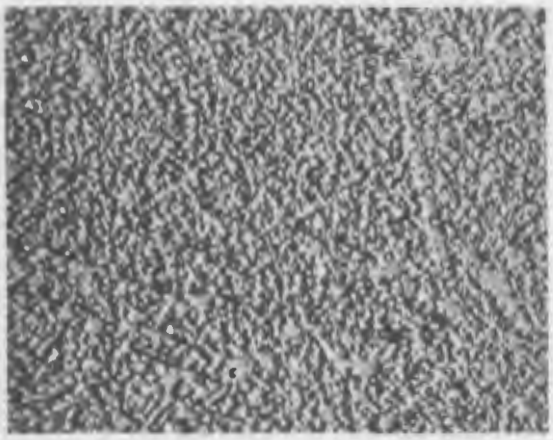

(b) (18,829)

Age 1 Hr. at 1400°C

(d) (18,831)

Age 1 Hr. at 1250°C

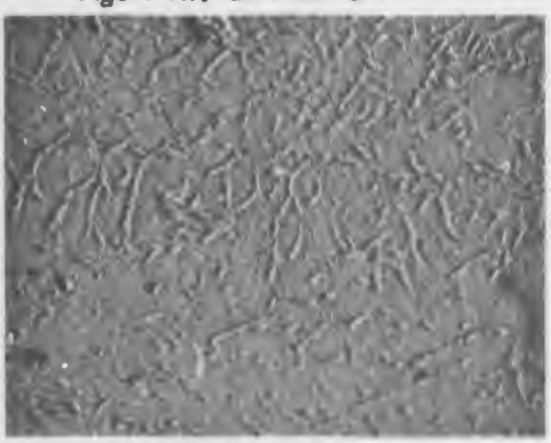

(c) (18,830)

Age 1 Hr. at 1300°C

(e) (18,832)

Age 1 Hr. at 1200°C

FIGURE 42 - Microstructure of VAM-98 (Cb-22W-2Hf-0.05C-0.04N) Solution Annealed 1 Hour at 1800°C, Water Quenched, then Aged 1 Hour at Indicated Temperature 1500X

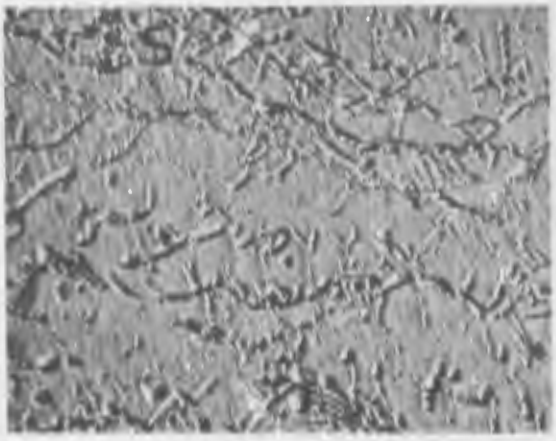

(e) (18,829)
As Solution Heat Treated at 1800°C + Water Quenched

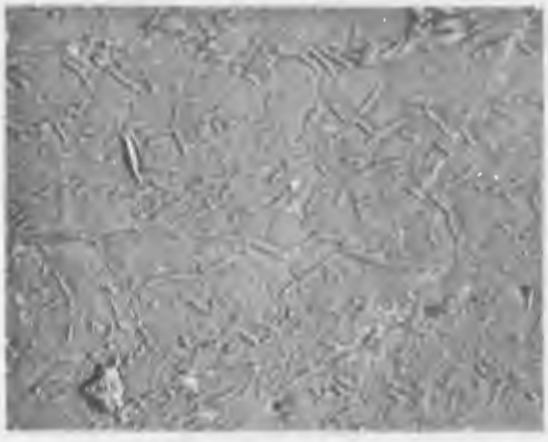

(f) (18,833)
Aged 1 Hr. at 1150°C

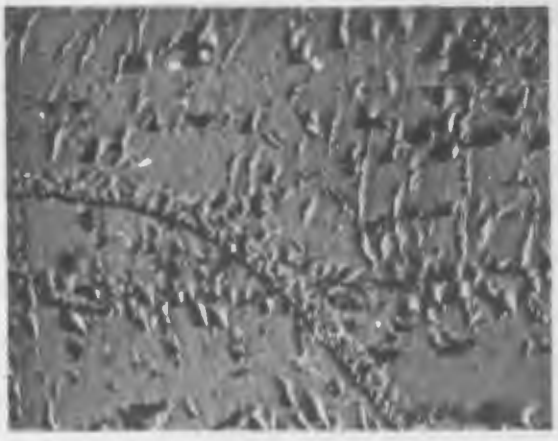

(h) (18,835)
Aged 1 Hr. at 1000°C

(g) (18,834)
Aged 1 Hr. at 1100°C

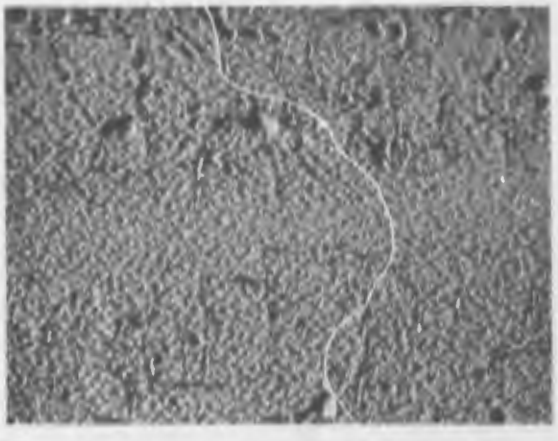

(i) (18,835)
Aged 1 Hr. at 1000°C

FIGURE 42 (Continued) - Microstructure of VAM-98 (Cb-22W-2Hf-0.05C-0.04N) Solution Annealed 1 Hour at 1800°C, Water Quenched, then Aged 1 Hour at Indicated Temperature 1500X

purity helium was admitted to the furnace at the termination of the solution anneal to increase the cooling rate. The time to cool below 1000°C was approximately 45 seconds. The solution annealed samples were then aged for various times and temperatures and the resulting hardness data are summarized in Figure 43. The most unusual aspect of the hardness curves is the presence of two pronounced aging peaks separated by a hardness minimum. An initial softening was noted in the 1500°C and the 1000°C isotherm as well as in the 1050°C and 1150°C isotherms which are not shown in Figure 43.

The first aging peak, designated peak "a" was observed after 4 hours at 1100°C at a hardness level of 390 VPN. The hardness curve of the 1100°C isotherm drops rapidly to a hardness of 276 VPN after 7 hours at 1100°C, followed by a very rapid rise to a hardness of 360 VPN after an 11 hour age (designated peak "b"). An identical trend was noted in the 1000°C isotherm where peak "a" occurred in approximately 16 hours, reaching a hardness of 409 VPN. The hardness minimum was 280 VPN in approximately 40 hours. Peak "b" occurred at ~100 hours, 370 VPN. Thus, from Figure 43 it can be seen that drastic changes in hardness can occur over relatively short time periods. For this reason the peaks were missed at the 1050°C, 1150°C and 1200°C isotherms because aging times were not properly selected. These data are remarkably similar to the aging curves for Cb-1 (Cb-30W-1Zr-0.06C-0.044N) reported by Chang[3] in his Figure 10. Chang showed aging peaks at the 1100°C isotherm at approximately 1 hour (peak "a") and at 10 hours (peak "b").

Since the precipitation (or pre-precipitation) reactions which lead to hardness peaks are thermally activated and the rate of formation is proportional to 1/t (reciprocal time), activation energies can be obtained by plotting the available $1/t_p$ data versus $1/T°K$ as shown in Figure 44. Such a plot yielded an activation energy for formation of the "a" peak of 57 ± 8 Kcal. This compares with 55 Kcal obtained from Chang's[3] data on Cb-1. The activation energy for formation of the "b" peak is 73 ± 8 Kcal. These data were used to predict the peak times for the 1200°C isotherm and the resultant extrapolated curve through the available data and calculated peaks are shown in Figure 43. Peaks "a" and "b" at

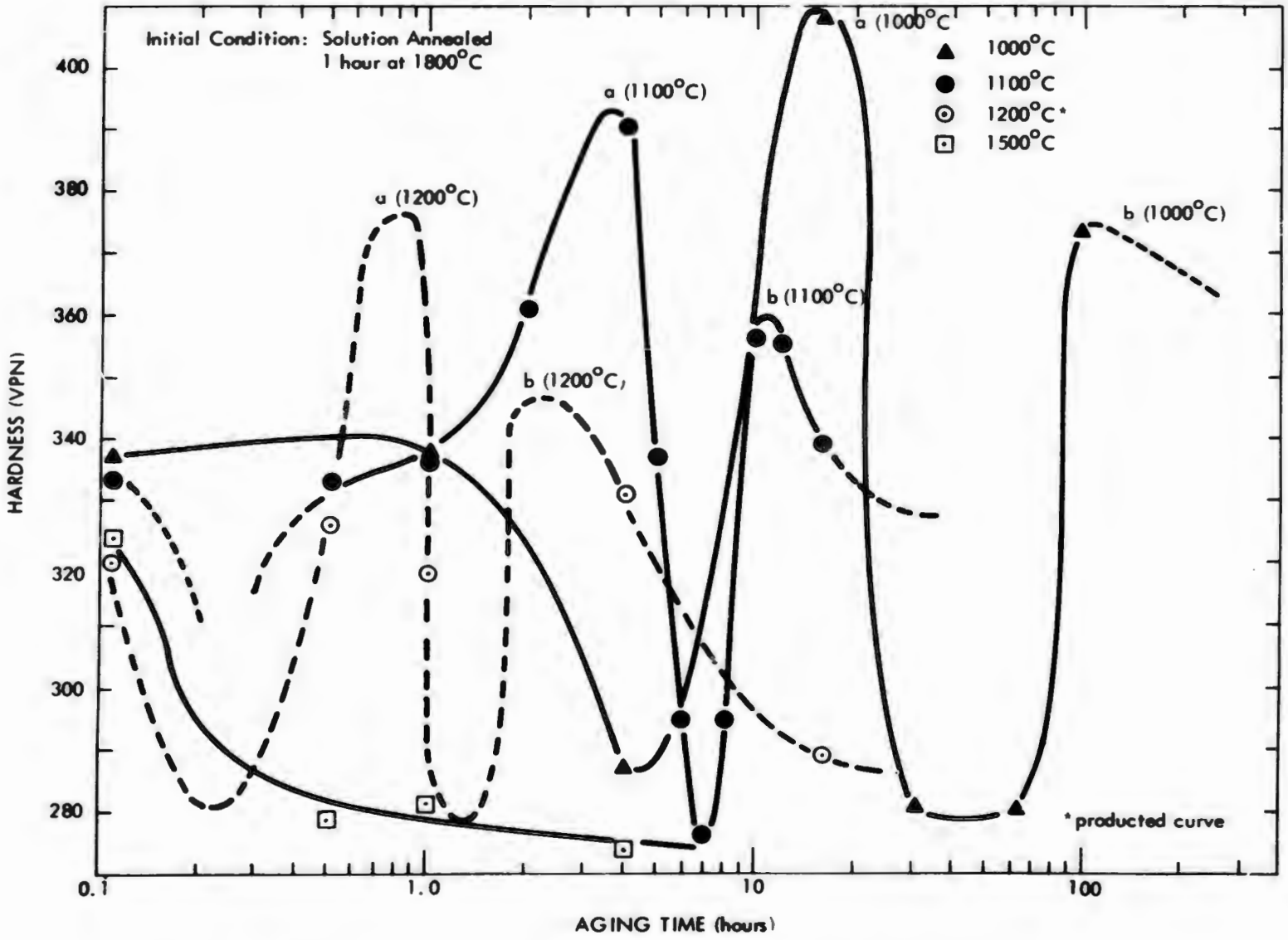

FIGURE 43 - Effect of Aging Time on the Hardness of VAM-98 (Cb-22W-2Hf-0.05C-0.04N)

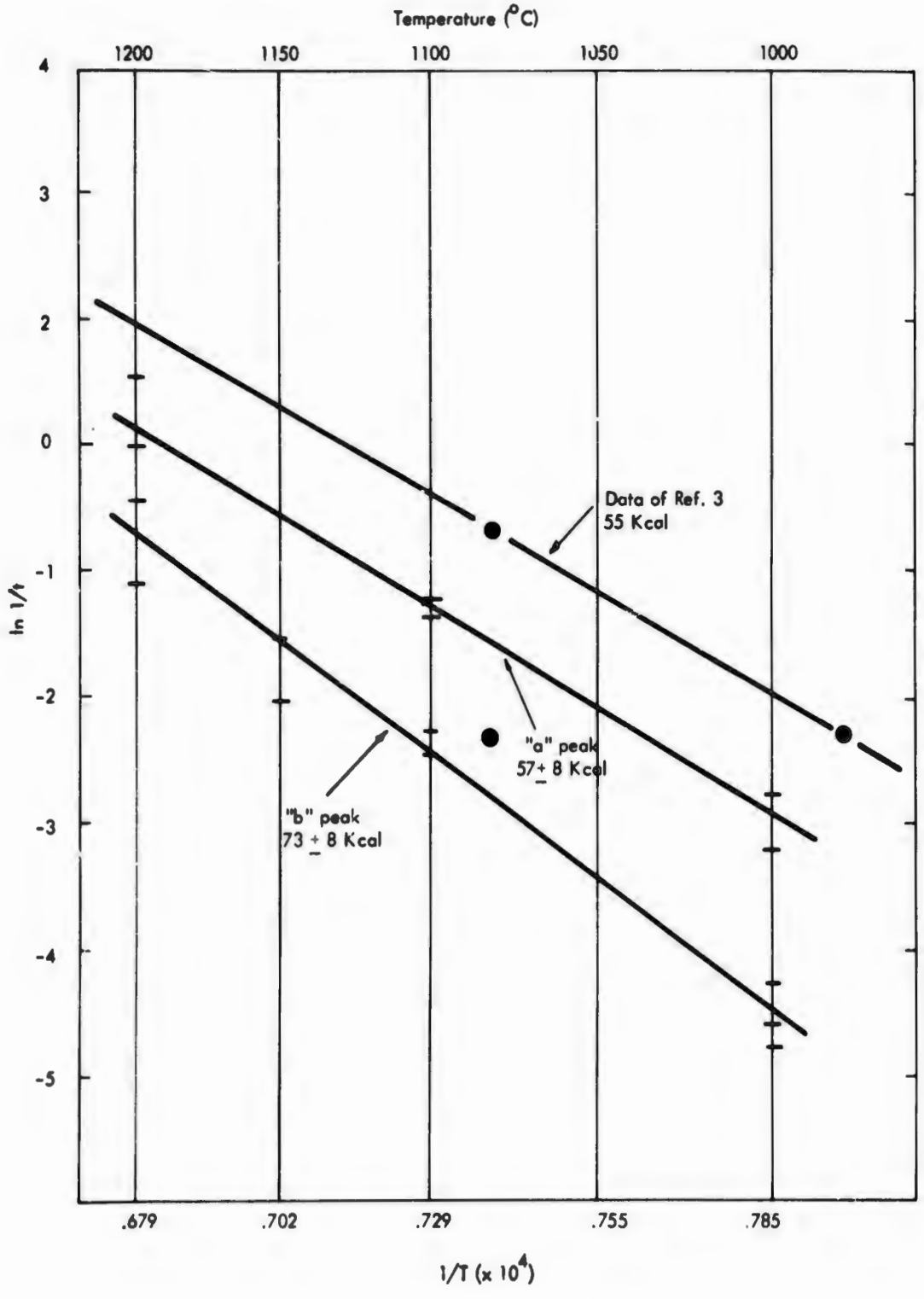

FIGURE 44 - Arrhenius Plot of Aging Data for VAM-98 (Cb-22W-2Hf-0.05C-0.04N)

1200°C should occur at about 0.8 hours and 0.2 hours. Confirmation of the existence of the peaks at 1200°C was not attempted during the present program.

A metallographic study including optical and transmission electron microscopy (TEM) was made to better characterize the aged microstructure. This study was conducted on samples aged at 1100°C.

The optical photomicrographs are shown in Figures 45 through 51. Figure 45 shows the as-solution annealed (1 hour at 1800°C) microstructure. The material is characterized by zeta carbide platelets, some substructure formation and a grain boundary film (Figure 46). The 2 hour aging treatment has caused considerable change in the structure with the appearance of a very fine background surface roughness which cannot be resolved optically. The larger platelets have not been drastically altered, however. The 4 hour aged material representing peak "a" is shown in Figure 47. Again the mottled background is apparent. This mottling may actually be an artifact since the etchant (H_2O, HNO_3 and HF) attacks nitride precipitates. The platelets seem to have taken on a more crystallographic relationship to the matrix with a substructure made up of regular polyhedra formed by the platelets. The structure associated with the interpeak valley are shown in Figures 48, 49 and 50 for the 6, 7 and 8 hour aging anneals, respectively.

The platelet formed substructure is very well developed in the material in these conditions. The mottled background has completely disappeared with the exception of a better developed substructure and platelet array. This material associated with the overaging (interpeak) valley is indistinguishable from the as-solutioned material. Figure 51 shows the optical microstructure of the material slightly over the aging peak (peak "b"). The background is again mottled and with the exception of the beginning of deterioration of the platelet and substructure array, the material is optically indistinguishable from the "a" peak material in Figure 47.

1500X

FIGURE 45. Microstructure of VAM-98 (Cb-22W-2Hf-0.05C-0.04N) Solution annealed 1 hour at 1800°C and helium cooled.

1500X

FIGURE 46. Microstructure of VAM-98 (Cb-22W-2Hf-0.05C-0.04N) Solution annealed 1 hour at 1800°C and helium cooled plus aged 2 hours at 1100°C.

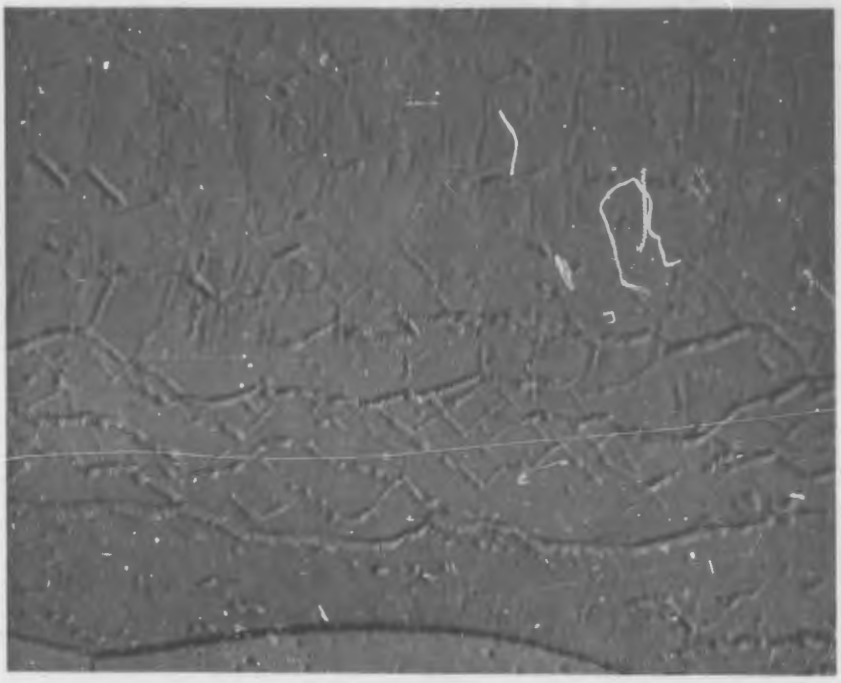

1500X

FIGURE 47. Microstructure of VAM-98 (Cb-22W-2Hf-0.05C-0.04N) Solution annealed 1 hour at 1800°C and helium cooled plus aged 4 hours at 1100°C ("a" aging peak).

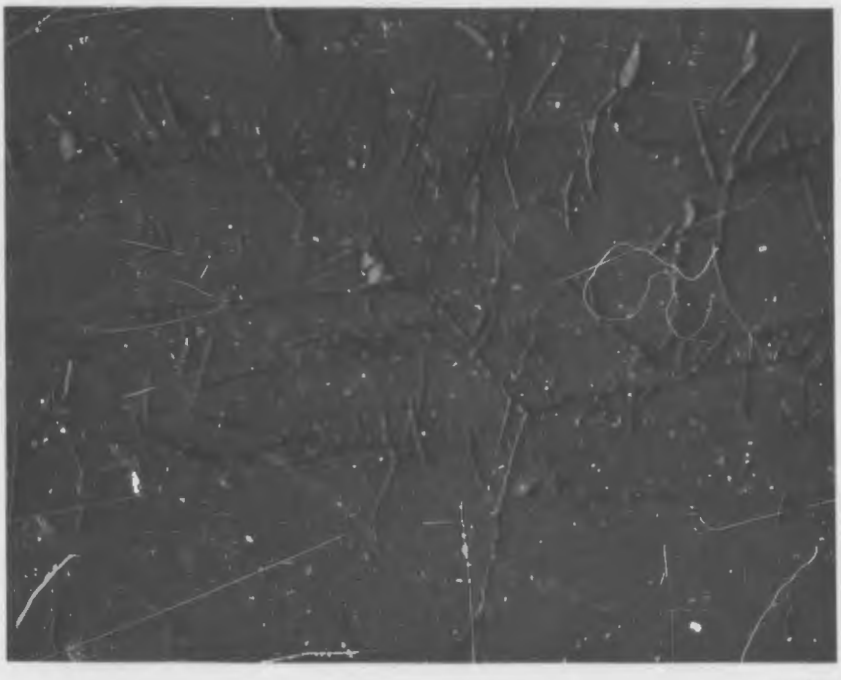

1500X

FIGURE 48. Microstructure of VAM-98 (Cb-22W-2Hf-0.05C-0.04N) Solution annealed 1 hour at 1800°C and helium cooled plus aged 6 hours at 1100°C.

1500X

FIGURE 49. Microstructure of VAM-98 (Cb-22W-2Hf-0.05C-0.04N) Solution annealed 1 hour at 1800°C and helium cooled plus aged 7 hours at 1100°C.

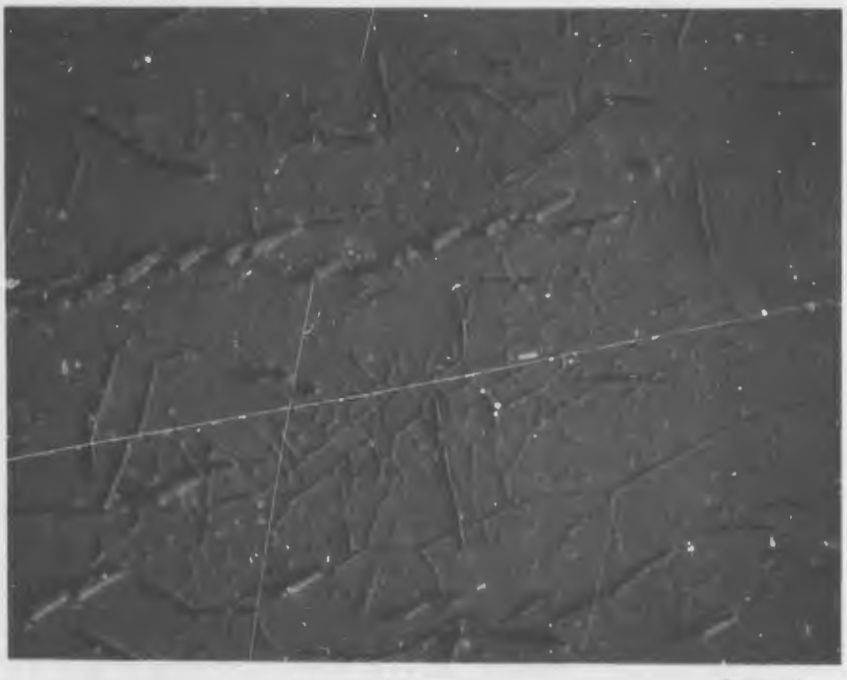

1500X

FIGURE 50. Microstructure of VAM-98 (Cb-22W-2Hf-0.05C-0.04N) Solution annealed 1 hour at 1800°C and helium cooled plus aged 8 hours at 1100°C.

1500X

FIGURE 51. Microstructure of VAM-98 (Cb-22W-2Hf-0.05C-0.04N) Solution annealed 1 hour at 1800°C and helium cooled plus aged 12 hours at 1100°C.

Electron Microscopy Study of VAM-98

The solution annealed and solution annealed plus aged Cb-22W-2Hf-0.05C-0.04N alloy was studied by transmission electron microscopy in four conditions: as-solution annealed; aged 4 hours at 1100°C (peak "a"); aged 7 hours at 1100°C (interpeak valley); and 12 hours at 1100°C (peak "b"). The thinning techniques were identical to those developed for B-88.

Approximately 40 mil slices were cut from longitudinal sections of the specimen to be examined. These slices were mechanically thinned by successive grinding on water cooled 120, 240, 320 and 400 grit silicon carbide papers and finally on 600 grit paper lubricated with stick wax. The final thickness of the slices was 3 to 5 mils after mechanical thinning. A number of 1/8 inch diameter discs were punched out of the specimen. The discs were then electro polished to a thickness of less than 2000 Å in a J.E.M. dual-jet thinning apparatus. The electrolyte consisted of 20 ml concentrated H_2SO_4, 10 ml Hf and 370 ml methyl alcohol. During electro polishing, which takes 5 to 15 minutes, the electrolyte temperature was maintained at -74°C by using dry ice in ethyl alcohol. The current was maintained at 5 to 10 ma by periodically adjusting the voltage and/or electrolyte flow rate as thinning progressed. The voltage ranged between 20 and 40 volts. Polishing was stopped at initial penetration and the foil was carefully washed. The resulting self-supporting foils were then inserted directly into the electron microscope for examination.

The range of microstructures obtainable in the as-solution annealed material are shown in Figure 52. The structure is similar to the as-solutioned B-88[2] with the exception that there is a small amount of coherent precipitates noted in Figure 52e, f, and h and in Figure 54. A Widmanstatten array of disorganized rafts of precipitates lay on {110} matrix planes as shown in Figure 52a, d, e, f, g, and h. The larger platelets which are the zeta phase are present throughout forming the larger substructure. A zeta platelet was captured in the plane of the foil in Figure 52c. The "faceting" or microrelief in Figure 52b is believed to be caused by anomolies in the thinning procedure and are due to preferential

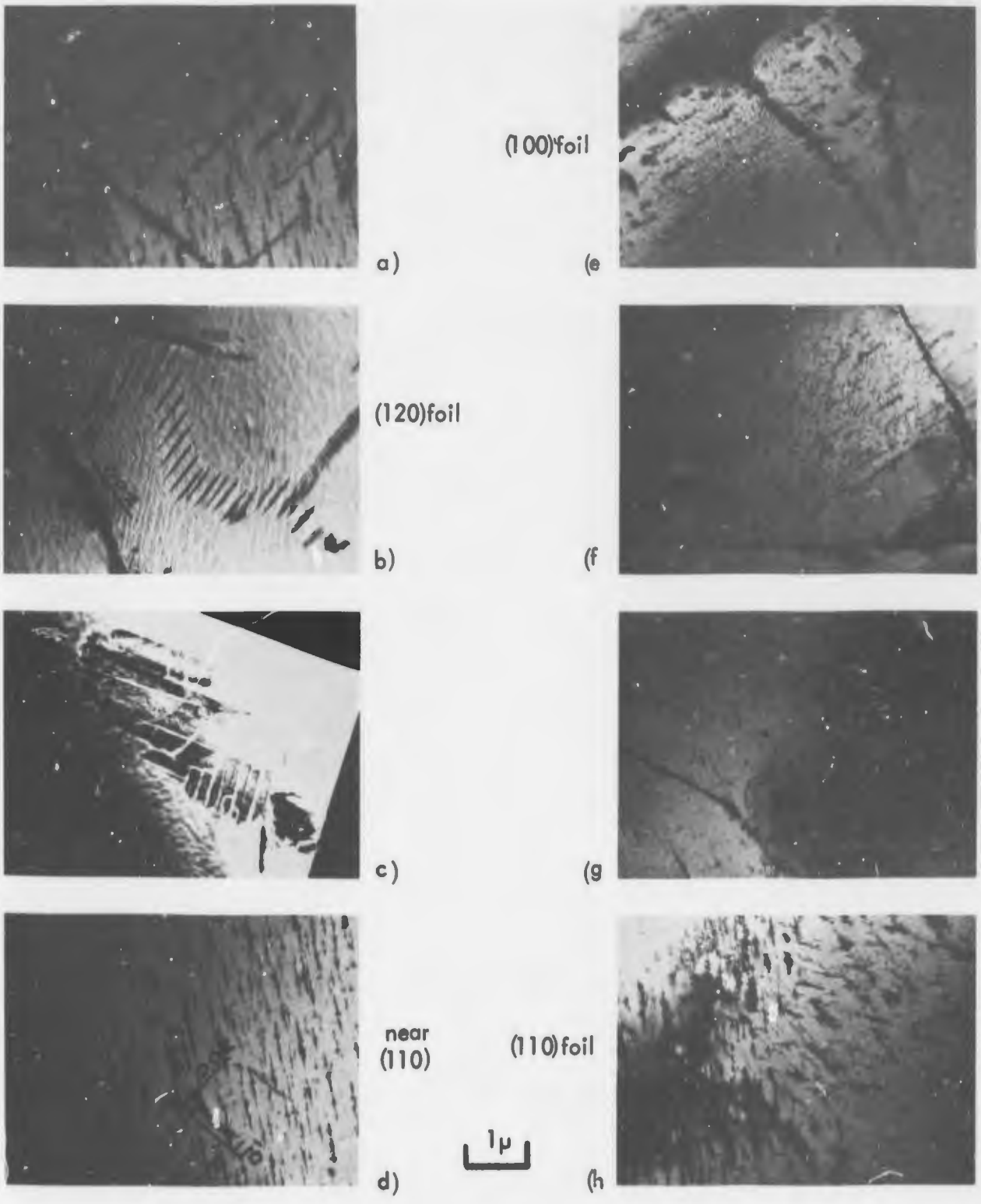

FIGURE 52. Transmission Electron Micrograph of VAM-98 (Cb-22W-2Hf-0.05C-0.04N) Solution annealed 1 hour at 1800°C and helium cooled.

attack by the electrolyte along certain crystallographic directions. An interesting feature of Figure 52f and at higher magnification in Figure 53 is the copious number dislocation loops which were apparently "punched out" during precipitation during cooling from the solutioni·g temperature since there has been no applied stress on specimens during heating. Other dislocations are shown to be entangled with grain boundary precipitates in Figure 52g and with the zeta substructure platelets in Figure 52f and 53.

With the exception of a small amount of coherent precipitates, more disorganized array of rafts of precipitates on matrix $\{110\}$ planes, the structure of the nitride containing VAM-98 is similar in appearance to B-88 in the as-solutioned condition.

Electron micrographs taken from samples aged 4 hours at 1100°C corresponding to peak "a" are shown in Figure 55. The Widmanstatten array of rafts of precipitates on matrix $\{110\}$ planes have disappeared. In their place are a general distribution of coherent precipitates which masked most other features. The larger substructure formed by the platelets of zeta (which transforms to a fcc NaCl/type carbide or carbonitride) is not shown in the TEM photos though they are readily apparent in the optical photomicrographs discussed earlier. Figure 55e shows a simple twist boundary separating two (120) oriented grains. The twist angle is approximately 15°. Coherent precipitates lie along the boundary showing coherency strains in only one side of the grain boundary. A narrow precipitate free zone about 0.5μ wide is associated with the boundary. Although the (200) reflection was generally the strongest diffraction spot, the coherency effects were noted to respond most strongly to the $\{\bar{2}\bar{1}3\}$ and then the $\{211\}$ diffraction vectors. In some cases it appears that contrast is obtained from the structure factor mechanism from platelets along $\{211\}$ and $\{\bar{2}\bar{1}3\}$ directions in the (120) foils shown in Figures 55b, c, d, and e.

The TEM observations of foils from specimen taken from the overaging valley between peak "a" and peak "b" (aged 7 hours at 1100°C) are shown in Figures 56 and 59. This material is very similar in appearance to the initial as-solution annealed condition. The

FIGURE 53. Transmission Electron Micrograph of VAM-98 (Cb-22W-2Hf-0.05C-0.04N) Solution annealed 1 hour at 1800°C and helium cooled. Foil showing numerous dislocation loops.

FIGURE 54. Transmission Electron Micrograph of VAM-98 (Cb-22W-2Hf-0.05C-0.04N) Solution annealed 1 hour at 1800°C and helium cooled; (001) foil showing some coherent precipitation.

a)

d) (120) foil

b) (120) foil

e) (120) foil

c) (120) foil

1μ

FIGURE 55. Transmission Electron Micrograph of VAM-98 (Cb-22W-2Hf-0.05C-0.04N) Solution annealed 1 hour at 1800°C and helium cooled; plus aged 4 hours at 1100°C.

a)

d) (311) foil

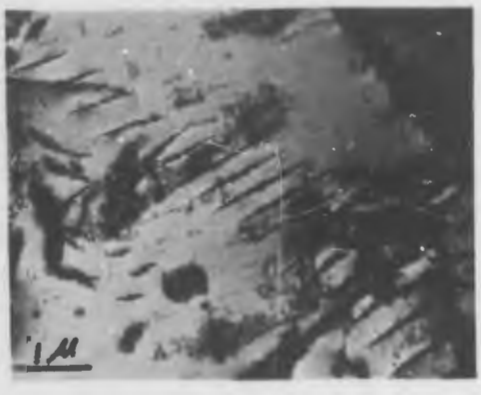

b)

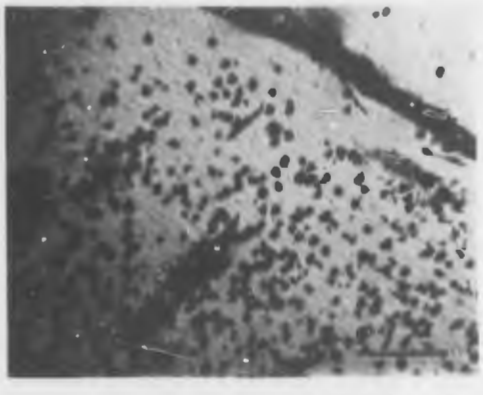

e) (120) foil

c) (120) foil

f) (311) foil

FIGURE 56. Transmission Electron Micrograph of VAM-98 (Cb-22W-2Hf-0.05C-0.04N) Solution annealed 1 hour at 1800°C and helium cooled; plus aged 7 hours at 1100°C.

FIGURE 57. Transmission Electron Micrograph of VAM-98 (Cb-22W-2Hf-0.05C-0.04N) Solution annealed 1 hour at 1800°C and helium cooled; plus aged 7 hours at 1100°C. Thin foil showing general precipitation formed substructure.

FIGURE 58. Transmission Electron Micrograph of VAM-98 (Cb-22W-2Hf-0.05C-0.04N) Solution annealed 1 hour at 1800°C and helium cooled; plus aged 7 hours at 1100°C.

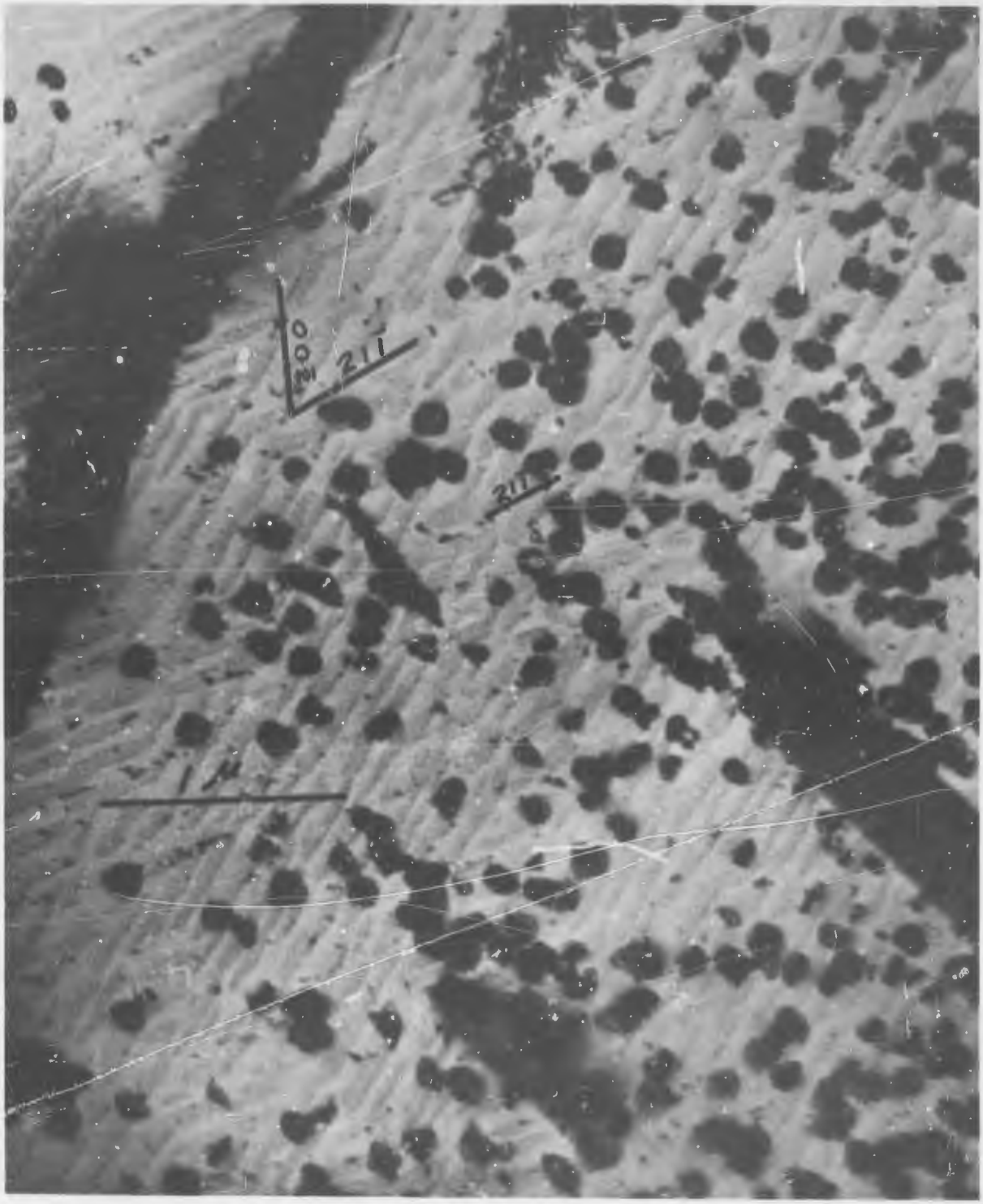

FIGURE 59. Transmission Electron Micrograph of VAM-98 (Cb-22W-2Hf-0.05C-0.04N) Solution annealed 1 hour at 1800°C and helium cooled; plus aged 7 hours at 1100°C. 120 foil showing coherent precipitates.

structures obtained were not at all what were expected. The larger platelets are in the same profusion and general distribution as in the initial condition and otherwise no great coarsening was noted as shown in Figures 56, 57 and 58. A few scattered areas of coherent precipitates were noted examples of which are shown in Figures 56 and 59. The coherency strains in the (120) foil in Figure 59 respond to operation by the $\{211\}$ g vector although g $\{002\}$ was the strong diffraction vector. The microrelief in the background is similar to that shown in thin areas in the initial as-solution annealed condition. Occasional well decorated dislocations associated with the coarser platelets were noted in Figure 56f.

The final condition studied was taken from just beyond peak "b" at 12 hours at 1100°C. The general range of observed structure are shown in Figure 60 with higher magnifications of the same areas in Figures 61, 62, and 63. The copious array of uniformly distributed coherent precipitates are similar to those observed at peak "a" with the exception that the diameter of the coherent strain contrast around the precipitates are about half of that observed at peak "a" (0.05μ for peak "b" versus approximately 0.1μ for peak "a"). Some decrease in coherent precipitate density are noted near the larger thin platelets as in Figure 60 and Figure 63. A definite precipitate free zone is apparent in the regions near the high angle grain boundary in Figures 60d, e, and Figure 62. The grain boundary shown in Figure 62 is free of larger precipitates but shows abundant punched dislocation in the precipitate free zone.

Phase Relationships

Interpretation of the aging phenomena requires accurate phase identification data. For this reason precipitated phases were extracted from the VAM-98 matrix by dissolution of the matrix in a bromine-methanol-tartaric acid solution. The phases extracted represent the larger discrete precipitates. Very fine precipitates (< 1000Å) would probably be lost during the rinsing process. Coherent precipitates would most likely be dissolved with the matrix. These qualifications limit the correlation of x-ray phase identification to the electron microscopy presented earlier and restrict the discussion to the larger substructure forming precipitates.

a)

d)

b) (120) foil

e)

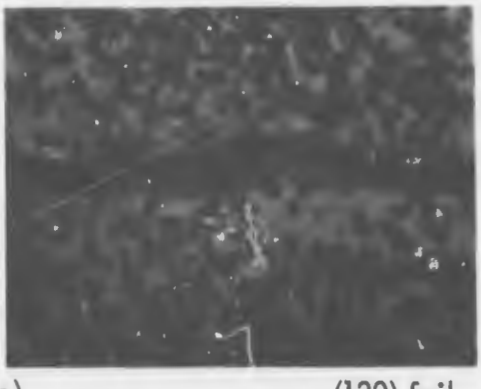

c) (120) foil

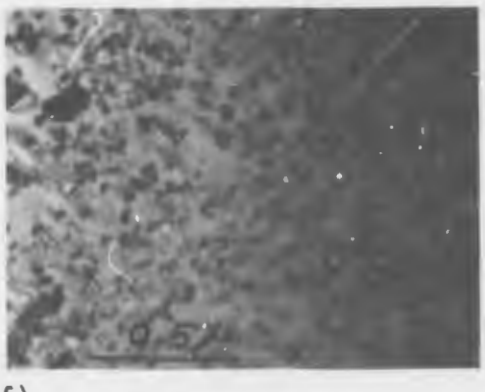

f)

FIGURE 60. Transmission Electron Micrograph of VAM-98 (Cb-22W-2Hf-0.05C-0.04N) Solution annealed 1 hour at 1800°C and helium cooled; plus aged 12 hours at 1100°C.

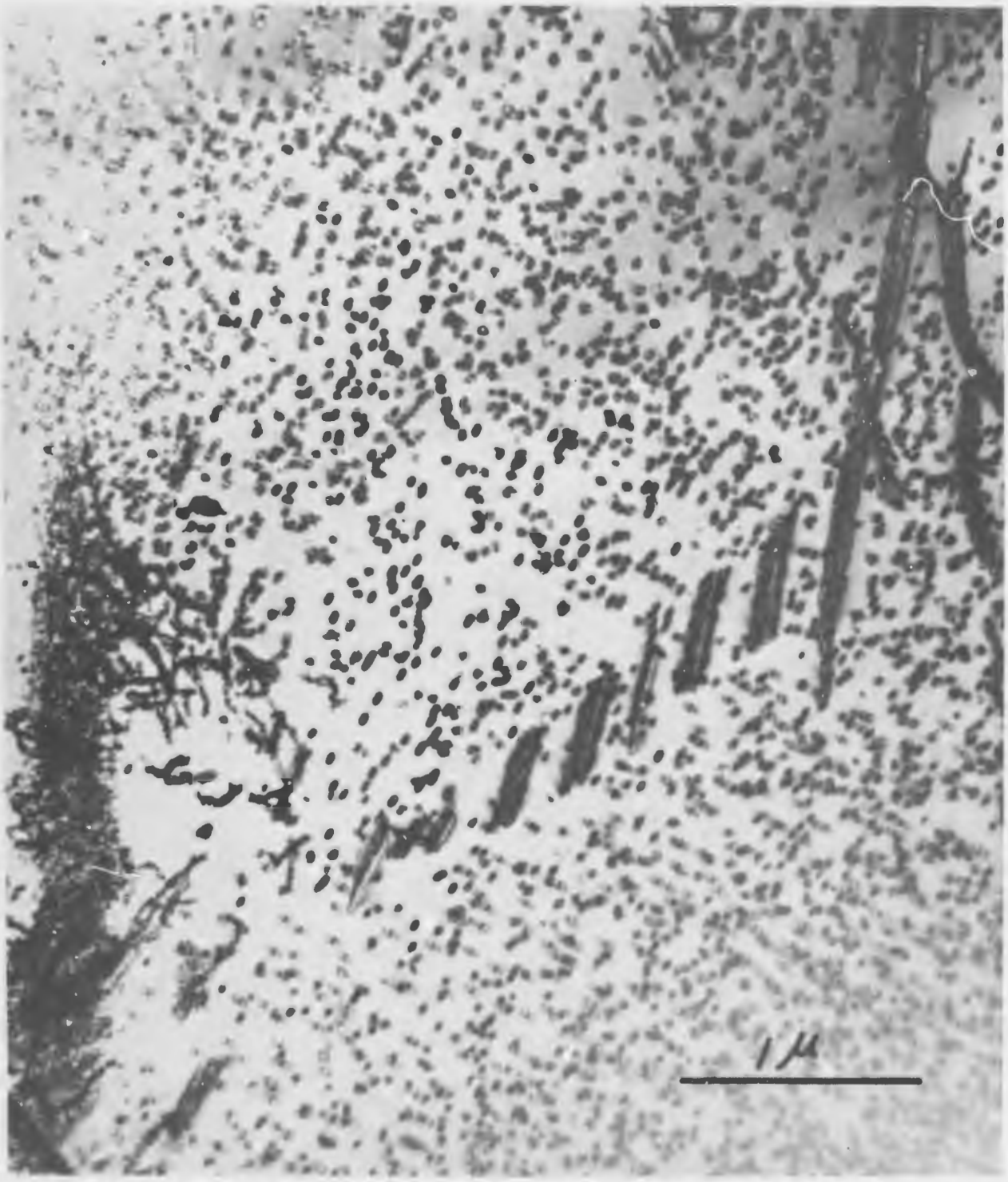

FIGURE 61. Transmission Electron Micrograph of VAM-98 (Cb-22W-2Hf-0.05C-0.04N) Solution annealed 1 hour at 1800°C and helium cooled; plus aged 12 hours at 1100°C.

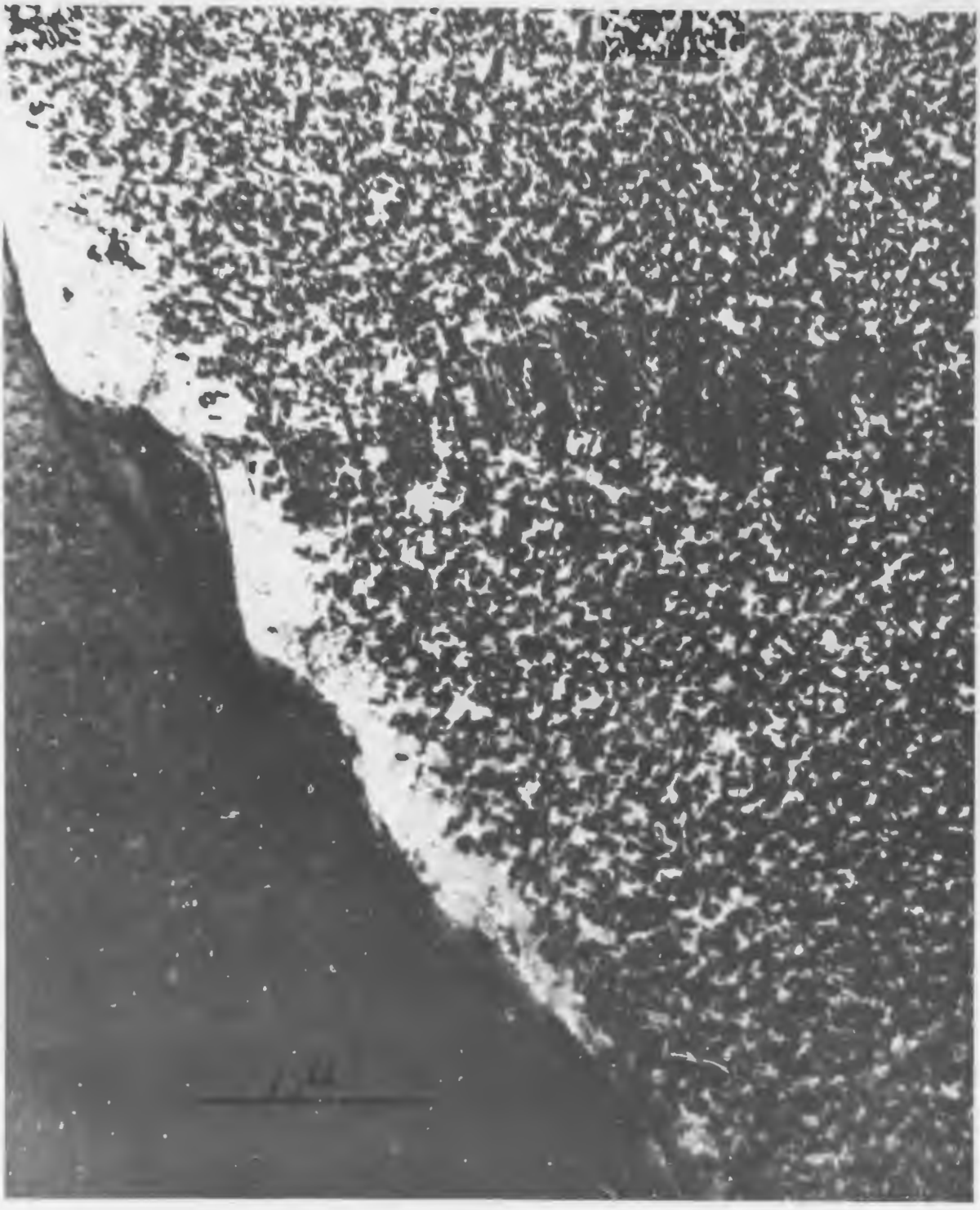

FIGURE 62. Transmission Electron Micrograph of VAM-98 (Cb-22W-2Hf-0.05C-0.04N) Solution annealed 1 hour at 1800°C and helium cooled; plus aged 12 hours at 1100°C. Grain boundary and associated P.F.Z.

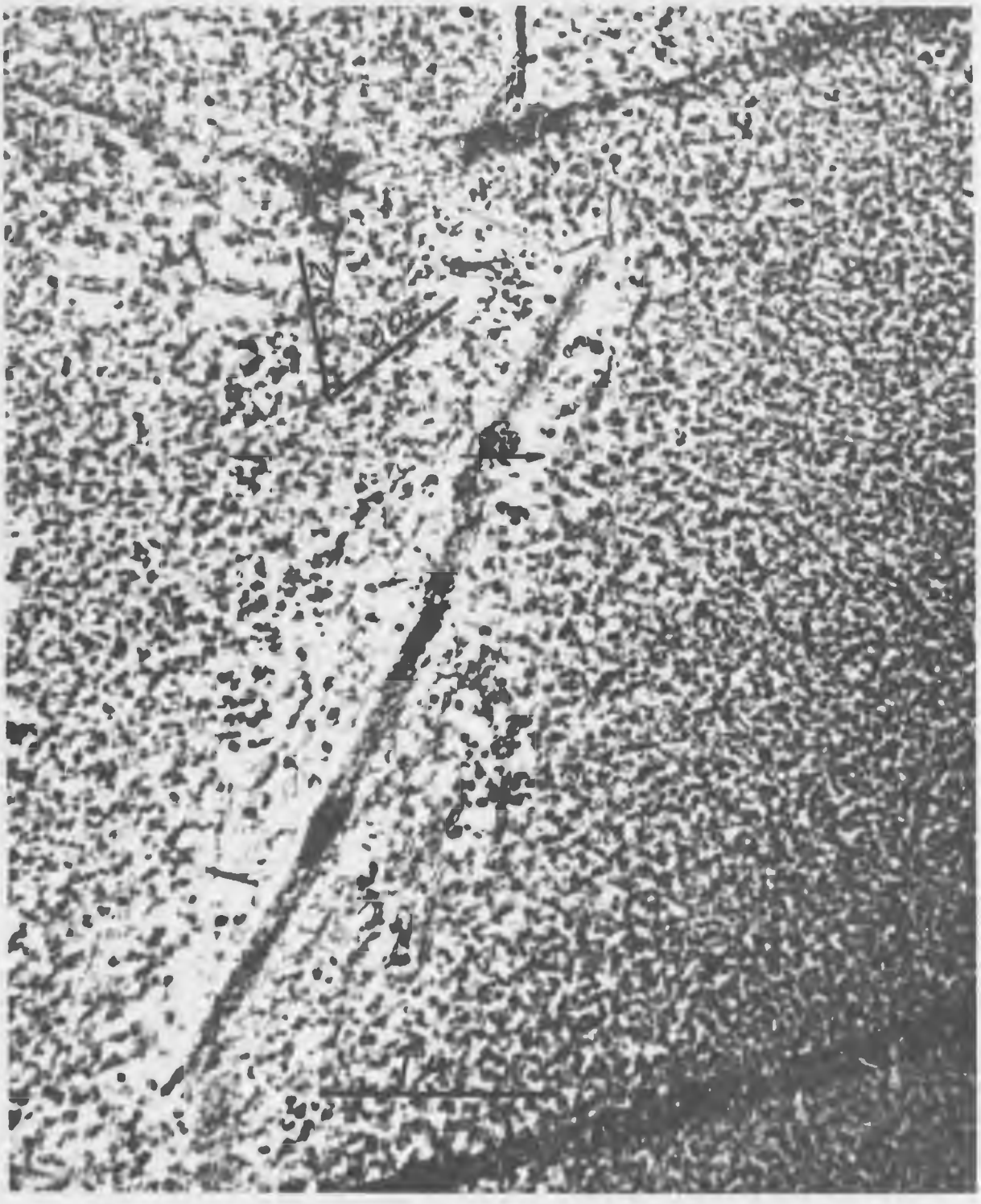

FIGURE 63. Transmission Electron Micrograph of VAM-98 (Cb-22W-2Hf-0.05C-0.04N) Solution annealed 1 hour at 1800°C and helium cooled; plus aged 12 hours at 1100°C. 120 foil showing coherent precipitates.

Phases were extracted for Debye-Scherer analysis from VAM-98 in the as-solution annealed (at 1800°C) and after several aging treatments at 1100°C, corresponding to the electron microscophy study presented previously. The phase identification data are summarized in Table 15. The sequence of precipitation events is related to the hardness behavior in Figure 64.

TABLE 15. Phase Identification Data on Carbonitride Phases Extracted from Cb-22W-2Hf-0.05C-0.04N (VAM-98)

Thermal Treatment Condition	Phases Present
A. - As solution annealed 1 hour at 1800°C	β (Matrix a_o = 3.28 Å) + Zeta
B. - As solution annealed 1 hour at 1800°C + 2 hours at 1100°C	β (Matrix a_o = 3.28 Å) + $(Cb, Hf)_2C$ (hex) (S) + Zeta (VW)
C. - As solution annealed 1 hour at 1800°C + 4 hours at 1100°C	β (Matrix a_o = 3.28 Å) + $(Cb, Hf)_2C$ (hex) (S) + Cubic (VW)*
D. - As solution annealed 1 hour at 1800°C + 6 hours at 1100°C	β (Matrix a_o = 3.28 Å) + Zeta (W)
E. - As solution annealed 1 hour at 1800°C + 8 hours at 1100°C	β (Matrix a_o = 3.28 Å) + Zeta (M)
F. - As solution annealed 1 hour at 1800°C + 10 hours at 1100°C	β (Matrix a_o = 3.28 Å) + $(Cb, Hf)_2C$ (hex) (M) + Cubic (VW)*
G. - As solution annealed 1 hour at 1800°C + 12 hours at 1100°C	β (Matrix a_o = 3.28 Å) + $(Cb, Hf)_2C$ (hex) (S) + Cubic (W)*
	* $a^o \approx 4.50$

These data show a most unusual behavior of the phase transitions during aging. The zeta carbide phase is present initially after solution annealing. The zeta phase apparently transforms to the hexagonal bimetal carbide upon aging to the first aging peak. Meanwhile the coherent nitride precipitate (HfN) is also forming. Upon overaging from peak "a" zeta reforms only to transform again to the hexagonal plus cubic ($a_o \approx 4.50$) after aging to peak "b". Again exactly as in the case of peak "a", a coherent precipitate forms simultaneously with the zeta → hex transformation of the larger precipitates. It appears that overaging from peak "b" would produce a transformation from hexagonal $(Cb, Hf)_2C$ to the cubic carbide (or carbonitride).

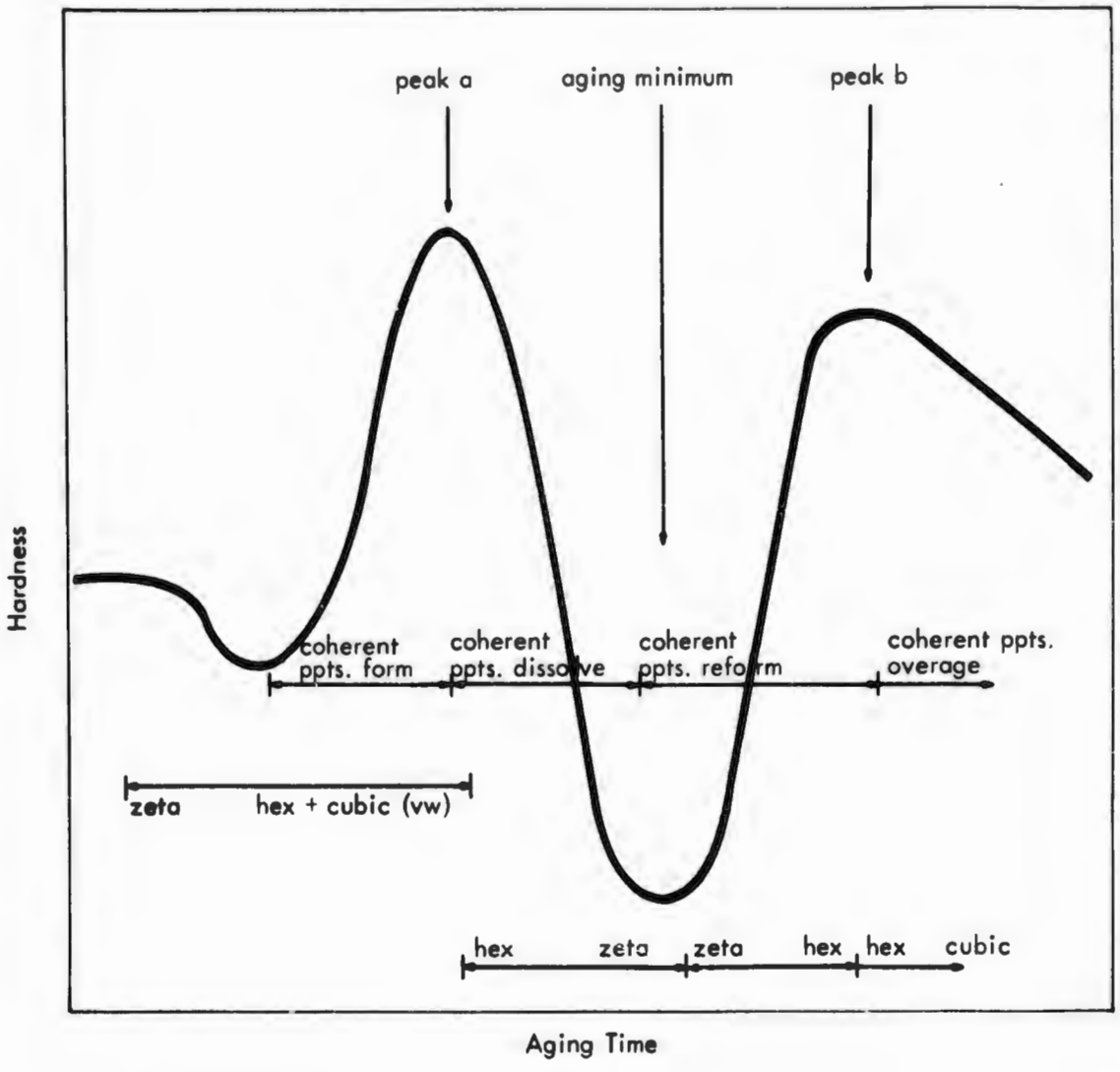

FIGURE 64. Schematic Representation of Aging Response of VAM-98 (Cb-22W-2Hf-0.05C-0.04N) at 1100°C

Discussion of Thermal Treatment Response

The general characteristics of the aging curves of the VAM-98 material solution annealed at 1800°C and cooled in helium are summarized by the following experimental observations.

1. Initial as-solutioned hardness of 330 VPN.
2. Rapid softening by approximately 50 VHN at short aging times (less than 0.5 hours.
3. Rapid increase in hardness to peak "a".
4. Very rapid decrease in hardness to a narrow overaging "valley".
5. Very rapid hardness increase to peak "b" followed by overaging.
6. The "a" peaks are approximately 30 VHN higher than the "b" peaks.
7. The "a" or "b" peaks are higher at the lower temperature aging isotherms.
8. The activation energy of formation of the "a" peak is 57 ± 8 Kcal/mole. The "b" peak requires a thermal activation of 73 ± 8 Kcal/mole.

The results of the optical and electron microscopy and Debye-Scherer studies as related to the 1100°C aging isotherm are as follows:

1. The initial as-solutioned material is characterized by a substructure made up of zeta platelets. Rafts of fine precipitates are found on (110) matrix planes.
2. Peaks "a" and "b" are associated with coherent precipitates less than 0.1μ diameter. A transformation of the zeta platelets to the hexagonal bimetal carbide (or carbonitride) accompanies the hardness increase to peak "a".
3. Zeta returns as a substructure network precipitate at the expense of the hexagonal bimetal carbide upon overaging from peak "a" to the interpeak valley. The coherent precipitate present at peak "a" returns to solution during overaging. This structure is very similar to the as-solutioned structure.
4. The observations on the second aging peak (peak "b") are almost identical to those on the "a" peak. Zeta disappears and the bimetal carbide reappears. Coherent

precipitation is again the most prominent feature in electron micrographs. Some cubic carbide ($a_o \approx 4.50$) was also observed at peak "b" and during overaging from peak "b".

The precipitation processes in an alloy such as the Cb-22W-2Hf-0.05C-0.04N containing three metallic constituents and two interstitial constituents must of necessity be complex. Many simplifications would be necessary to explain the observations outlined above. The initial decrease in hardness suggest a reversion process, i.e., zones forming during cooling from the solutioning temperature being resolutioned at lower temperatures. The annealing out of a super saturation of vacancies may also be associated with this initial decrease.

The formation of coherent precipitates associated with peak "a", their dissolution associated with the overaging valley, and the formation of coherent precipitates associated with peak "b" could be explained by two different species of precipitates. The peak "a" precipitates, though metastable, can form because of a lower free energy barrier than the more stable peak "b" precipitate species.

The reformation of zeta platelets during the overaging from peak "a" is very confusing but must represent a vital link in the aging sequence.

The unusual aging response of the nitrogen containing alloy prompted a careful review of the experimental procedures to determine if some error in technique was responsible for the occurrence of the double aging peak. The hardness measurements were rechecked, and found to agree with the original data. Furthermore the aging runs were conducted over a considerable time period, and the trends were confirmed by additional aging runs. In addition, the possibility of variation in nitrogen content from specimen to specimen was also considered as a possible cause of the unusual aging response. Specimens were submitted for a recheck of the nitrogen analysis, and the results are summarized in Table 16.

TABLE 16 - Chemical Analysis of VAM-98 as a Function of Thermal Treatment

CONDITION	ANALYSIS (W/O)		
	N	O	C
As-swaged	0.042	0.015	0.052
Solution Annealed 1 hour at 1800°C	0.035	--	--
Solution Annealed 1 hour at 1800°C plus aged 2 hours at 1100°C *	0.038	0.009	--
*close to peak "a"			

These results show no significant variation in nitrogen level in the swaged, solution annealed, and the aged samples. In addition, hafnium analyses were obtained on samples in various conditions and no significant variation in hafnium concentration was observed.

The most positive confirmation of the existence of the aging peaks is provided by the transmission electron micrographs corresponding to peaks "a" and "b". (Figures 55 and 61). These micrographs clearly show the presence of coherent precipitates which directly correlates with the hardness data.

The precipitation behavior of the nitrogen containing alloy is obviously complex and more detailed studies are required to define the precise precipitation sequence and kinetics to permit the exploitation of the potential of alloys of this type.

C. MECHANICAL PROPERTY EVALUATION

The pronounced aging response of the Cb-22W02Hf-0.05C-0.04N alloy indicated that with selection of the proper thermal treatment significant improvement in intermediate temperature yield strength could be realized. Tensile and creep rupture data were obtained on specimens of VAM-98 in various thermal conditions.

Tensile Results

Tensile specimens having a 0.1 inch gage diameter and a 1 inch gage length were machined from as-swaged rod and annealed 1 hour at 1800°C and helium cooled. A number of the solution annealed specimens were then aged at 1100°C, and tensile tests were conducted at room temperature and 760°C (1400°F). The results are tabulated in Table 17. The tensile results at 1400°F were quite disappointing. The yield strength values were on the order of 50,000 psi in both the solution annealed and the solution annealed plus aged conditions, which is only slightly higher than obtained for the nitrogen free B-99 alloy. Hardness measurements were made on as-solution annealed specimens and the hardness levels ranged from 260 to 290 VPN, which is considerably lower than the 330 VPN obtained on the solution annealed specimens used for the hardness and metallographic studies reported in the previous section. Furthermore, the specimens aged for 4 hours and 14 hours at 1100°C showed no significant hardening response as would be expected from the results of the initial aging studies. The lack of aging response explains the relatively low 1400°F yield strength values of the aged tensile specimens but the reason for the difference between the initial results and the tensile specimens is not clear. Specimen VAM-98-T17 was submitted for chemical analysis following tensile tests and the nitrogen level was determined to be 0.032 w/o. Several duplicate as-swaged samples were submitted at the same time and they analyzed 0.033 and 0.042 w/o nitrogen. This indicates that nitrogen was not lost during heat treatment of the tensile specimens. A metallographic specimen which did show a hardness peak analyzed 0.038 w/o N_2, hence it does not appear that the nitrogen content is too low. A possible explanation for the difference between the response to heat treatment of the tensile specimens and the metallographic specimens is a difference in cooling rate from the solution annealing temperature. Experiments are currently in progress to resolve this problem, utilizing both brine and tin quenching of tensile specimens.

The room temperature ductility of both solution annealed and solution annealed plus aged specimens was quite low. The transition temperature of VAM-98 would be

TABLE 17 - Tensile Data for VAM-98 (Cb-22W-2Hf-0.05C-0.04N)

Specimen Number	Test Temperature (°C)	Test Temperature (°F)	0.2% Yield Strength (psi)	Ultimate Strength (psi)	Elongation (%) Uniform	Elongation (%) Total	Reduction in Area (%)	Condition
VAM-98-T8	--	1400	51,700	91,400	11.4	14.2	47.3	Annealed 1 hour at 1800°C; helium cooled
VAM-98-T17	--	1400	49,590	84,250	10.8	14.1	54.7	Annealed 1/2 hour at 1800°C; helium cooled
VAM-98-T7	--	1400	48,400	79,400	9.4	13.9	54.3	Annealed 1 hour at 1800°C; helium cooled plus aged 14 hours at 1100°C
VAM-98-T1	RT	RT	----	69,200*	0.6	0.6	0.0	Annealed 1 hour at 1800°C; helium cooled
VAM-98-T2	RT	RT	104,200	106,100*	0.65	0.65	1.53	Annealed 1 hour at 1800°C; helium cooled plus aged 4 hours at 1100°C
VAM-98-T3	RT	RT	100,400	102,300*	0.74	0.74	2.43	Annealed 1 hour at 1800°C; helium cooled plus aged 12 hours at 1100°C
VAM-98-T4	RT	RT	103,900	105,800*	0.64	0.64	1.08	Annealed 1 hour at 1800°C; helium cooled plus aged 7 hours at 1100°C

*True Fracture Stress

expected to be higher than that of B-99 because of the former's higher total interstitial level. However, by solution annealing at either lower temperatures and/or shorter times to reduce the primary grain size it should be possible to achieve satisfactory room temperature ductility in this alloy.

Creep-Rupture Results

Creep rupture tests were conducted at 1095 and 1205°C (2000 and 2200°F) on specimens which had been solution annealed 1 hour at 1800°C and aged 14 hours at 1100°C. The creep data are listed in Table 18. The results were identical to those obtained on VAM-97 which is the nitrogen free analog to VAM-98. Considering the lack of aging response exhibited by the tensile specimens this similarity in properties is to be expected. Further creep rupture testing was deferred pending solution of the problem of the lack of response of the tensile and creep specimens to heat treatment.

Specimen No.	Test Temperature (°C)	(°F)	Stress (psi)	Rupture Time (hrs)	Minimum Creep Rate (%/hr.)	Transition Time (hrs.)	Red. in Area (%)	Elong. (%)	Prior Treatment
VAM-98-25	1205	2200	40, 000	5.7	.3140	3.5	28.3	9.33	Solution annealed 1 hr at 1800°C plus aged 14 hrs at 1100°C
VAM-98-26	1205	2200	30, 000	57.3	.0188	39.9	22.9	6.67	" "
VAM-98-28	1095	2000	50, 000	43.0	.0374	30.0	30.0	9.33	" "
VAM-98-29	1095	2000	50, 000	42.9	.031[illegible]	34.7	23.9	9.33	Solution anneal 1 hr at 1800°C

TABLE 18 - Creep Rupture Data for VAM-98 (Cb-22W-2Hf-0.05C-0.04N)

V. REFERENCES

1. R. T. Begley, J. L. Godshall, and D. L. Harrod, "Development of Columbium Base Alloys," AFML-TR-65-385, January 1966.

2. R. T. Begley, J. A. Cornie, and R. C. Goodspeed, "Development of Columbium Base Alloys," AFML-TR-67-116, November 1967.

3. W. H. Chang, "Influence of Heat Treatment on Microstructure and Properties of Cb-Base and Cr-Base Alloys," ASD-TDR-62-211, Part IV, March 1966.

4. R. L. Ammon and R. T. Begley, "Pilot Production and Evaluation of Tantalum Alloy Sheet," Summary Phase Report, June 15, 1963.

5. A. Taylor and N. Doyle, "Solid-Solubility of Oxygen in Nb and Nb Rich Nb-Hf, Nb-Mo and Nb-W Alloys," J. Less Common Metals, Part I Nb-O System, 13, 1967, 399, 412; Part II Ternary Systems Nb-Hf-N, Nb-Mo-N, and Nb-W-N, 13, 1967, 413-430.

6. R. T. Begley, J. L. Godshall, and R. Stickler, "Precipitation Hardened Cb-Hf-N Alloys," in Plansee Proceedings, 1964, F. Benesovsky, Metallwerk Plansee AG, Reutte Tyrol, 1965.

7. Ostermann, Untersuchungen Uber Ausscheidungen in Zwei Kohlenstaffhaltigen Nioblegierungen, PhD Thesis, Technischen Hochschule Aachen, 1966.

8. R. T. Begley, R. W. Buckman, J. L. Godshall, and R. Stickler, "Development of Columbium-Base Alloys," AFML-TR-57-344, Part VII, April 1963.

9. R. T. Begley, R. L. Ammon, and R. Stickler, "Development of Niobium Base Alloys," WADC-TR-57-344, Pt. VI, February 1963.

10. A. L. Titchner and M. B. Bever, "The Stored Energy of Cold Work," Progress in Metal Physics, Vol. 7, 1958, p. 326-328.

11. J. T. Michalak and H. W. Paxton, "Some Recovery Characteristics of Zone-Melted Iron," Trans. AIME, Vol. 221, 1967, p. 850.

12. R. T. Begley, D. L. Harrod, and R. E. Gold, "High Temperature Creep and Fracture Behavior of the Refractory Metals," in Refractory Metal Alloys; Metallurgy and Technology, Plenum Press, New York, 1968.

13. R. T. Begley, W. N. Plotte, R. L. Ammon, and A. I. Lewis, "Development of Niobium Base Alloys," WADC-TR-57-344, Part V, January 1967.

14. R. T. Begley, R. W. Buckman, Jr., J. L. Godshall, and R. Stickler, "Development of Columbium-Base Alloys,"WADC-TR-57-344, Part VII, April 1963.

15. R. W. Buckman, Jr. and R. C. Goodspeed, "Considerations in the Development of Tantalum Base Alloys," in Refractory Metal Alloys: Metallurgy and Technology, Plenum Press, New York, 1968.

16. H. Inouye, "Equilibrium Solid Solutions of Nitrogen in Nb-1% Zr Between 1200 and 1800°C," ORNL TM-1355, February 1966.

BLANK PAGE

APPENDIX I

STRUCTURAL CHANGES DURING CREEP DEFORMATION OF B-88 (Cb-28W-2Hf-.067C)

APPENDIX I - TABLE OF CONTENTS

LIST OF FIGURES

LIST OF FIGURES (Continued)

LIST OF FIGURES (Continued)

LIST OF TABLES

I-I. INTRODUCTION

Although B-88 and similar carbide hardened columbium alloys display high creep strength when compared to other materials, it is unlikely that their full strength potential has been realized. In the recrystallized condition B-88 can accommodate only 1.5 to 2.5 percent plastic strain prior to the onset of third stage creep. If the transition to tertiary creep could be extended to higher strain values the useful rupture life of these alloys could be extended significantly. Effecting such an improvement in the rupture life of B-88 and similar alloys requires a better understanding of the factors which control high temperature deformation and fracture behavior than now exists.

Equally important is a better understanding of the specific mechanism(s) by which carbide precipitates contribute to the strength of alloys of this type, and the effect of exposure time, temperature, and strain on the precipitate morphology. Precipitate stability is of considerable concern in precipitation hardened alloys, but generalizations are of little usefulness in establishing a basis for developing improved properties. Specific information on precipitate identity, distribution, and morphology, and their change with anticipated service exposure conditions is required.

The object of this study was to describe the changes in structure which occur as a function of creep deformation of B-88 at 1205°C (2200°F), using transmission electron microscopy (TEM) as the primary means of observation.

Previous TEM studies had been conducted on B-88 in the reference condition (extruded, swaged, annealed 1 hour at 1700°C) as a function of creep exposure at 1315°C (2400°F)[1]. The reference heat treatment provided a largely fully recrystallized structure of elongated grains with a well developed substructure in bands between the recrystallized areas. This structure was quite variable and TEM studies revealed a host of features which made structural characterization very difficult. The results did show, however, significant coarsening of the carbide precipitates after relatively short exposures at 1315°C (2400°F).

In the current study, B-88 specimens were annealed 1 hour at 1800°C prior to test to provide a more uniform structure for evaluation. This treatment resulted in a fully recrystallized structure with a grain size of approximately 0.075 mm. Creep tests were conducted at 1205°C (2200°F) to observe structural changes in a temperature range where the precipitate contribution to creep strength is quite significant[2].

I-II. EXPERIMENTAL METHODS

The material used in this study was the alloy B-88 (Heat No. VAM 88). The alloy was consolidated by consumable double vacuum arc-melting into water cooled copper molds. The ingots were extruded at a 5:1 reduction ratio at 1700°C and swaged to bar stock at 1300°C. The creep specimens were annealed 1 hour at 1800°C which is 100C° in excess of the carbon solvus.

The specimens were creep tested in a Satec Model VC-100 stress-rupture unit. These are lever loaded machines with tantalum sheet heating elements. Creep tests were conducted at less than 5×10^{-6} torr at 2200°F (1205°C). Plastic strain was measured with a dial gauge on the load train and by measurements before and after the creep test. The specimens were cooled from the creep test while fully loaded to prevent recovery of the creep produced dislocation arrangements during cooling.

Samples for metallographic and EM replica examination were ground on 240, 400, and 600 grit silicon carbide papers, and then polished through 30, 15 and 6 micron diamond abrasive on hard finish cloth. The mechanical polish was continued on a short-pile cloth charged with a slurry of Linde B alumina and water. The specimens were then acid polished by adding a solution of 10% chromic acid, 25 parts H_2SO_4, and 10 parts solution of 48% HF to the polishing cloth while still charged with Linde B. Final definition of precipitates and grain boundaries were accomplished by etching in a solution of 1 part concentrated HNO_3, 1 part 48%HF, and 2 parts glycerine.

Surface replicas for E.M. were prepared using a two stage parlodion-carbon technique. The replicas were shadowed with chromium and examined using a JEM-6A electron microscope.

Thin foils of B-88 (Cb-28W-2Hf-0.067C) were prepared by a process which was developed for this alloy. Approximately 40 mil slices were cut from longitudinal sections of the specimen to be studied. These slices were mechanically thinned by successive grinding on water cooled 120, 240, 320, and 400 grit silicon carbide papers and finally on 600 grit paper lubricated with stick wax. The final thickness of the slices was 3 to 5 mils after mechanical thinning. A number of one-eighth inch diameter discs were punched out of the specimen. The discs were then electropolished to a thickness of less than 2000 $\mathring{A}$ in a G.E.M. dual-jet thinning apparatus. The electrolyte consists of 20 ml concentrated H_2SO_4, 10 ml HF and 370 ml methyl alcohol. During electropolishing, which takes 5 to 15 minutes, the electrolyte temperature was maintained at -74°C by using dry ice in ethyl alcohol. The current was maintained at 5 to 10 ma by periodically adjusting the voltage and/or electrolyte flow rate as thinning progressed. The voltage ranged between 20 and 40 volts. Polishing was stopped at initial penetration and the foil was carefully washed. The resulting self-supporting foils were then inserted directly into the electron microscope for examination.

I-III. PHASE RELATIONSHIPS

During an earlier study[1] the equilibrium phase relationships of the carbon dilute columbium rich region of the Cb-W-Hf-C system were established over the temperature range 1200 to 1800°C. Figures 1 and 2 summarize the results of this study. Figure 1 gives the phase fields of alloys of the type discussed here as a function of temperature. The B-88 composition is a solid solution above 1700°C. Below 1700°C the equilibrium phase is the NaCl type FCC carbide $(Cb,Hf)C_{1-x}$. The composition of the cubic carbide in the three-phase region varies with temperature as shown in Figure 2.

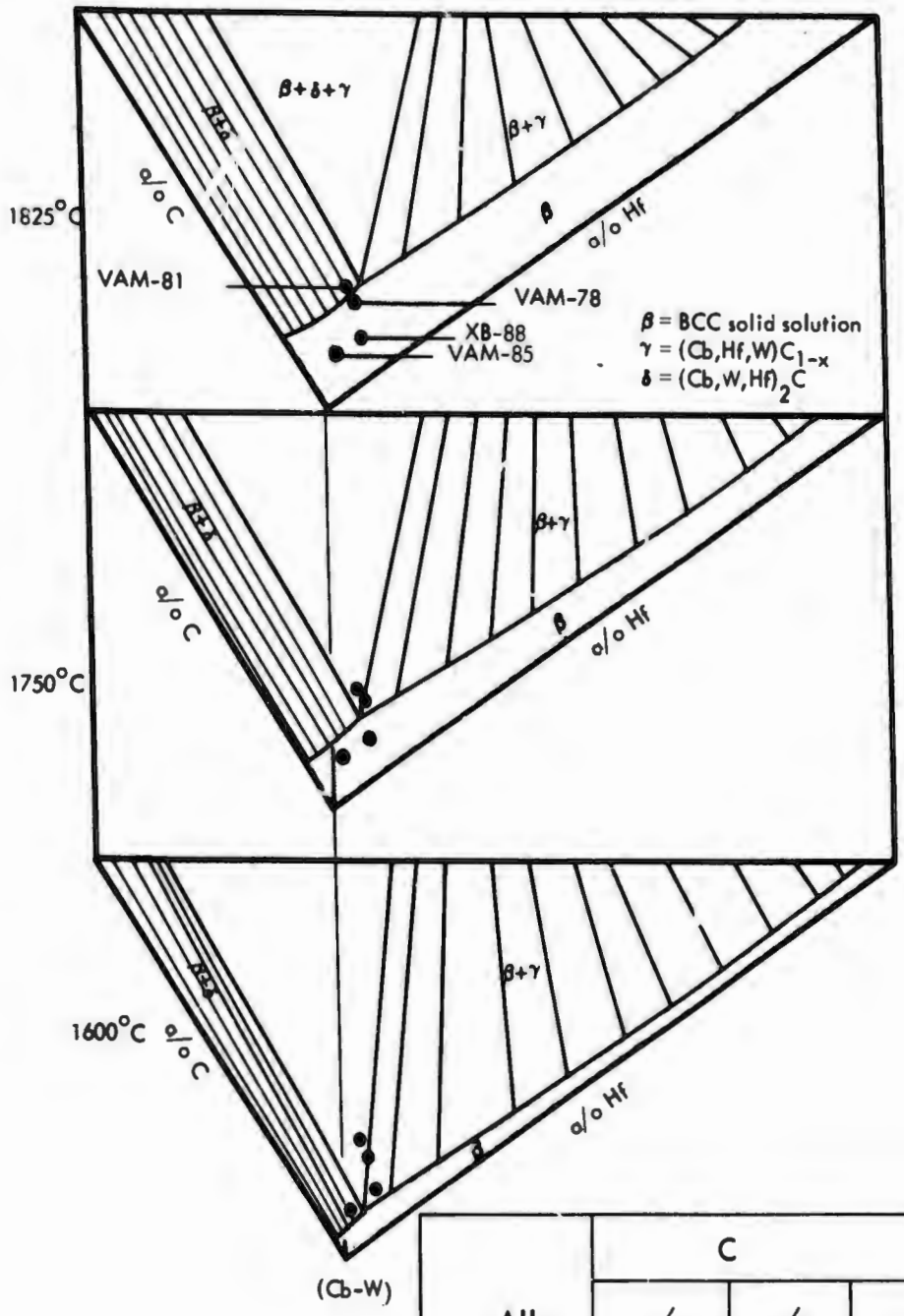

Alloy	C		Hf		W	
	w/o	a/o	w/o	a/o	w/o	a/o
XB-88	0.067	0.63	2.0	1.2	28	16.5
VAM-78	0.13	1.27	2.0	1.4	22	12.1
VAM-81	0.167	1.62	2.0	1.4	22	12.0
VAM-85	0.067	0.63	1.0	0.7	22	12.0

FIGURE 1 - Schematic Representation of (Cb,W)-Hf-C Pseudo Ternary System

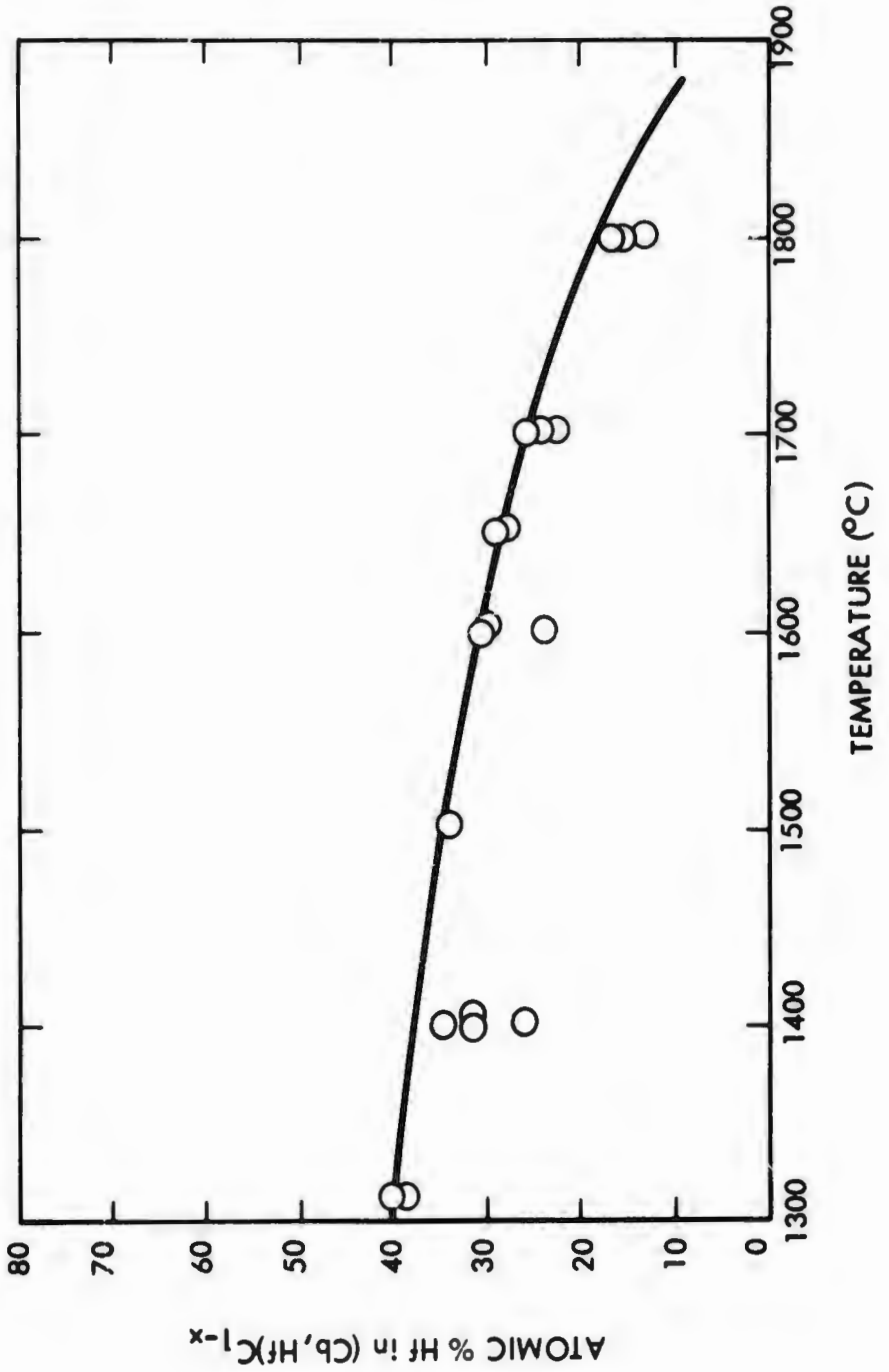

FIGURE 2. Variation of Composition of $(Cb,Hf)C_{1-x}$ with Temperature as Determined by Lattice Parameter Measurements

The equilibrium phase relationships do not fully define the precipitates developed in the B-88 alloy. When B-88 is annealed above the carbon solvus a metastable zeta type carbide forms Widmanstatten precipitates. Extractions of the precipitates are shown in Figure 3. The complex nature of the zeta phase is shown by the selected area electron diffraction pattern in Figure 3. The zeta phase has been shown to form during cooling from above the carbon solvus[1].

The zeta phase forms because the hafnium necessary to form the equilibrium carbide is unavailable due to its slow diffusivity. Carbon, on the other hand, can readily migrate large distances to nucleation sites during cooling from above the solvus and participate in the formation of the metastable zeta phase. The zeta phase contains about the same molarity (moles/cc) with respect to tungsten and hafnium as the matrix phase. Thus the matrix material at any active site may serve as food for zeta formation. The zeta phase has been shown by Ostermann[3] to transform readily to the equilibrium structure after annealing at temperatures below the carbon solvus. The rate of transformation appears to be related to the rate of hafnium diffusion.

Transformations to the equilibrium phase during aging are not limited to the metastable zeta phase. The equilibrium cubic phase formed during heating just below the carbon solvus (1700°C) has a hafnium content of <25 a/o. The equilibrium phase at 1205°C (2200°F) contains approximately 45 to 50 a/o Hf. The data on Figure 2 have been translated to Figure 4 to show the variation of carbide composition, and thus phase relationships with temperature. The low hafnium cubic carbides formed during cooling from above the carbon solvus undergo a change of approximately 20 to 25 a/o Hf while equilibrating at 1205°C (2200°F). It appears that cubic carbides precipitating during aging at 1205°C first form as the low hafnium cubic $(Cb,Hf)C_{1-x}$ phase but upon aging slowly transform to the equilibrium hafnium content. Such a transformation takes over 100 hours at 1205°C.

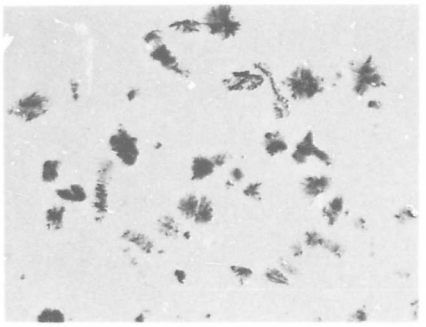

(a) 3200X

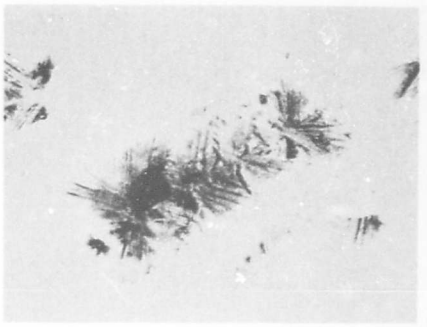

(b) 8000X

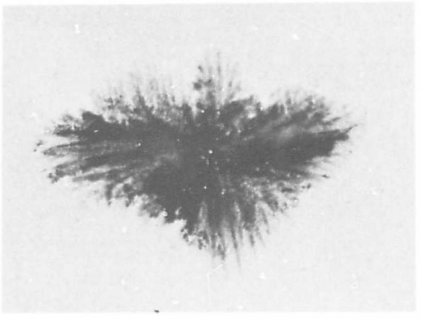

(c) 20,000X

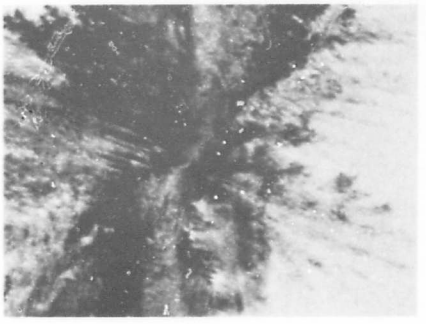

(d) 50,000X

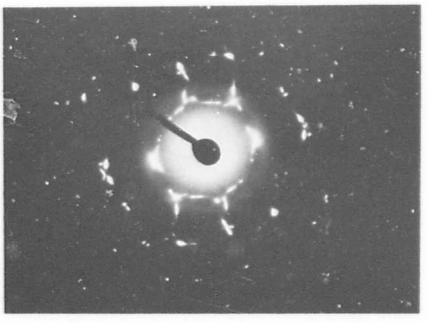

(e) SAED

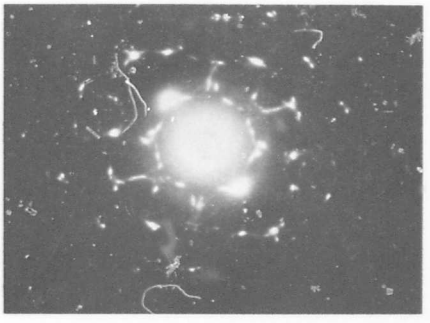

(f) SAED

FIGURE 31 - Electron Micrographs and Selected Area Electron Diffraction Patterns of Extracted and Redispersed Zeta Phase (Specimen Heat Treatment: 2 Hours at 2000°C Plus 1 Hour at 1800°C)

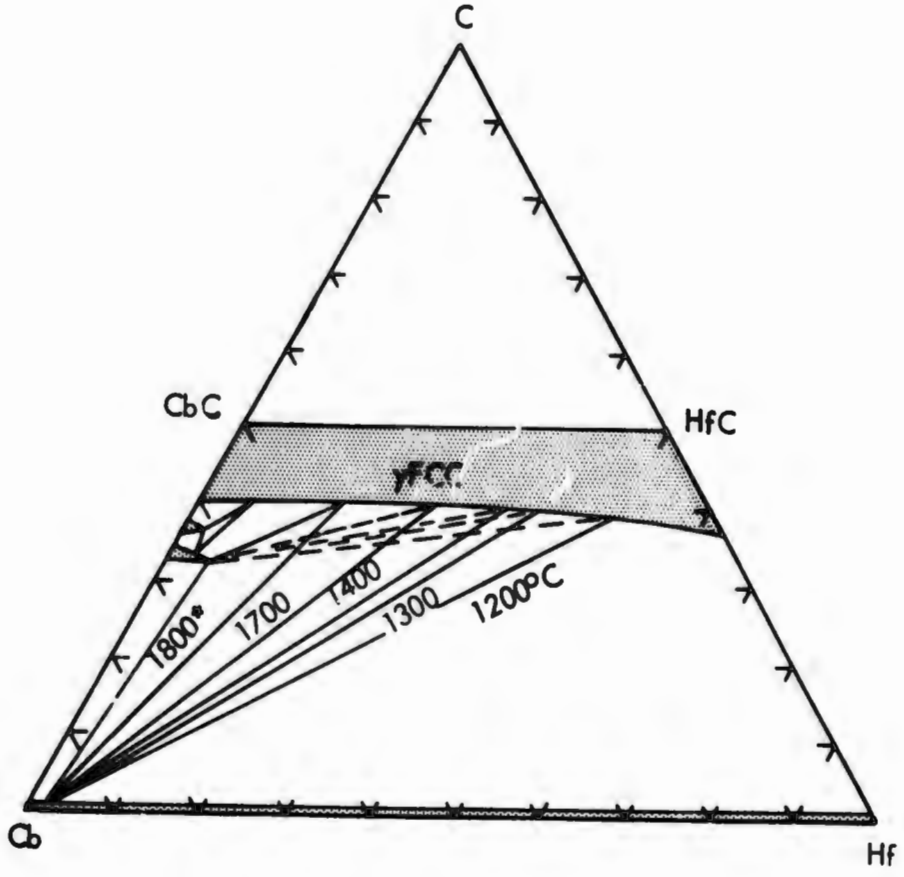

*From Stecher and Nowotny (Ref. 4)

FIGURE 4. Variation of γ Rich Corner of (Cb,W)-Hf-C System with Temperature

It should be obvious, considering the initial instability of B-88, that the precipitate morphology and thus the creep behavior must be affected by this built-in metastability. The description of this metastability is one of the objects of this investigation.

I-IV. EXPERIMENTAL DATA

The plan of this work was to describe the variation in microstructure, phase morphology, phase identity, and phase composition with creep exposure at 2200°F (1205°C) at a stress of 34,000 psi. Therefore, samples for phase extraction, microscopy, E.M. replication and thin foil E.M. studies were taken from specimens given the initial 1 hour at 1800°C heat treatment and after various degrees of creep. The creep data are given in Table 1. One specimen was thermally exposed 176 hours at 1205°C following the solution annealing treatment prior to creep testing to determine the effect of thermal exposure per se on creep strength. Aging was accomplished in an ion pumped furnace operation at 10^{-8} torr to prevent contamination.

TABLE 1

Specimen No.	Temp. (°F)	Stress (psi)	Creep Time (Hrs.)	Plastic Strain (%)	Stage of Creep at Termination of Test	Min. Creep Rate (%/hr)	Creep Rate at Test Termination (%/hr)
A-5	2200	34,000	1.5	0.33	Primary	0.067	0.067
A-3	2200	34,000	30.0	0.67	Secondary	0.012	0.012
A-2	2200	34,000	107.8	1.00	Secondary	0.006	0.006
A-1	2200	34,000	167.8	1.66	Tertiary	0.0081	0.02
A-6	2200	34,000	154.5	4.67		0.0120	Specimen tested to failure.

The locations of the specimens for optical and electron metallographic study with respect to the reference creep curve are shown in Figure 5. Specimens were cut parallel to the stress axis of the 0.18 inch diameter gauge of creep test specimens after the creep exposures. Specimens for bromine extraction of the carbides were also taken from the gauge length of the

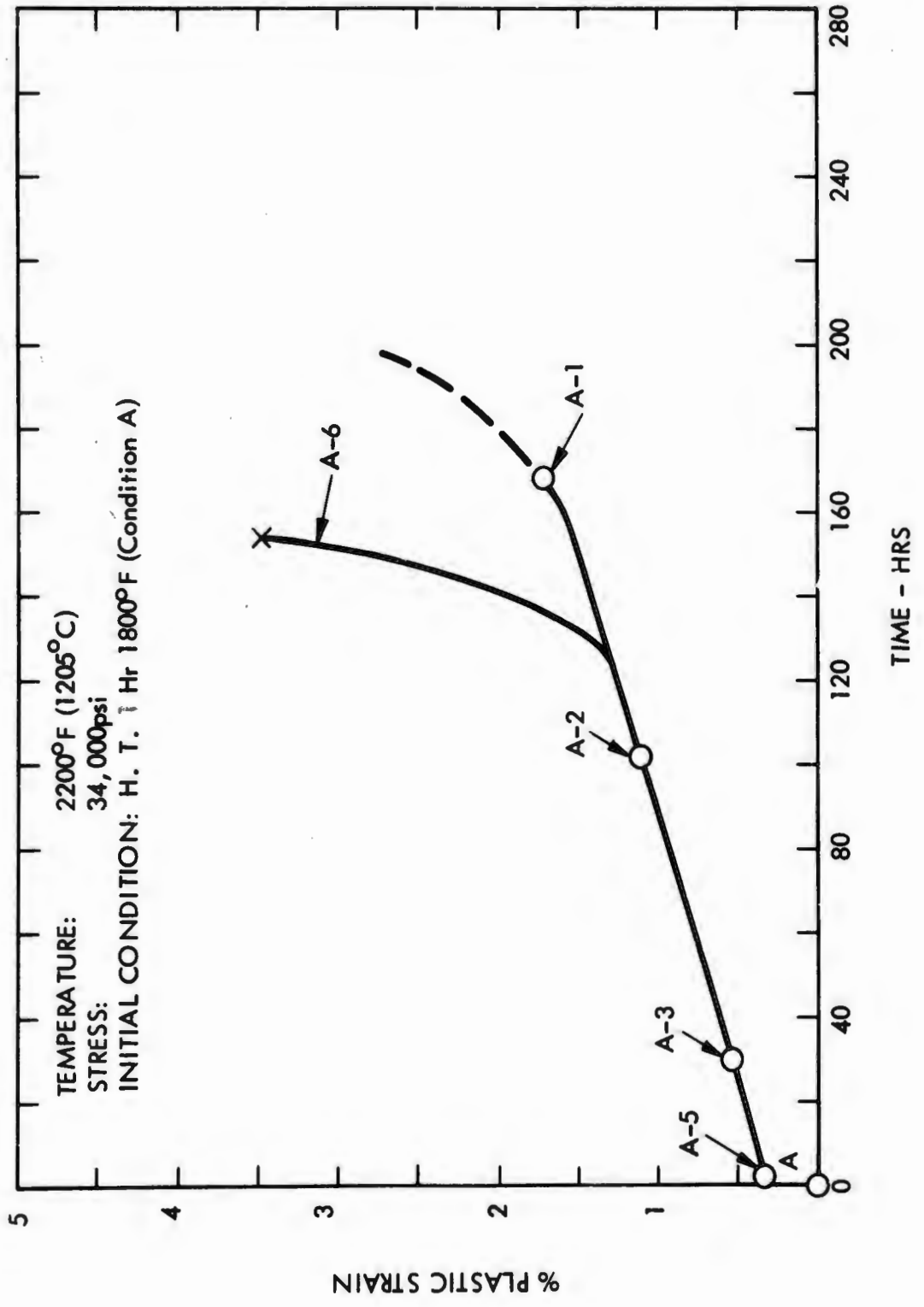

FiGURE 5. Condition of Specimens Evaluated by Optical and Electron Microscopy

creep specimen. The bulk extraction residues were examined by Debye Scherrer x-ray techniques and by TEM of the redispersed bulk extractions. The results of Debye Scherrer analysis of the extracted residues are given in Table 2. Also given in Table 2 are the compositions of the extracted cubic carbides which were determined from comparison of the lattice parameters to the data of Stecher et al.[4]

TABLE 2

Specimen No.	Creep Time at 2200°F	Phases Present	a_o - Å	a/o Hf in MC_{1-x}
A (as solution H. T.)	---	Zeta weak M_2C (hex) VVW		
		MC_{1-x} (cubic) M (broad)	4.47	14
A-5	1.5 hr.	M_2C (M) MC_{1-x} (W) Zeta (VW)	4.47	14
A-3	30.0 hr.	MC_{1-x} (S) (Broad)	4.57	35
A-2	107.8 hr.	MC_{1-x} (S) (Broad)	4.57	35
			4.58	36
A-1	167.8 hr.	MC_{1-x} (S) (Broad)	4.57	35
			4.58	36

The above data show a phase change from the metastable zeta to the NaCl type FCC MC_{1-x} carbide. The carbide in turn changes composition from 14 to 36 a/o during creep test. The two different sets of MC_{1-x} patterns in the longer time creep test extractions indicate that carbides are forming from two different sources, i.e., coarse precipitates vs. fine precipitates The broadness of the lines indicate a very fine particle size.

A. Characterization of the Initial Condition (Specimen A)

The optical micrographs of B-88 after one hour at 1800°C are shown in Figure 6. A well developed precipitation formed cellular substructure with a diameter of about 3 microns was characteristic of the material. The cell structure occurred in bands parallel to the stress axis. The precipitates were identified as the zeta phase (probably forming the larger plate-like and cell forming precipitates) with a small amount of the cubic carbide present. The cubic carbide had a lattice parameter of 4.47 Å with diffuse x-ray diffraction lines. This corresponds to a hafnium content of about 41 a/o.

The surface replicas of B-88 in the initial condition in Figure 7 shows considerable substructure bounded by carbide platelets. Also shown in Figure 7 are continuous carbide precipitates along all of the grain boundaries. The cell structure does not appear to form along crystallographic directions, although parts of the cell forming precipitates appear to form preferentially along crystal directions as shown in Figure 7C.

This material was also characterized by T.E.M. Many large areas viewable at 3,000X were obtained on the several foils utilized in this study. The transmission photographs given in Figure 8 show the discrete precipitate nature of the cell structure (Figures 8A and 8B). These observations are consistent with the optical and surface replicas described above. The stress axis is located by the lineage of the large platelike substructure formed from the precipitate in Figure 8A. This substructure forms parallel to the working axis of the swaged rod upon annealing.

Figure 8B is shown at a magnification of 40,000X in Figure 9. This area shows the finer Widmanstatten type precipitates within one of the subcells. Figure 10 shows a zeta platelet parallel to the plane of the foil. Such individual zeta platelets apparently form the cell walls of the structure seen optically in Figure 6 and by T.E.M. in Figure 9.

(a) 150X

(b) 1500X

(18,545)

FIGURE 6. Pre-Test Condition of B-88, Heat Treated 1 Hour at 1800°C Plus Quick Cool in He Gas.

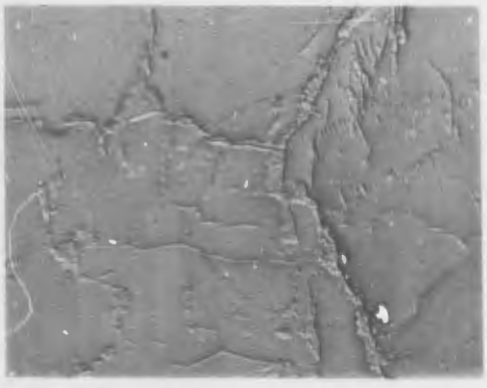

(a) (#3) 3,000X

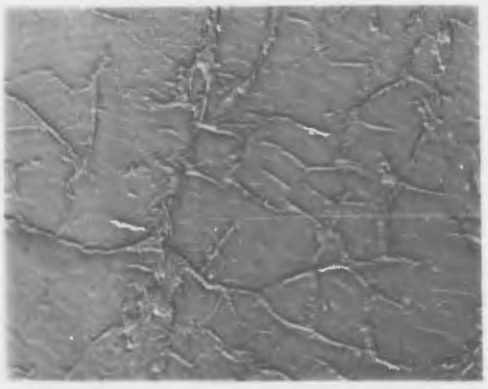

(b) (#5) 3,000X

(c) (#6) 10,000X

(0588-)

FIGURE 7. Surface Replicas of B-88 As Heat Treated 1 Hour at 1800°C Plus Quick Cool in He Gas. (Pre-Test Condition).

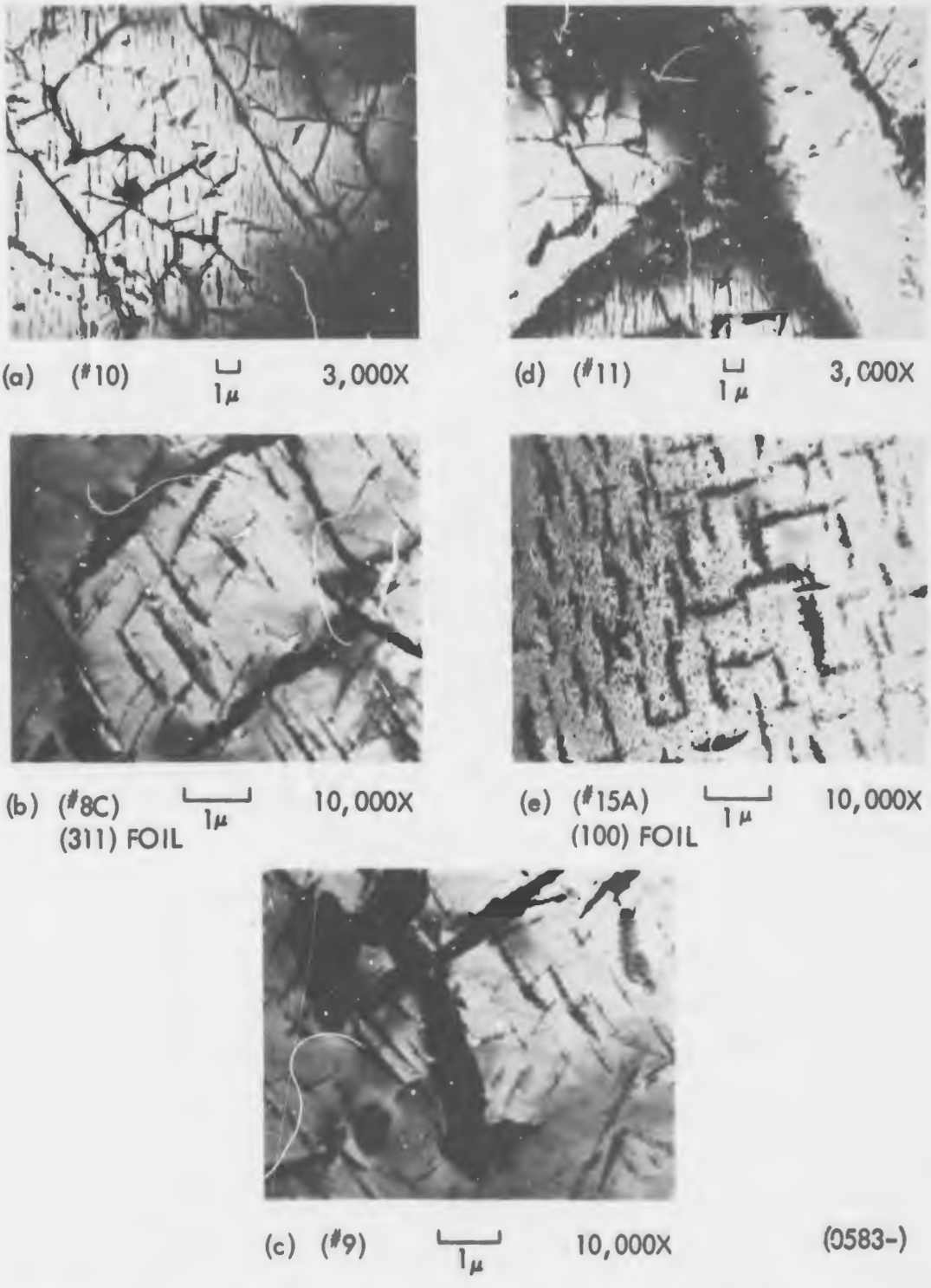

FIGURE 8. TEM of B-88 As Heat Treated 1 Hour at 1800°C Plus Quick Cool in He Gas. (Pre-Test Condition).

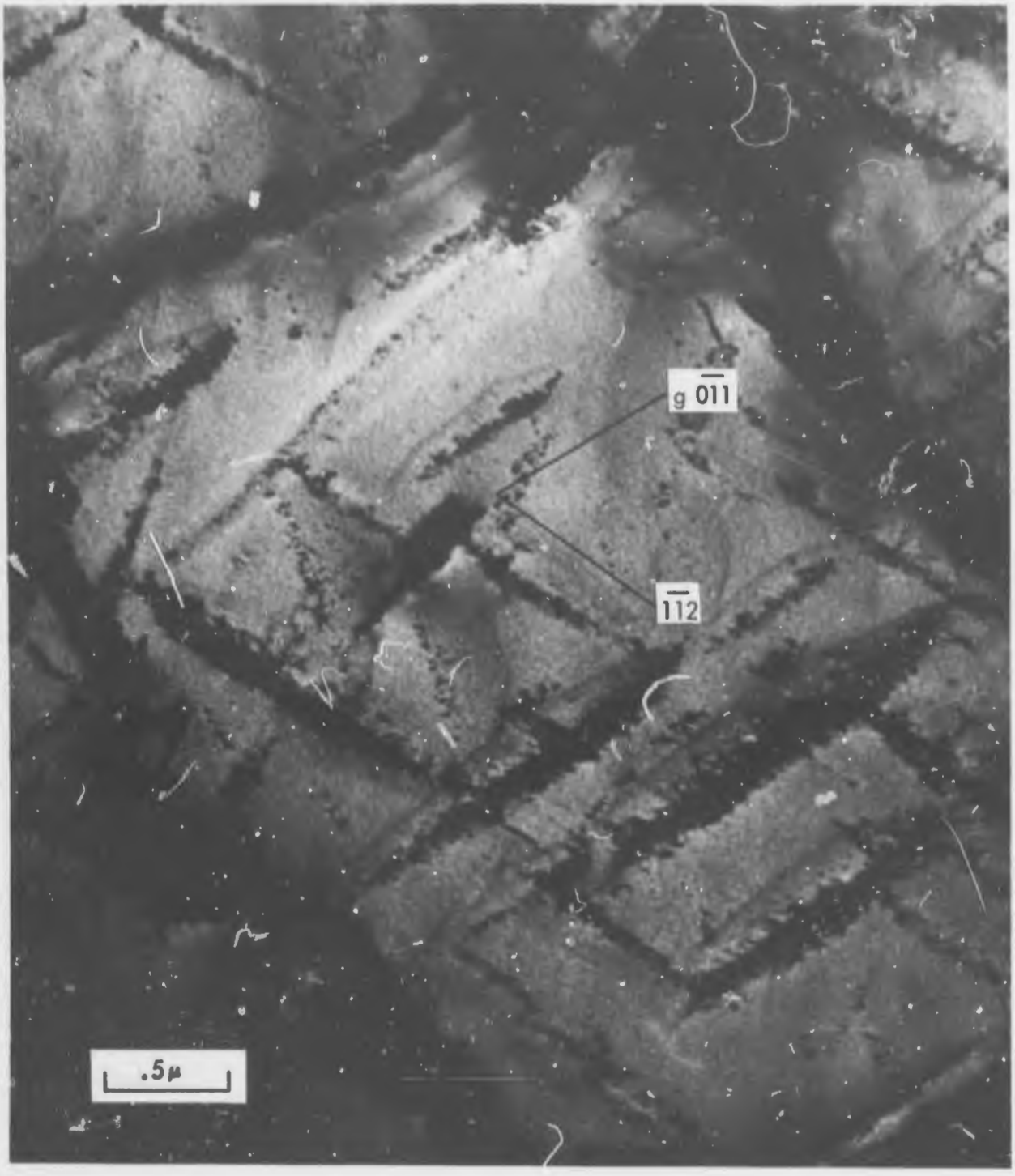

(0583-8C)

FIGURE 9. TEM of B-88 as Heat Treated 1 Hour at 1800°C Plus Quick Cool in He Gas.(311) Foil

.5μ (0583-6)

FIGURE 10. TEM of B-88 as Heat Treated 1 Hour at 1800°C Plus He Cool, Showing Zeta Platelet in Plane of Foil.

The extremely fine precipitate forming along crystallographic directions in all of these photographs was not expected. In some cases (Figure 8E) the precipitates appear to be clusters of smaller precipitates on the order of 500 Å diameter. This could possibly be a decomposition product. Selected area electron diffraction patterns of areas such as in Figure 8B and 8E show the fine precipitates to form on (110) planes. Since the cubic carbide XRD patterns from extraction residues were very diffuse, we can assume that the fine precipitates are the cubic (Cb, Hf) C_{1-x}. This assumption is consistent with the phase relationships phenomena for B-88 discussed earlier. T.E.M. photographs of the bulk extruded phases from the alloy in the initial conditions are shown in Figure 11. The zeta phase and a trace of the hexagonal phase were identified here. The finer precipitates shown in Figures 8, 9, and 10 were not retained during the bromine extraction and redispersion process. The morphology of the zeta platelets in the bulk extractions (Figure 11A) corresponds nicely with that shown in Figure 10.

B. Specimen A-5, Creep Tested 1.5 hours at 2200°F to 0.33% Plastic Strain

The substructure of the specimen creep tested into primary strain appears smaller (sub-grain diameter of approximately 1 micron) and more generally distributed as shown in Figure 12. The grain boundaries are still host to a continuous carbide. X-ray diffraction results show a cubic plus a hexagonal carbide present with a few unidentified lines that may be from the zeta phase. The surface replicas in Figure 13 show some of the various substructure forms ranging from cells in (13a)and (13d) to parallel rows of platelets in Figures (13b) and (13 c).

The TEM photograph in Figure 14 shows the cell structures are still composed of long platelike or blade-like precipitates which have transformed from the zeta phase to either cubic (MC_{1-x}) or the hexagonal M_2C carbides. The finer uniformly distributed Widmanstatten type precipitates observed in the as-heat treated alloy have not changed their distribution during the 1.5 hours at 2200°F as shown in Figures 14 and 15. The EDP pattern of the (111) foil in Figure 15 shows that the oriented plate-like precipitates lie parallel to the <110> crystallographic directions and indeed on (110) planes. A few undecorated dislocations are

(a) (#2a)

1μ

(b) (#3)

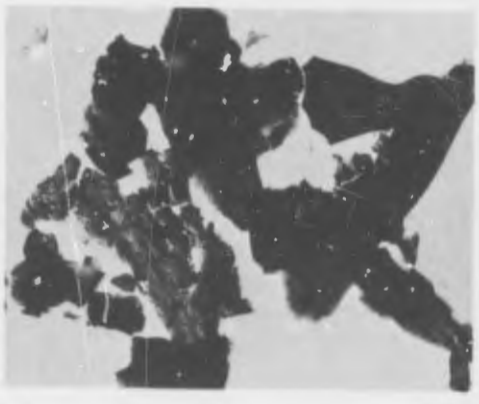

(c) (#5)

(#0593 -)

FIGURE 11. T.E.M. of Redispersed Bulk Extraction from B-88 (Specimen A) as H.T. 1 Hr. at 1800°C.

(a) 150X

(b) 1,500X

(18,549)

FIGURE 12. Specimen A-5 As Creep Tested 1.5 Hr. at 2200°F (1205°C) at 34,000 psi, Plastic Strain = 0.33%

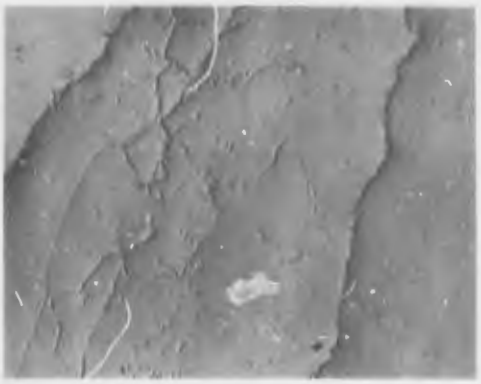

(a) (#4) 3,000X

(c) (#6) 10,000X

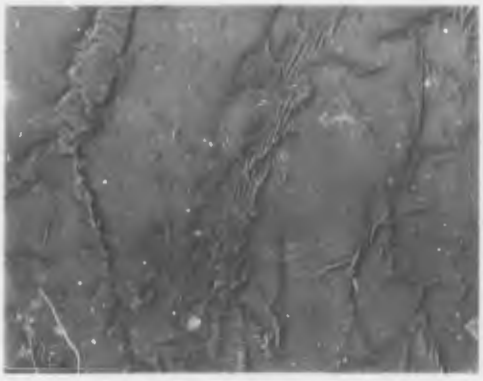

(b) (#7) 10,000X

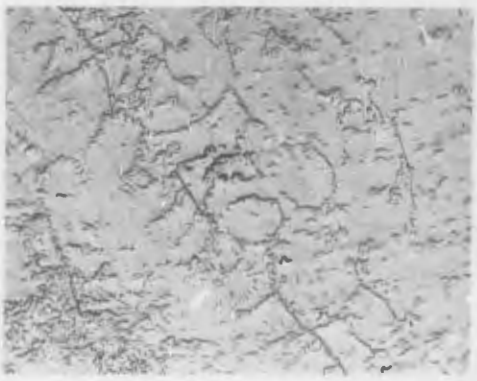

(d) (#5) 3,000X

(e) (#5) 10,000X

(0592-)

FIGURE 13. Surface Replicas of Specimen A-5 (B-88) As-Creep Tested 1.5 Hr. at 2200°F (1205°C) at 34,000 psi, 0.35% Plastic Strain.

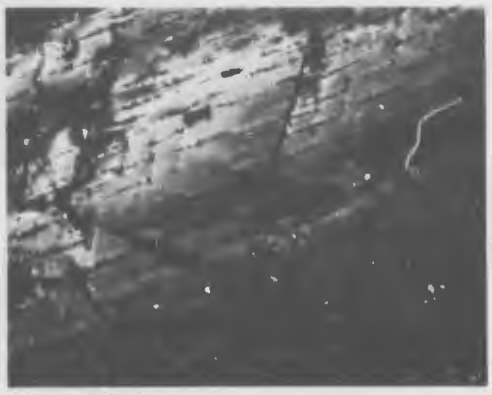

(a) (#3a)

(d) (-14)

(b) (111) Foil (-13a)

(e) (-12)

(c) (-11)

1μ

(f) (-6a)

(#0584-)

FIGURE 14. TEM of B-88 (Specimen A-5) Creep Tested 1.5 Hr. at 2200°F, 34,000 psi to 0.33% Plastic Strain Mag = 10,000X

(#0584-13A)

FIGURE 15. TEM of B-88 (Specimen A-5) Creep Tested 1.5 Hour at 2200°F, 34,000 psi, 0.33% Plastic Strain (111) Foil.

apparent after 0.33 percent plastic strain. Strongly decorated dislocation substructures were occasionally observed as shown in Figure 16. Close examination of the precipitates on the dislocation substructure show dense core precipitates which are bound with fins apparently on preferential growth planes. The nodes on dislocation intersections are decorated with heavier blocky precipitates about 0.15μ in diameter.

TEM photographs of the bulk extraction residue in Figure 17 show platelet type precipitates of varying morphologies. Transmission photographs of the bulk extraction residue of the sample creep tested into the primary stage are shown in Figure 17. With the exception of the presisting zeta platelets in Figure 17a, 17c and 17d, the morphology of these precipitates are greatly different from those extracted from the as-solutioned material shown in Figure 11. There is a predominance of much faceted, "lacey" material which measures 10 to 15μ in breadth by less than 2000 Å in thickness (since they are transmissive to electrons) as shown in Figures 17a and b. Some of the lacey precipitate contains a single thicker spine as shown in Figures 17a and 17d. These lacey precipitates probably occur on grain boundaries and derive their faceted or lacey appearance from the structure at the boundary. The spines are interpreted as precipitate decoration of grain edges (grain edges are equivalent to triple points in two dimensions). The zeta platelets and many of the more uniform platelets shown in Figures 17c and 17e are most probably associated with the substructure network. The fan-shaped zeta precipitate in Figure 17b is readily identified from earlier work (see Figures 3 and 11). The uniform platelets in Figures 17a and 17e were identified as the cubic carbide by electron diffraction pattern (EDP). The lacey or faceted precipitates in 17a, 17b and 17d may be the hexagonal M_2C carbide although we could not determine this from the EDP due to the highly faulted nature of these platelets.

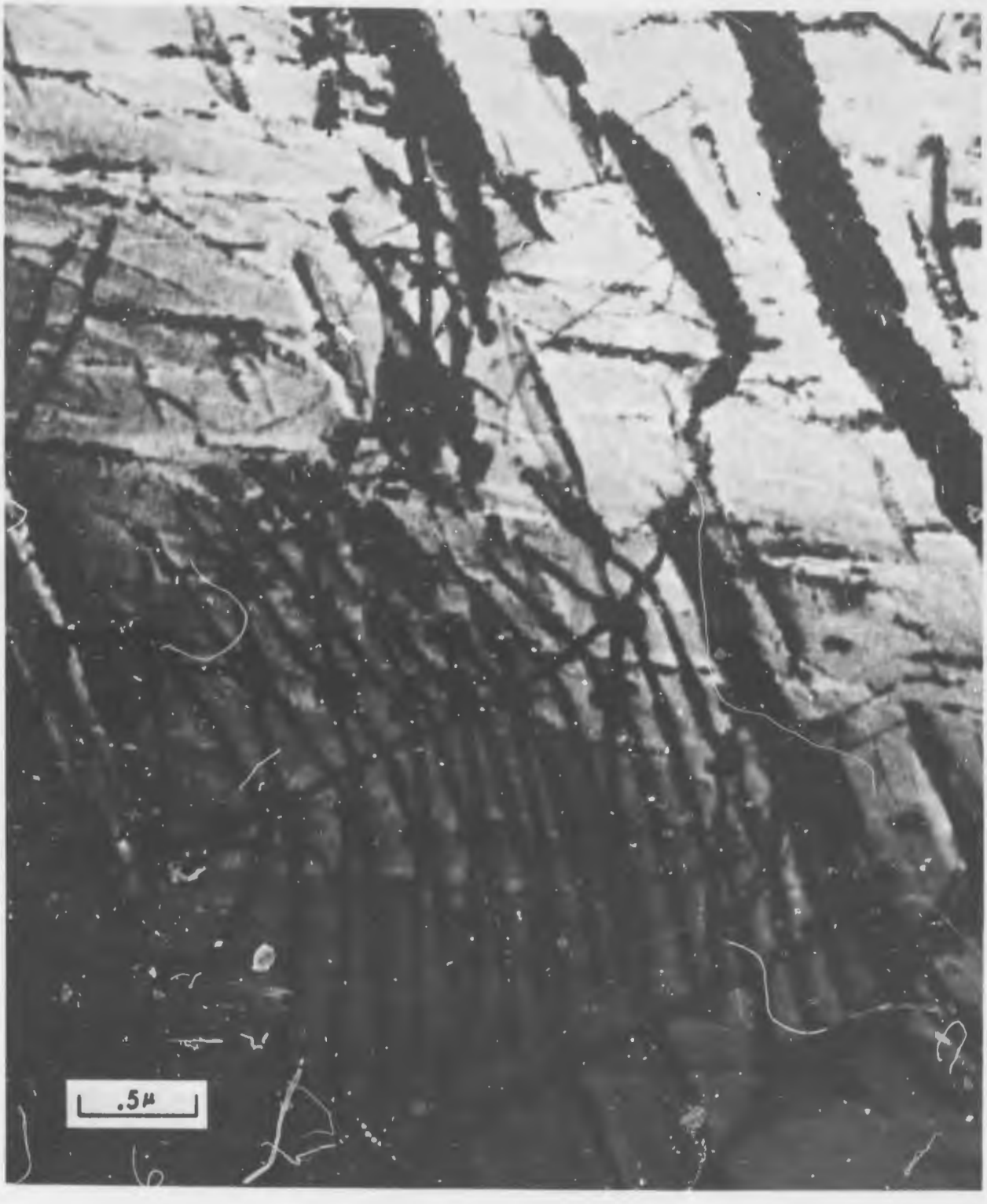

(0584-11)

FIGURE 16. TEM of B-88 (Specimen A-5) Creep Tested 1.5 Hr. at 2200°F, 34,000 psi to 0.33% Plastic Strain

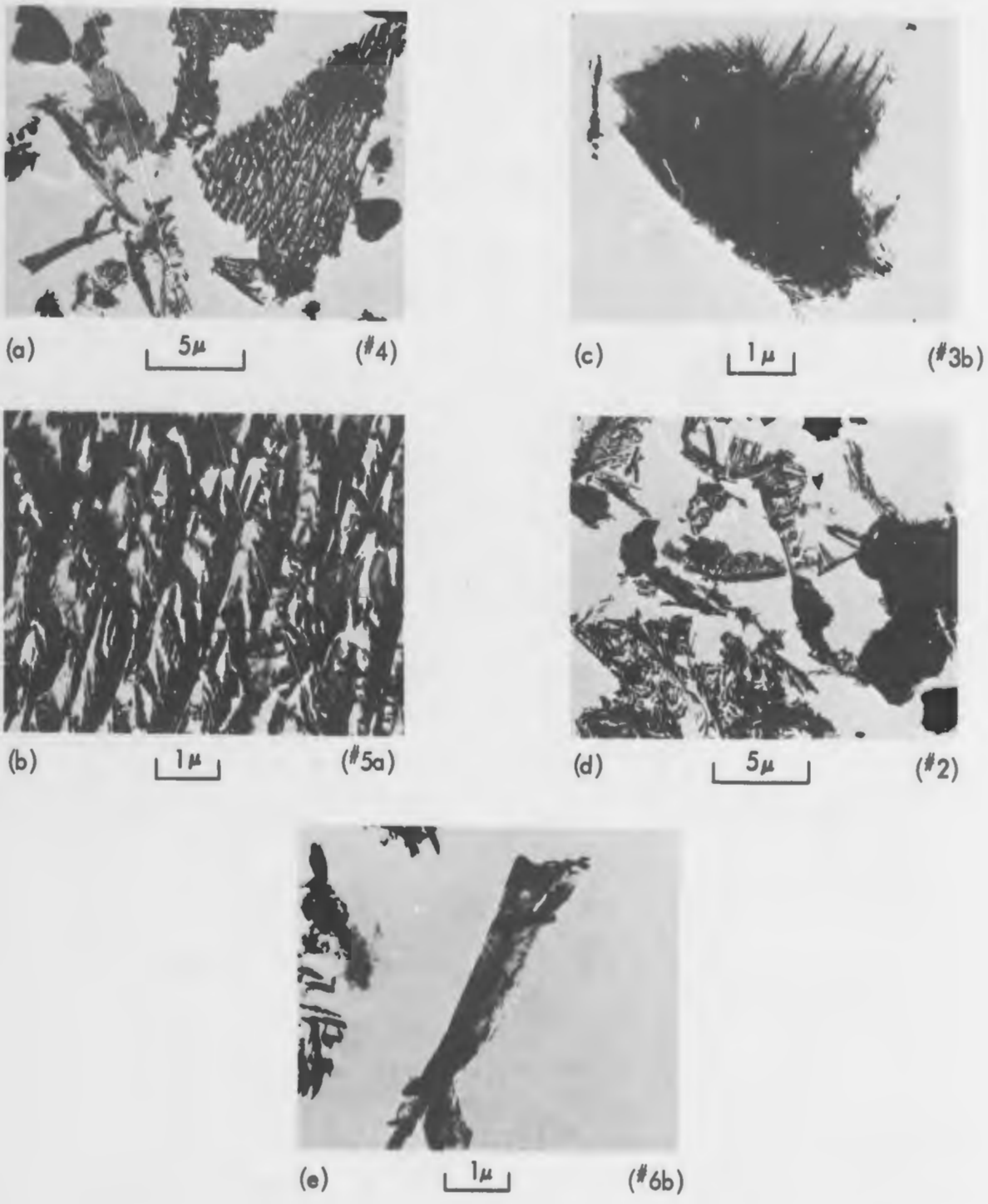

(0597-)

FIGURE 17. TEM of Bulk Extractions from B-88 (Specimen A-5) Creep Tested 1.5 Hr. at 2200°F (1205°C) 34,000 psi to 0.33% Plastic Strain

C. Specimen A-3, Creep Tested 30 Hours at 2200°F to 0.67% Plastic Strain

The optical photomicrographs of Figure 18 show that the fine cell structure is beginning to decompose into more randomly distributed precipitates. This trend is also apparent from the surface replicas in Figure 19. Another important observation is the relative freedom of continuous grain boundary precipitates in Figures 18b and 19c.

The transmission photos in Figure 20 on first glance look similar to the initial condition. The electron diffraction patterns of the area in Figure 20 shows the precipitates to lie parallel to <110>directions and are probably on (110) planes. However, these carbides appear to be more continuous than the Widmanstatten carbides in the initial condition. Figures 20e, 20f, 22, and 23 show the dislocations to be apparently associated with the carbides. These figures show considerable dislocation curvature and in Figure 21 (top) a perfect dislocation loop. The "lattice work" formed by the Widmanstatten precipitates shows strong interactions with the undecorated dislocations. The parallel "stack-up" array of the large (but thin) precipitates in Figure 20a is probably due to decoration of a precipitation substructure formed during the earlier stages of creep and may be considered to be a further stage of the decoration taking place on the dislocation substructure in Figure 16 from the specimen which had been creep tested at 2200°F for 1.5 hours.

The transmission photagraphs of the bulk extracted carbide of this specimen in Figure 24 show that the larger thin lacey platelets and the zeta platelet existing after 1.5 hours at 1205°C (Figure 17) have decomposed. Those presented in Figure 24 are longer blade-like precipitates which probably form within the matrix similar to the precipitates shown in Figures 20 and 23. Although some of the Widmanstatten precipitates forming the "lattice work" in Figures 20 (d, e, f) are probably represented in Figure 24, we feel that many of the very fine precipitates are lost during decantation during the bulk extraction process. The lattice parameter of the extracted carbides corresponds to a hafnium content of 35 a/o or a 16 a/o increase over that of the initial cubic carbide.

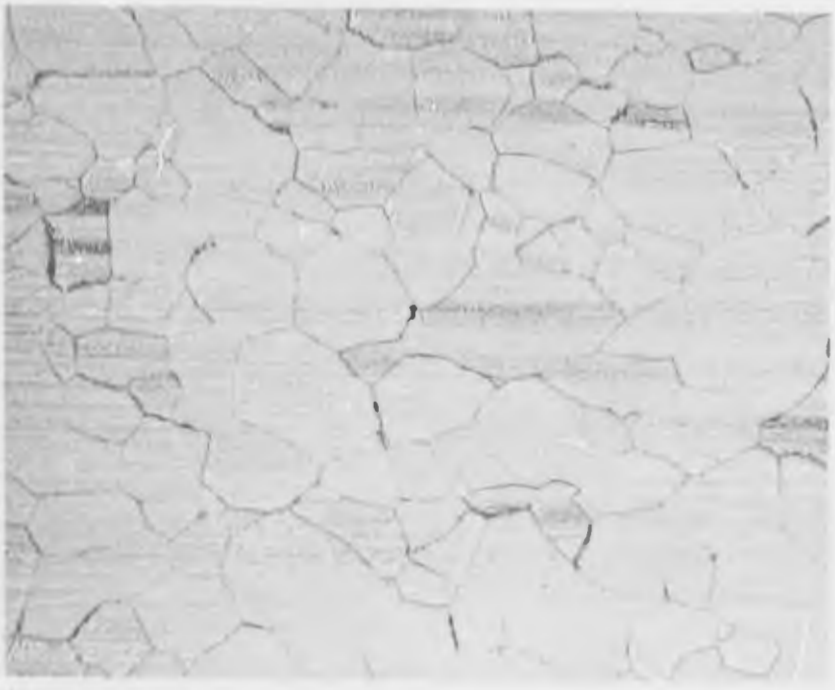

(a) 150X

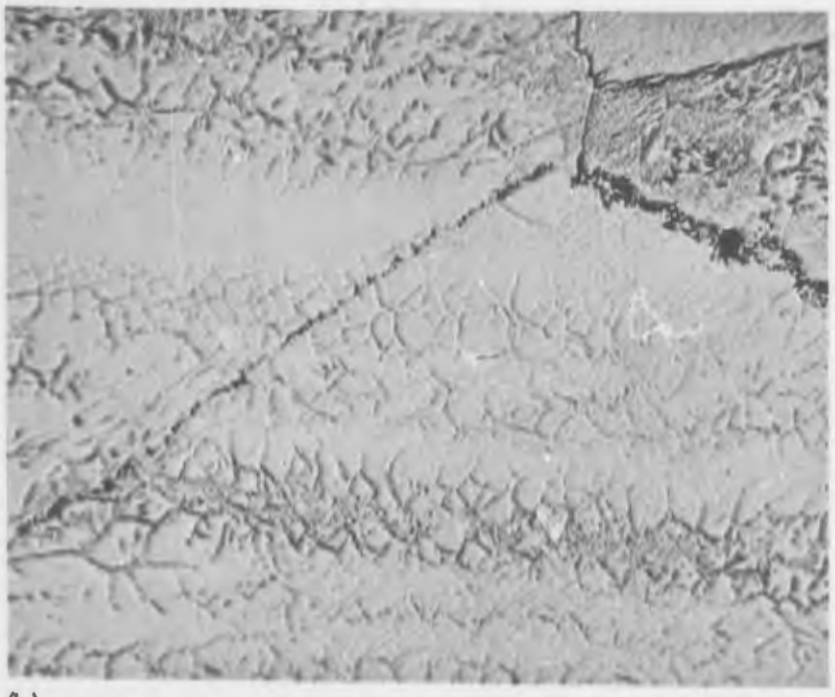

(b) 1,500X

(18,548)

FIGURE 18. Specimen A-3 (B-88) As Creep Tested 30 Hours at 2200°F (1205°C) at 34,000 psi, 0.67% Plastic Strain.

(a) (#5) 3,000X

(c) (#4) 3,000X

(b) (#2) 10,000X

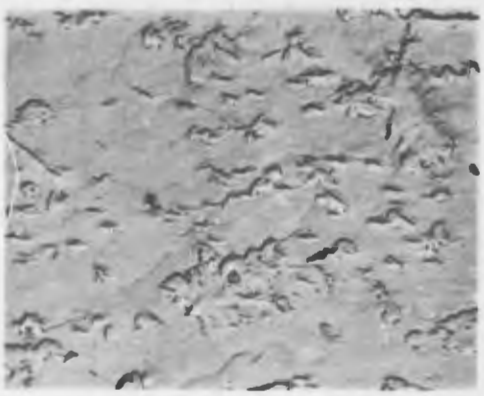

(d) (#3) 10,000X

(0591-)

FIGURE 19. Surface Replicas of Specimen A-3 (B-88) As Creep Tested 30 Hours at 2200°F (1205°C) at 34,000 psi, 0.67% Plastic Strain.

(a) (#16) 5μ (3000X)

(d) (#2a) 1μ (10,000X)

(b) (#4) 5μ (5000X)

(e) (#7c) 1μ (10,000X)

(c) (#5) 5μ (5000X)

(f) (#12) 1μ

(0585-)

FIGURE 20. TEM of B-88 (Specimen A-3) Creep Tested 30 Hours at 2200°F (1205°C) at 34,000 psi, 0.67% Plastic Strain

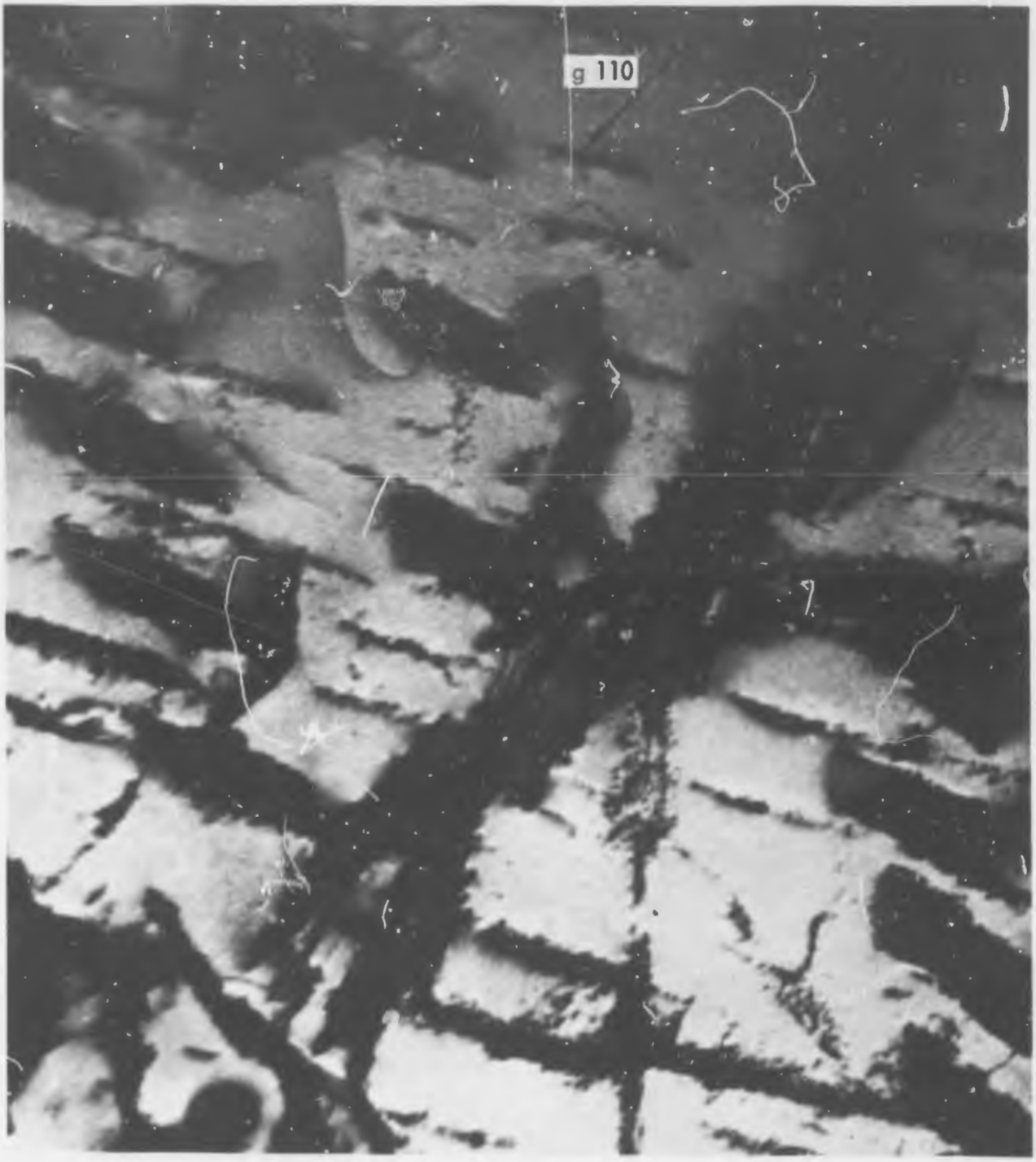

(0585-11a)

FIGURE 21. TEM of B-88 (Specimen A-3) Creep Tested 30 Hours at 2200°F at 34,000 psi, 0.67% Plastic Strain.

(#0585-12)

FIGURE 22. TEM of B-88 (Specimen A-3) Creep Tested 30 Hours at 2200°F at 34,000 psi, 0.67% Plastic Strain

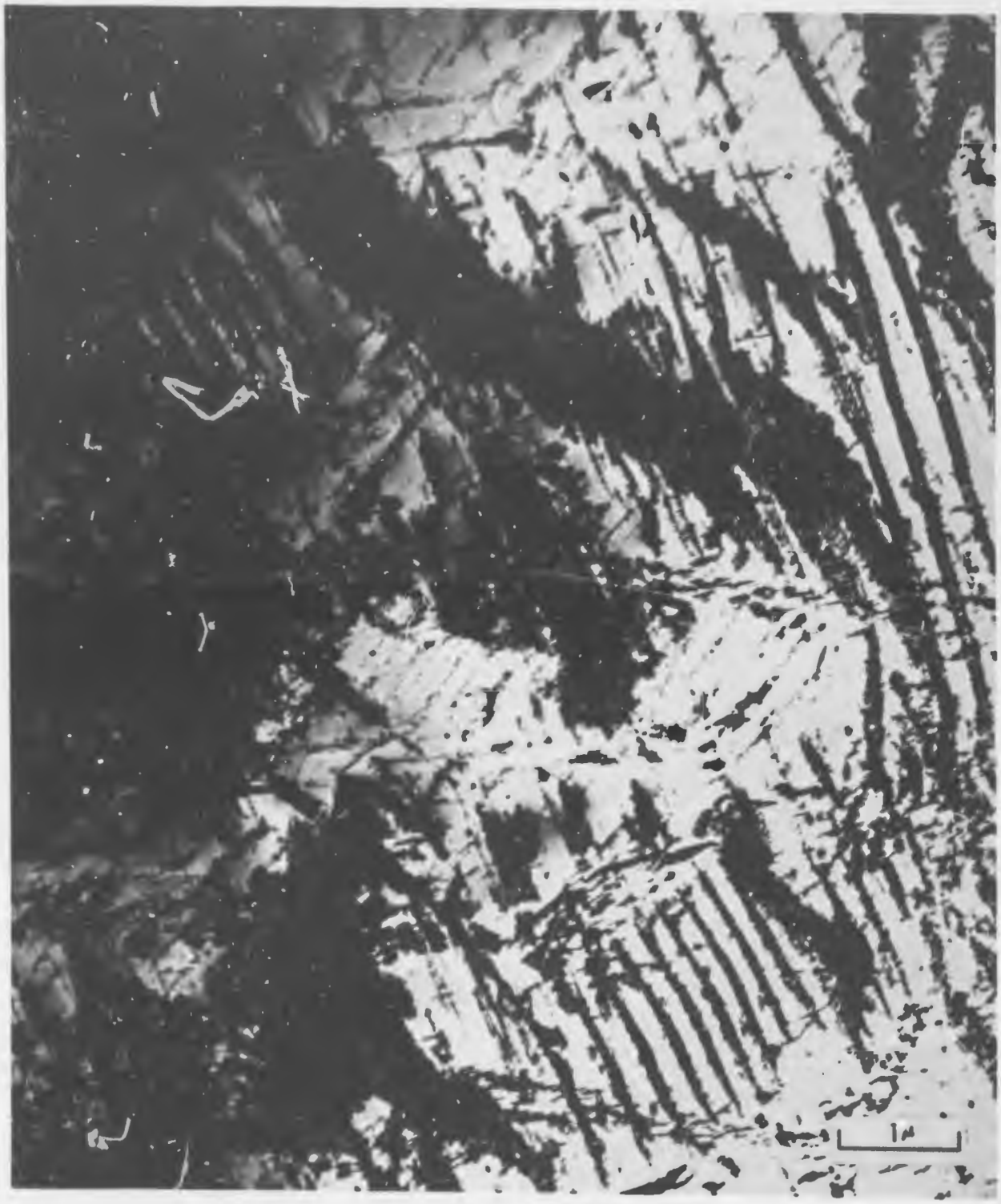

(#0585-4)

FIGURE 23. TEM of B-88 (Specimen A-3) Creep Tested 30 Hours at 2200°F at 34,000 psi, 0.67% Plastic Strain.

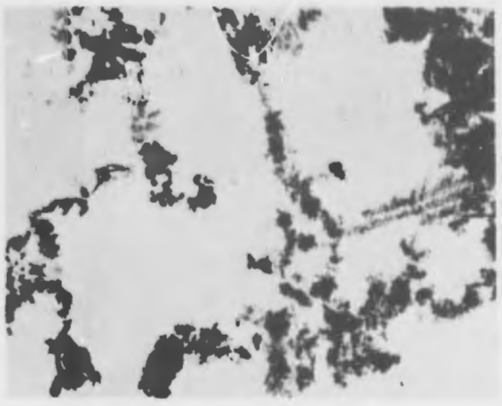

(a) #1a 1 μ 10,000X

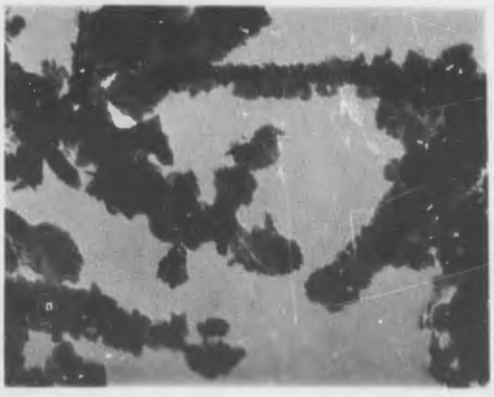

(b) #2a 30,000X

1 μ

(#0596)

FIGURE 24. TEM of Bulk Extractions from B-88 (Specimen A-3) Creep Tested 30 Hours at 2200°F, 34,000 psi, 0.67% Plastic Strain.

D. Specimen A-2, Creep Tested 107.8 Hours at 2200°F to 1.0% Plastic Strain

This specimen was tested approximately two-thirds of the way through second-stage creep before removal and sectioning. Therefore, the grain boundary separation in the 1500X optical micrographs in Figure 25 was unexpected. Since this could possibly be an etching affect, we evaluated surface replicas of this material. The replicas in Figures 26a and 26b show voids formed along boundaries and grain boundary separation on some boundaries normal to the stress axis. This observation places the onset of void formation and grain boundary sliding back to mid-second stage area.

The optical and surface replica micrographs show that the original precipitate substructure has almost completely transformed and dispersed throughout the matrix. Extracted precipitates from the A-2 specimen were the cubic carbide with a lattice parameter of 4.587 Å. Much line broadening was observed indicating either very fine (thin) precipitates or a range of composition. These parameters correspond to a hafnium content of 35 a/o and thus does not represent any significant change from the previous condition.

The microstructure of the specimen tested for 108 hours at 1205°C (2200°F) as viewed by transmission electron microscopy are shown in Figures 27 through 33. The range of structures and precipitate morphologies observed are shown on Figure 27. Some coarsening of the "lattice work" Widmannstatten precipitates have occurred although they still have about the same interplatelet spacing and still are on matrix (110) planes as demonstrated in Figures 27a and 29. A better appreciation for the range of structures obtainable is shown in the 3000X montage photographs in Figure 28. These photographs from a traverse across a (111) oriented grain show remnants of the original substructure (which defines the stress axis of this particular foil). Precipitation decorated pile-ups are shown near the grain boundary in frame no. 12b and in the lower portion of frame no. 12e. A number of highly curved dislocations appear, in areas where diffraction conditions permit, associated with the substructure

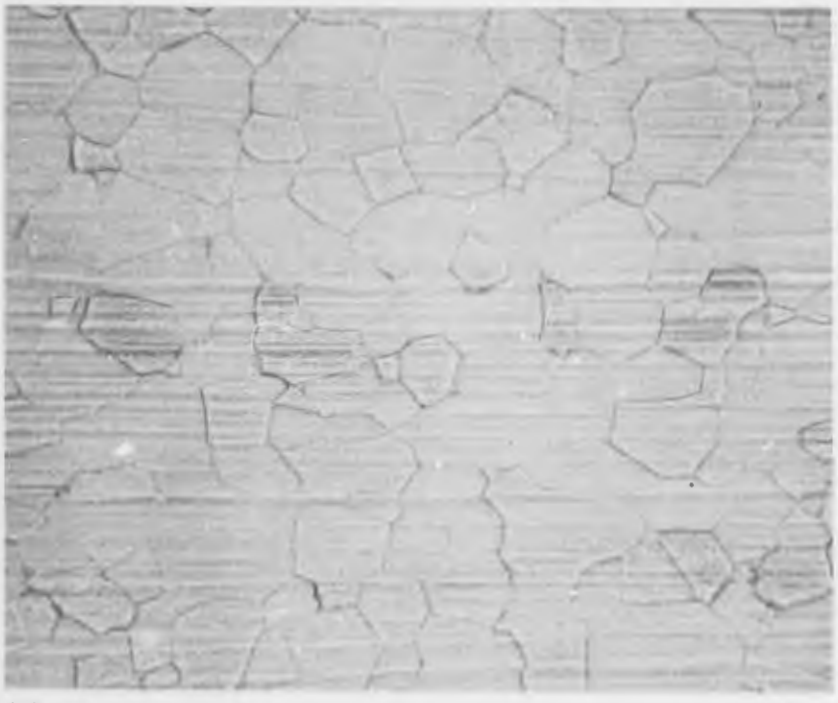

(a) 150X

(b) 1,500X

(18,547)

FIGURE 25. Specimen A-2 As Creep Tested 107.8 Hours at 2200°F (1205°C) at 34,000 psi, 1.0% Plastic Strain.

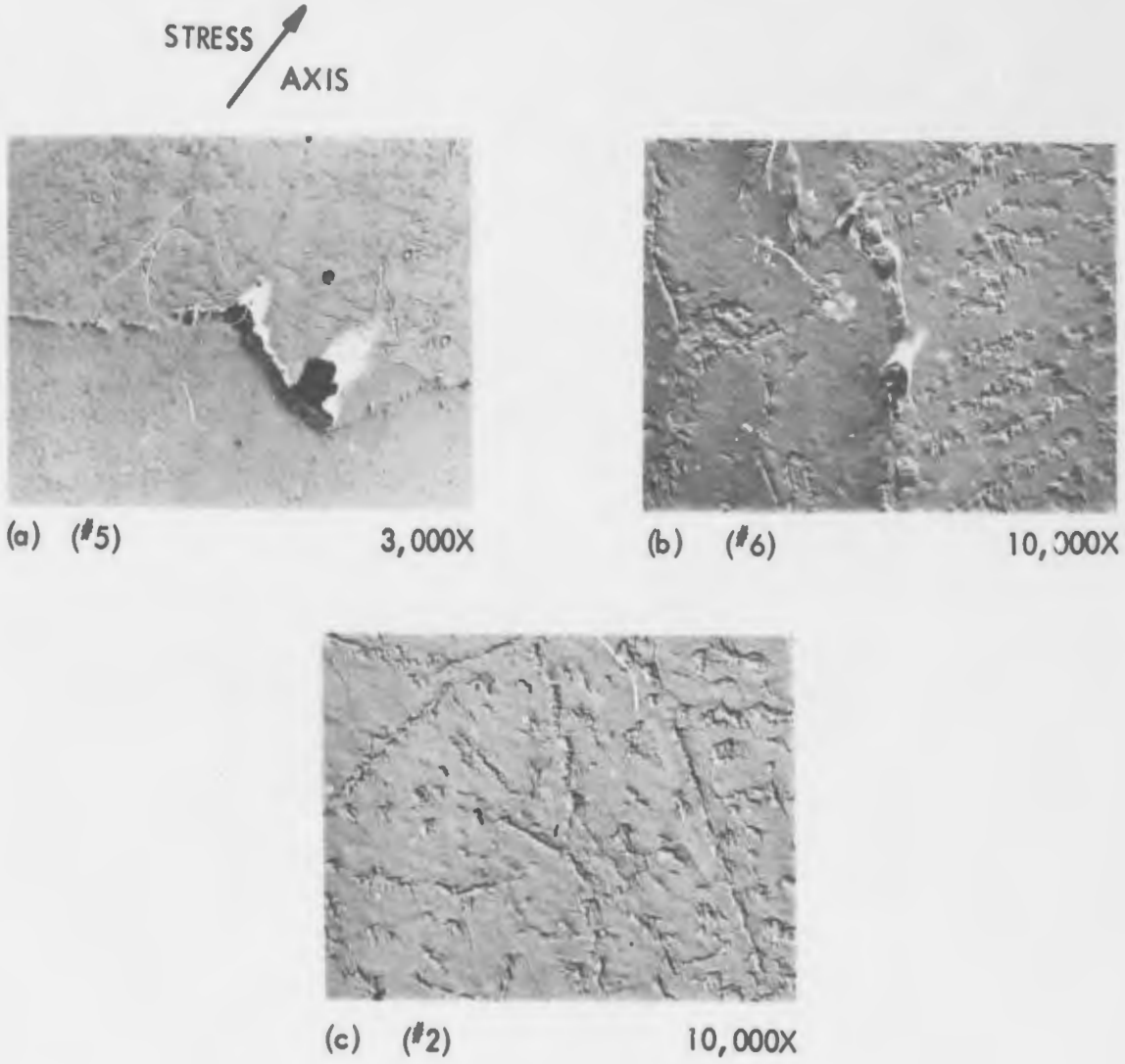

(0590)

FIGURE 26. Surface Replicas of Specimen A-2 (B-88) As Creep Tested 107.8 Hours at 2200°F (1205°C) at 34,000 psi, 1.0% Plastic Strain.

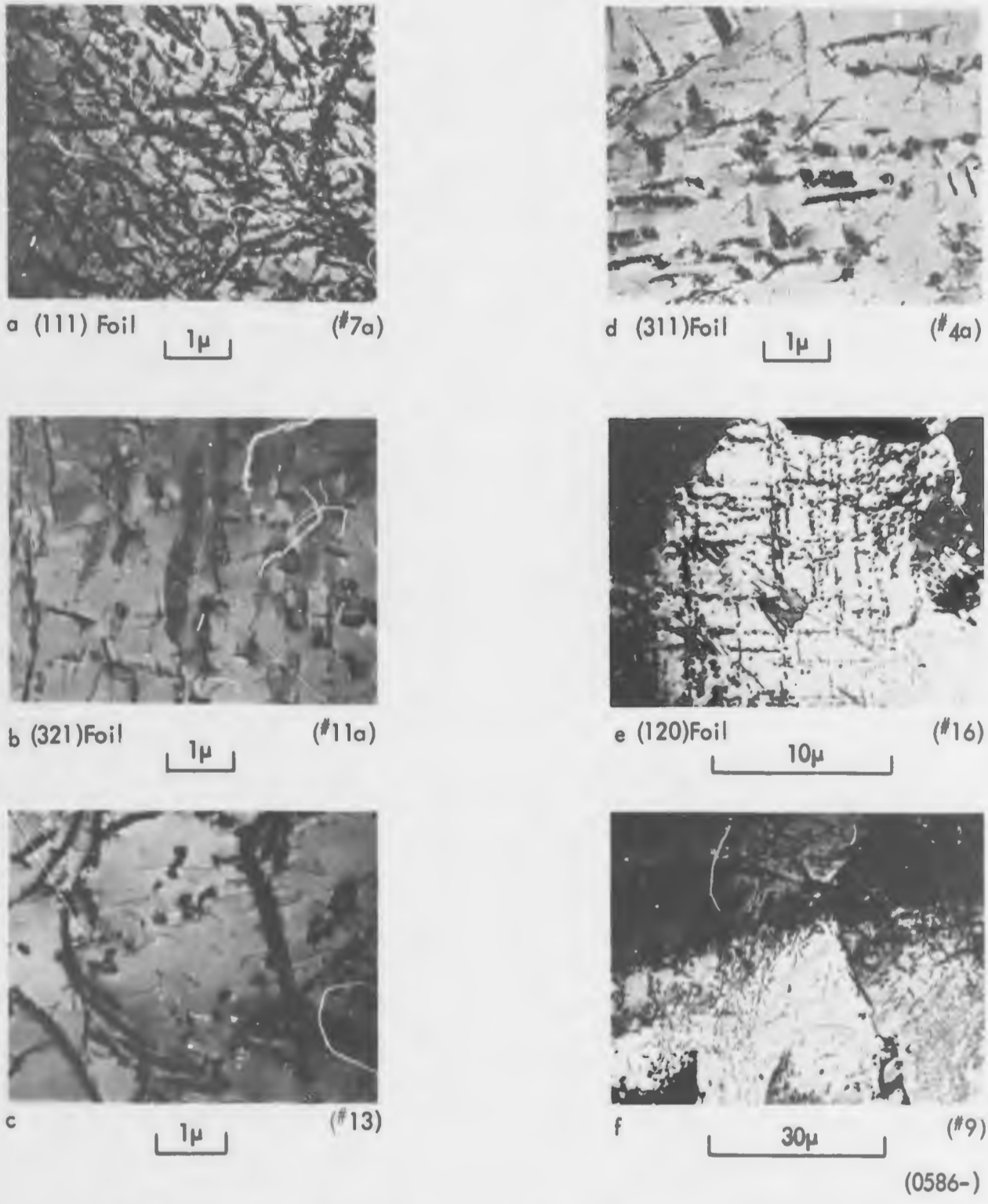

FIGURE 27. TEM of B-88 (Specimen A-2) Creep Tested 107.8 Hours at 2200°F (1205°C) at 34,000 psi, 1.0% Plastic Strain.

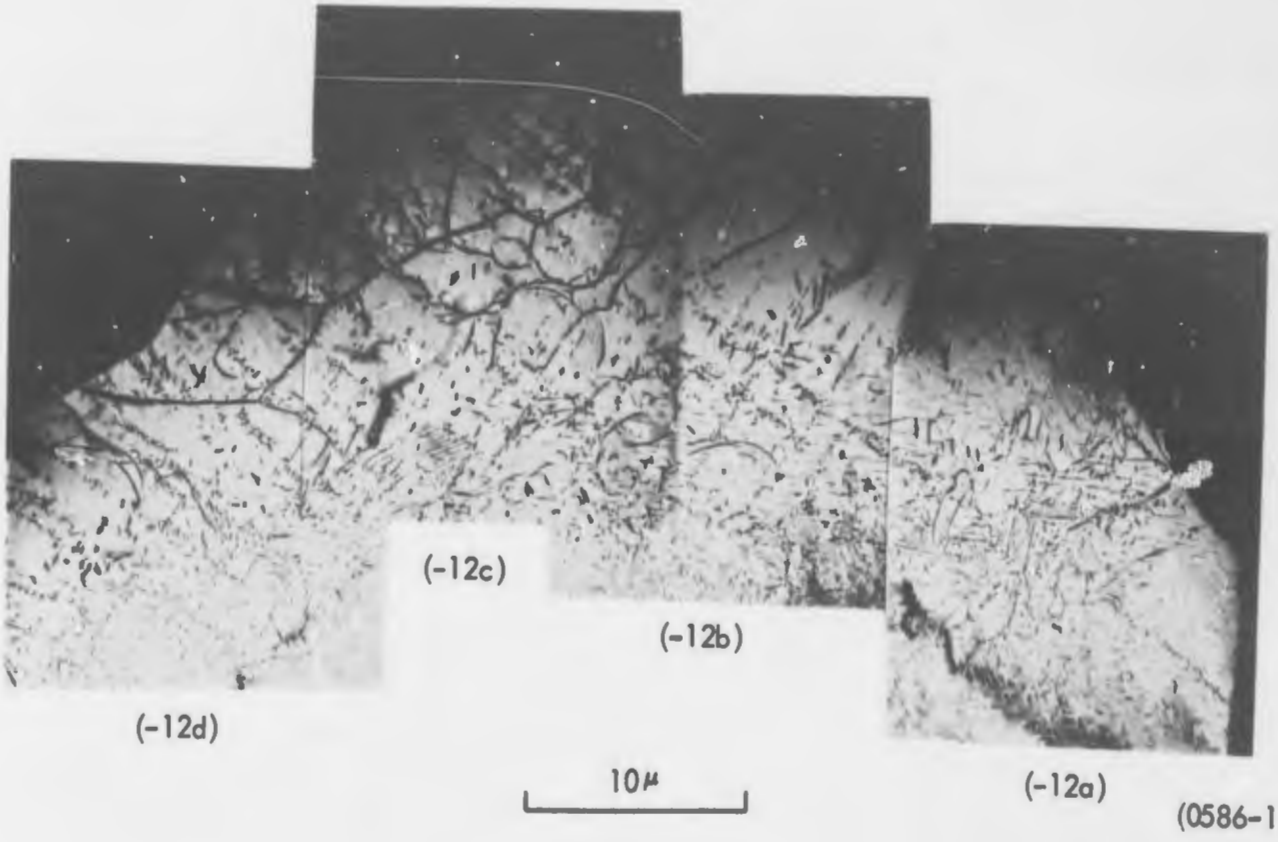

FIGURE 28. Composite Photograph TEM of (111) Foil of B-88 (Specimen A-2) Creep Tested 107.8 Hours at 2200°F (1205°C), 34,000 psi to 1.0% Plastic Strain - Magnification; 3000X.

precipitates and the finer (110) Widmanstatten or lattice work precipitates. Figure 29 shows the intimacy of the interaction of dislocations with the lattice work (110) platelets. The dislocations entangled in the lattice work are probably immobile. The lattice work platelets in the (321) foil of Figure 30 are shown in edge view (upper part of photograph) and approximately in plane view. The dislocations that bound the precipitate in the plane of the foil in the lower center portion of the photograph are probably similar to the dislocations that are shown to be intertwined with the end-on plates in the upper portion of Figure 30. Figure 31 shows many dislocations, apparently resulting from Frank-Read sources, and some loops in the (120) foil. In addition, a few coherent precipitates (see arrows) were noted. The larger platelet structure appears to be a decorated dislocation structure with fins connecting to coarser, more heavily decorated cores.

This specimen also showed considerable grain boundary migration as illustrated in Figures 32 and 33. The migrating boundary in Figure 32 is sufficiently clear of precipitates for thickness fringes to be readily visible. The area swept out by boundary migration in Figure 33 shows tangles of dislocations and precipitates on (110) planes in the same orientations as in the parent grain. These dislocations would be expected since this boundary lies at approximately 45 degrees to the stress axes hence, shear in addition to boundary migration was occurring during the creep test. The migrated portion of the boundary is much decorated with precipitates and was probably immobile. The boundary in Figure 32 being relatively free of pinning obstructions, was probably still moving at the termination of the test.

E. Specimen A-1, Creep Tested 168 Hours at 2200°F to 1.66% Plastic Strain

This specimen was allowed to reamin in third stage creep for 10 to 20 hours before the test was discontinued. The optical micrographs in Figure 34 show that the initial substructure forming precipitate substructure has completely disappeared and the cubic carbides have transformed to a more stable form. Numerous W type voids at boundaries normal to the stress axis as well as small type voids were observed. These observations are consistent with the electron micrographs of the replicas shown in Figure 35. Also of interest in Figure 35 is the grain boundary migration.

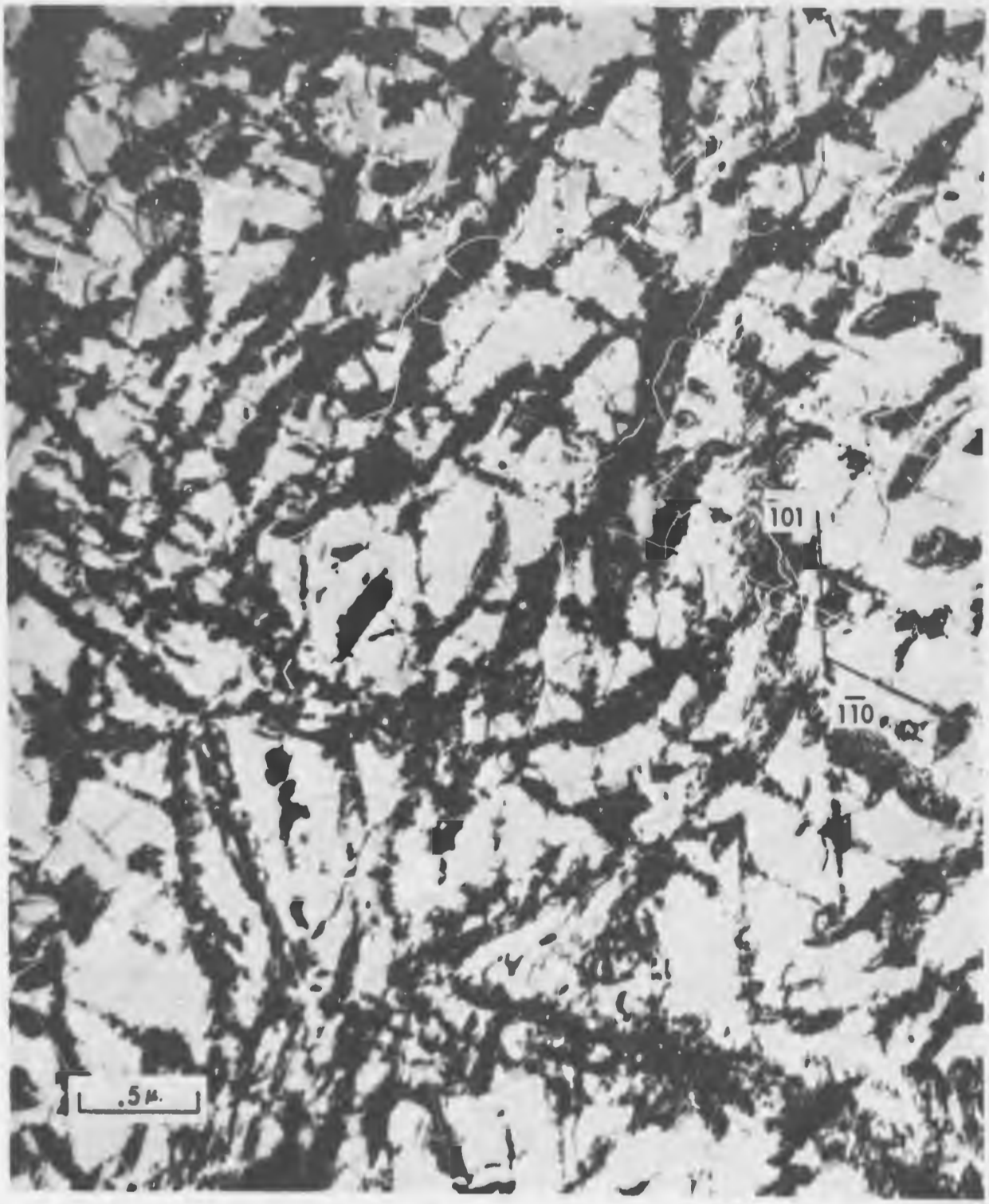

(0586-7a)

FIGURE 29. TEM of B-88 (Specimen A-2) Creep Tested 107.8 Hours at 2200°F, 34,000 psi, 1.0% Plastic Strain (111) Foil.

(#0586-11a)

FIGURE 30. TEM of B-88 (Specimen A-2) Creep Tested 107.8 Hours at 2200°F (1205°C) at 34,000 psi to 1.0% Plastic Strain (321 Foil.

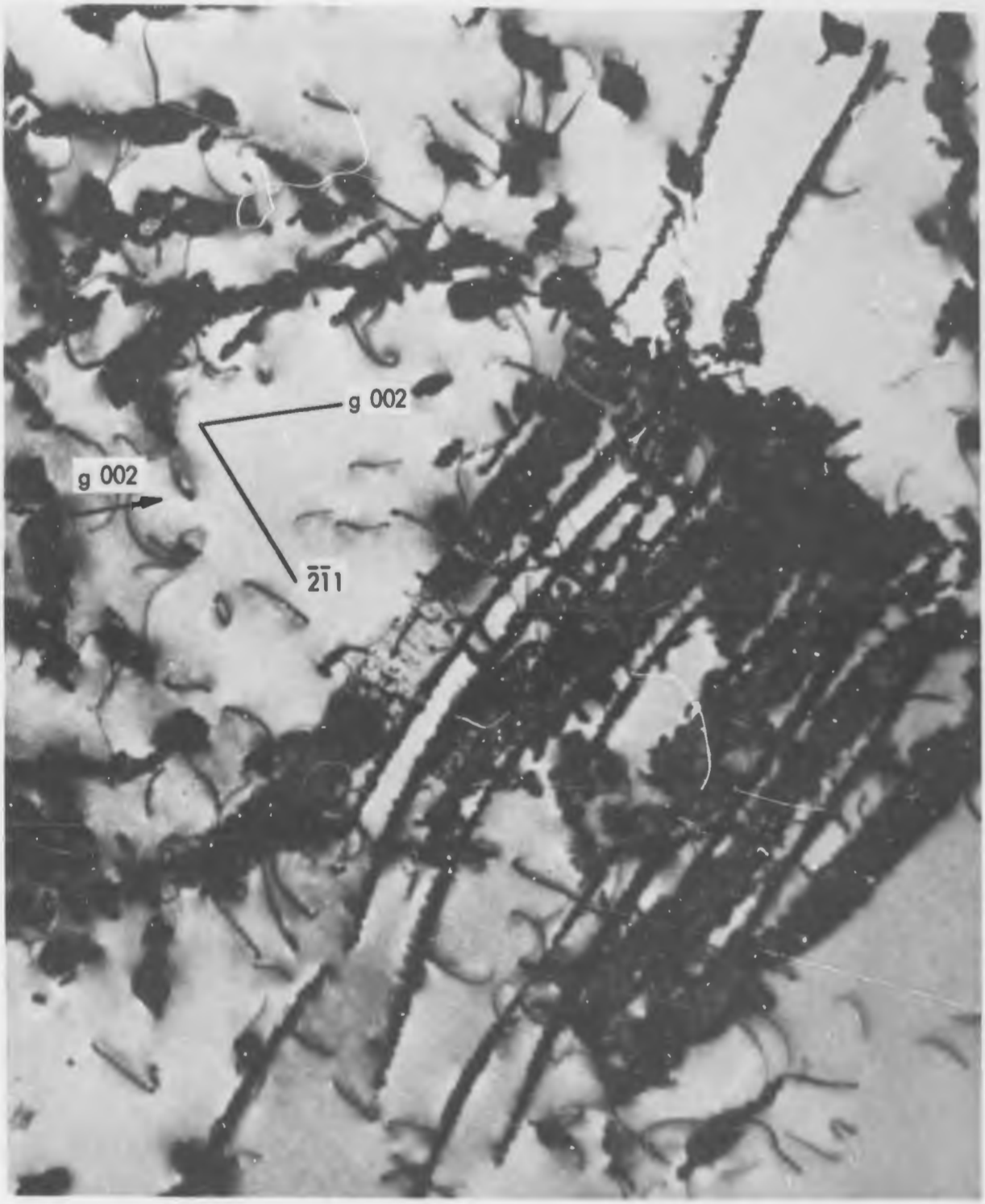

(#0586-15A)

FIGURE 31. TEM of (120) Foil of B-88 (Specimen A-2) Creep Tested 107.8 Hours at 2200°F, 34,000 psi, 1.0% Plastic Strain.

10 μ

(#0536-9)

FIGURE 32. TEM of B-88 (Specimen A-2) Creep Tested 107.8 Hours at 2200°F 34,000 psi, 1.0% Plastic Strain, Showing Grain Boundary Migration During Creep.

(#0586-1)

FIGURE 33. TEM of B-88 (Specimen A-2) Creep Tested 107.8 Hours at 2200°F (1205°C) at 34,000 psi to 1.0% Plastic Strain, Showing Grain Boundary Migration.

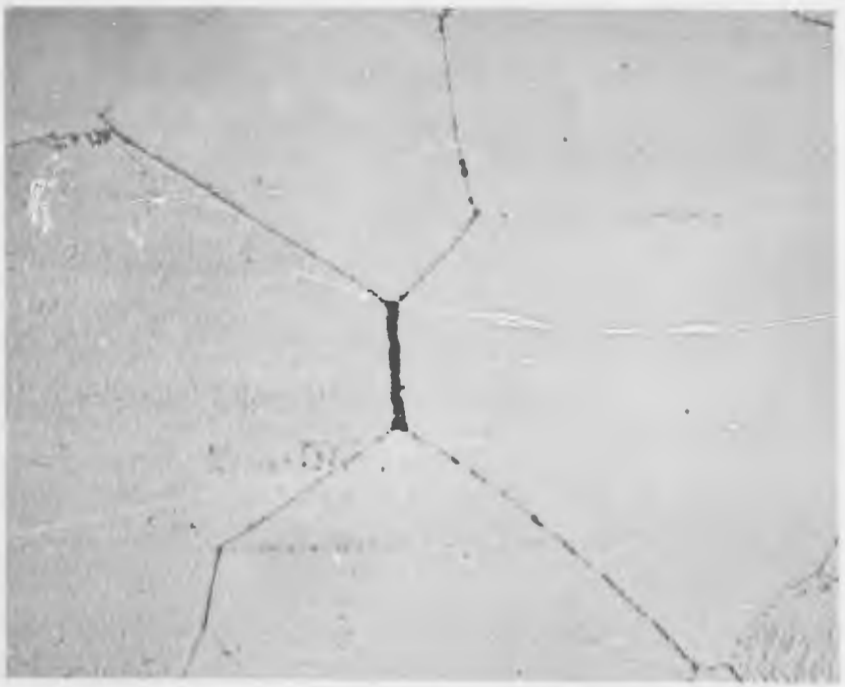

(a) 500X

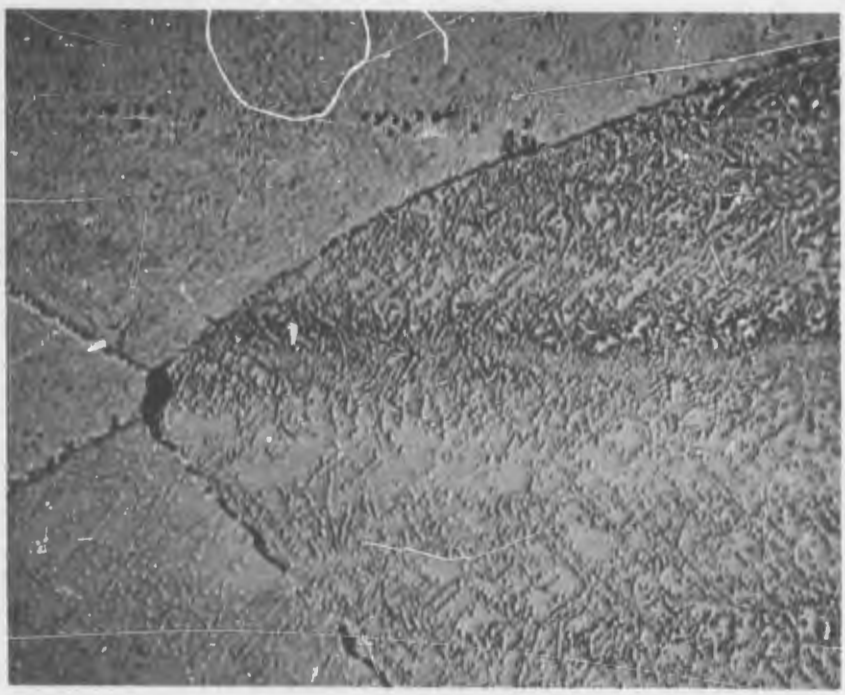

(b) 1,500X

(18.546)

FIGURE 34. Specimen A-1 (B-88) As Creep Tested 168 Hours at 2200°F (1205°C) at 34,000 psi, 1.66% Plastic Strain.

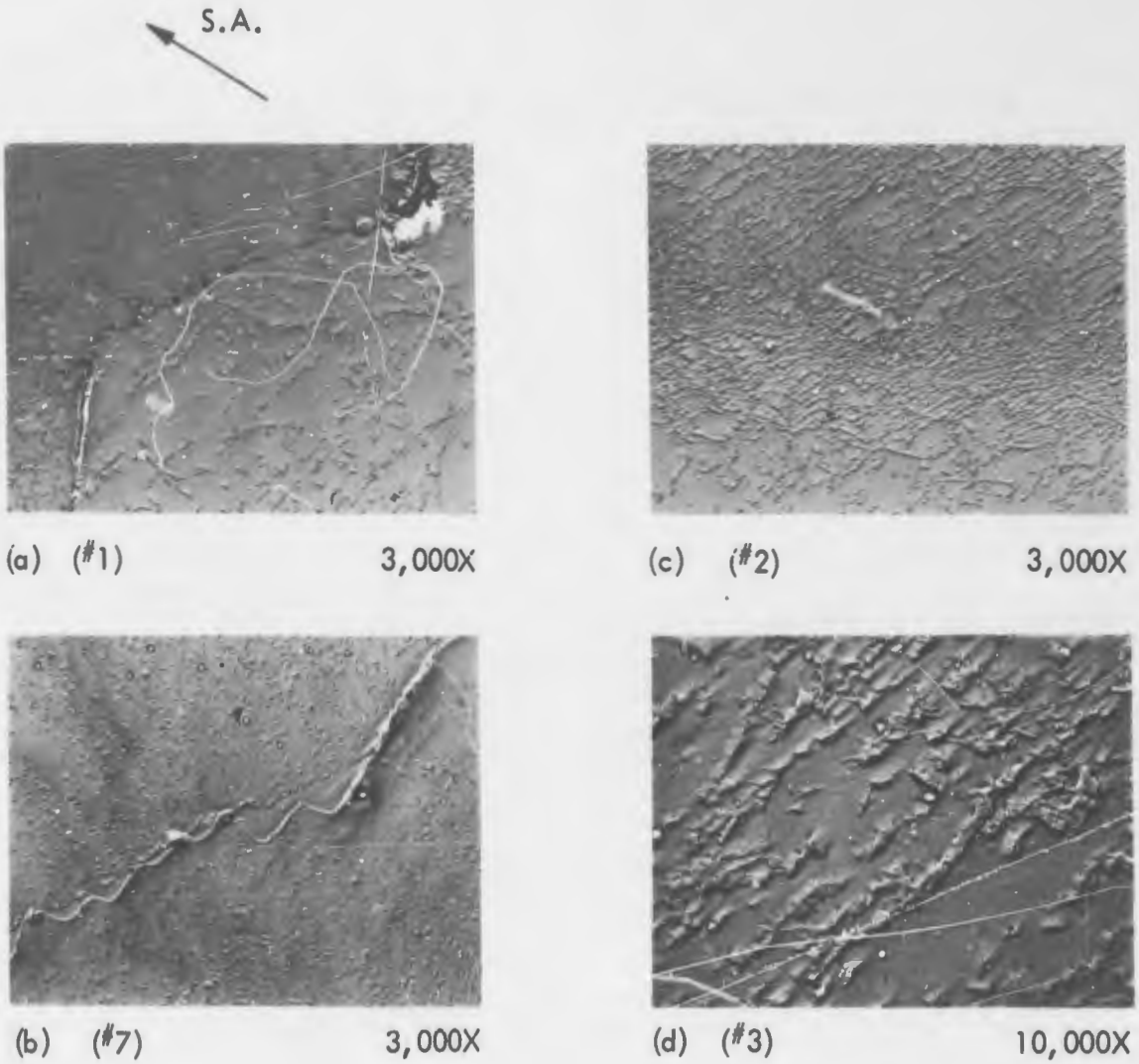

(0589-)

FIGURE 35. Surface Replicas of Specimen A-1 (B-88) As Creep Tested 168 Hours at 2200°F (1205°C) at 34,000 psi, 1.66% Plastic Strain.

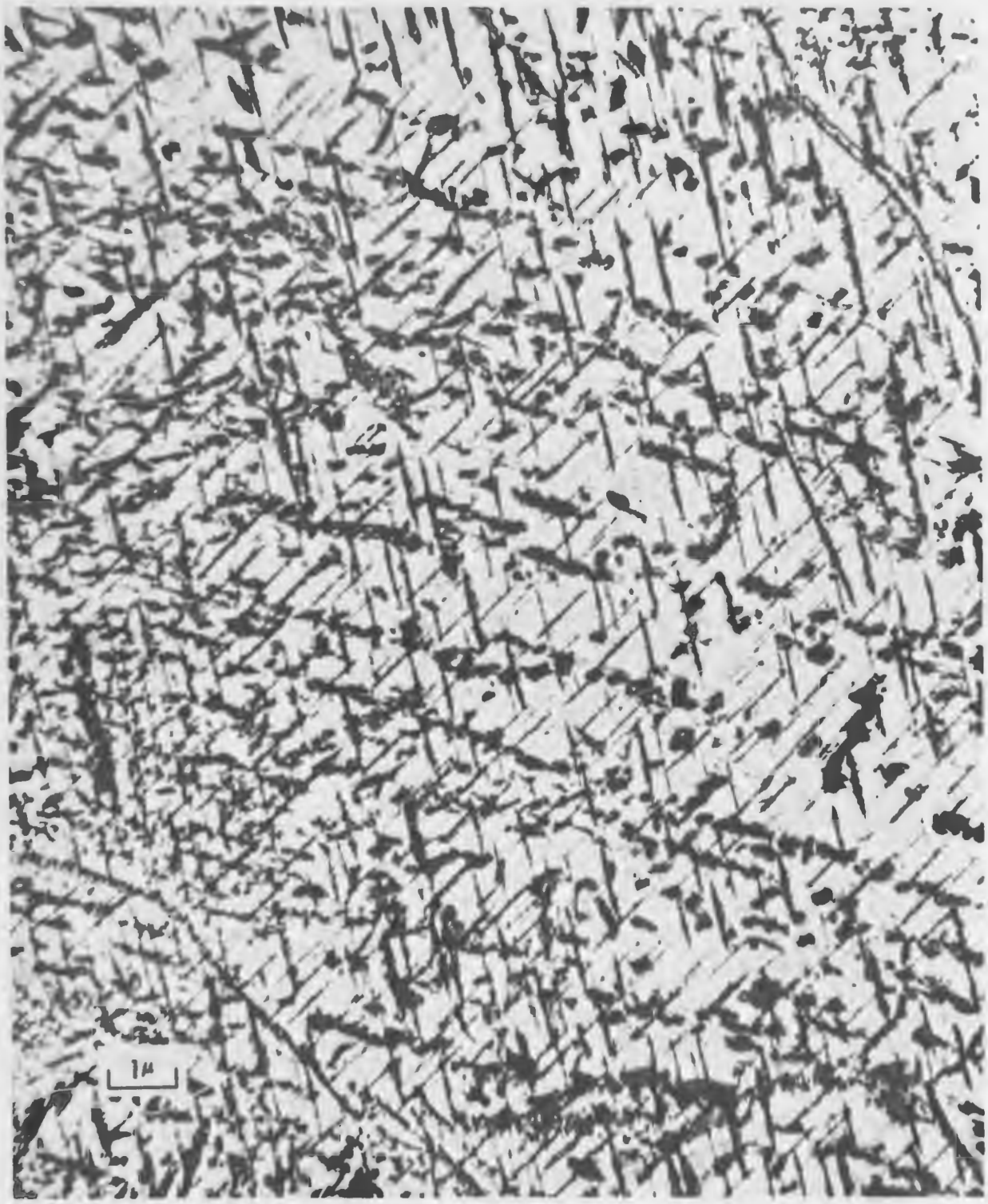

(#0587-7)

FIGURE 36. TEM of (111) Foil of B-88 (Specimen A-1) Creep Tested 168 Hours at 2200°F, 34,000 psi into 3rd Stage Creep. Plastic Strain = 1.66%.

The transmission photographs of this specimen is shown in Figures 36 through 40. Figure 36 shows at a lower magnification a (111) foil where the precipitation on all of the possible (110 planes is represented. By reference to Figure 8 for the material in the initial condition we see that the individual carbides in the Widmanstatten array of platelets on (110) matrix planes are now more continuous. However, the initial array or the spacings between platelets has not greatly changed from the initial condition. Figure 37 is a (100) foil showing the precipitates on (110) passing through the foil thickness. The strong dislocation precipitate interaction is evident. A small number of coherent precipitates are visible with the vector of zero contrast perpendicular to g [011] . This effect is also apparent in the (311) foil of Figure 38. Figure 39 shows a migrating grain boundary which is almost entirely free of precipitation. Of interest here are the dislocations passing through the boundary of Point A and terminating at the foil surface. Figure 40 shows that the dimension of the bulk extracted precipitate has considerably diminished. Very few thick blocky precipitates have formed and the large platelets have completely disappeared. The superimposed E.D.P. on Figure 40B show these platelets to be the $MC_{(1-x)}$ cubic carbide. Two distinct lattice parameters were observed here (4.57 Å and 4.58 Å) corresponding to a hafnium content of 35 and 36 a/o.

I-V. CONCLUSION

The significant observations during this study were:

1. The Hf content in the cubic carbides changed from 10 a/o in the initial condition to 36 a/o after 168 hours at 2200°F. The change in precipitate morphology is a consequence of the carbides striving for equilibrium. The Widmanstatten platelets on matrix (110) planes have remained relatively constant in morphology throughout creep, coarsening only by becoming more continuous. The zeta platelets comprising the initial grain boundary film and the substructure array transfer quickly to the cubic carbide. The original substructure almost completely dissappears by the time of entry to 3rd stage creep.

(#0587-1)

FIGURE 37. TEM of (100) Foil of B-88 (Specimen A-1) Creep Tested 168 Hours at 2200°F, 34,000 psi into 3rd Stage Creep. Plastic Strain = 1.66%.

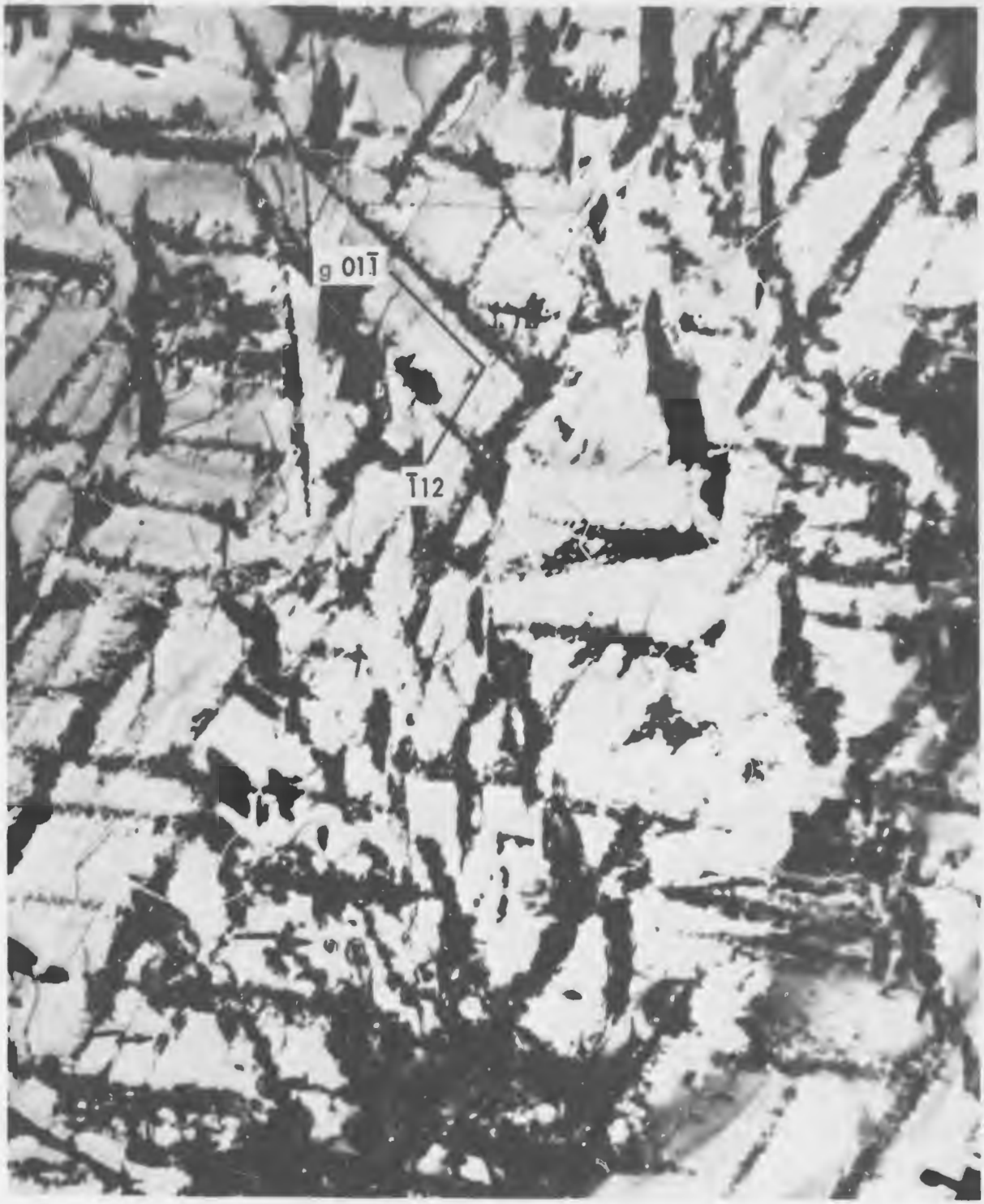

(0587-2b)

FIGURE 38. TEM of (311) Foil of B-88 (Specimen A-1) Creep Tested 168 Hours at 2200°F, 34,000 psi into 3rd Stage Creep. Plastic Strain = 1.66%.

(0587-6)

1μ

FIGURE 39. TEM of B-88 (Specimen A-1) Creep Tested 168 Hours at 2200°F at 34,000 psi into 3rd Stage Creep, Plastic Strain = 1.66%.

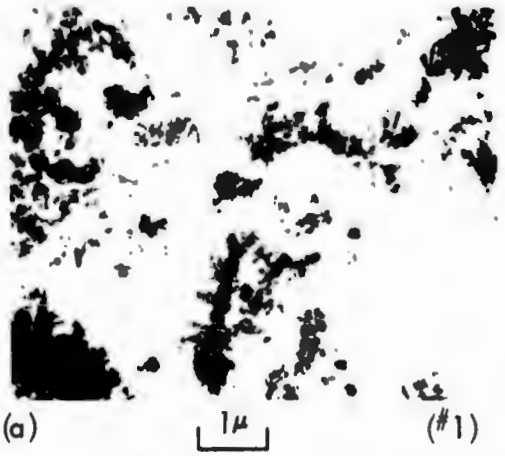

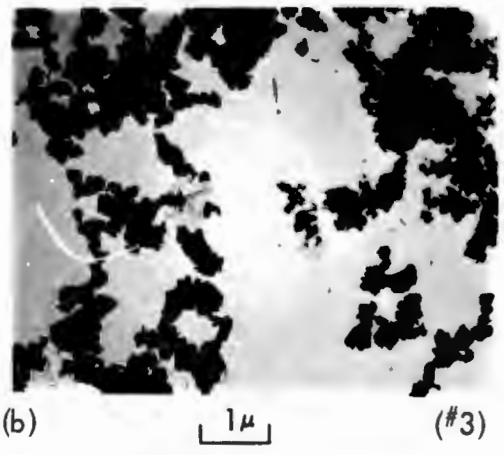

FIGURE 40. TEM of Bulk Extractions from B-88 (Specimen A-1) Creep Tested 168 Hours at 2200°F, 34,000 psi into 3rd Stage Creep, Plastic Strain = 1.66%

2. Grain boundary voids form during second stage creep. The early entry into third stage creep is a consequence of this fact. Grain boundary migration and associated grain boundary shear was demonstrated.

3. The fine and relatively stable "lattice work" of platelet like precipitates on (110) matrix planes appear to be an effective barrier to dislocation motion. This observation may explain why columbium alloys containing carbon are stronger in creep after solutioning than in the wrought condition.

4. The relatively coarse grain boundary participates undergo morphological changes during creep (or aging) at 1205°C (2200°F) and become less continuous.

5. Very few undecorated dislocations were observed in the specimen tested into the primary stage of creep (1.5 hours). Undecorated dislocations were observed during later stages of creep but most of them appeared to be tightly bound and immobilized by the "lattice work" precipitates. The dislocation density is much less than expected. It appears that much of the creep elongation is due to the grain boundary effects.

The above observations lead to a way of improving the creep life of B-88. If the alloy was periodically solution heat treated during use, the initial creep resistance and phase morphology and distribution could be reestablished. In addition, voids formed during second stage creep could be re-solutioned, thus extending the amount of total creep elongation. Certain aging treatments may be possible which would solution the grain boundary precipitates. The removal of these precipitates from grain boundaries would enhance grain boundary migration and hence, increase the amount of deformation before the onset of third stage creep.

REFERENCES

1. R. T. Begley, J. A. Cornie, and R. C. Goodspeed, Development of Columbium Base Alloys, AFML-TR-67-116, Air Force Materials Laboratory, Wright Patterson A.F.B., Ohio, Nov. 1967.

2. R. T. Begley, D. L. Harrod and R. E. Gold, "Refractory Metal Alloys," Machlin, Begley, and Weisert, ed. Plenum Press, New York, 1968.

3. Ostermann, Friedrich, Phase Stability in Carbon Containing Nb Base Alloys, PhD Thesis, University of Aachen, West Germany, (1965).

4. P. Stecher, F. Benesovsky, A. Neckol, and H. Nowotny, Untersuchungen in der Systemen Titan (Zirkonium, Hafnium), Niob - Kohlenstoff, Monatsh. for Chemie, 95, 6, pp 1630-45 (1964).

UNCLASSIFIED

Security Classification

DOCUMENT CONTROL DATA - R & D

(Security classification of title, body of abstract and indexing annotation must be entered when the overall report is classified)

1. ORIGINATING ACTIVITY (Corporate author)

Westinghouse Electric Corporation
Astronuclear Laboratory
Pittsburgh, Pennsylvania 15236

2a. REPORT SECURITY CLASSIFICATION

Unclassified

2b. GROUP

3. REPORT TITLE

Investigation of the Effects of Thermal Mechanical Variables on the Creep Properties of High Strength Columbium Alloys

4. DESCRIPTIVE NOTES (Type of report and inclusive dates)

Final Report April 1967 - January 1969

5. AUTHOR(S) (First name, middle initial, last name)

Cornie, J. A.
Begley, R. T.

6. REPORT DATE	7a. TOTAL NO. OF PAGES	7b. NO. OF REFS
August 1969	260	20

8a. CONTRACT OR GRANT NO	9a. ORIGINATOR'S REPORT NUMBER(S)
F33615-67-C-1443	
b. PROJECT NO. 7351	AFML-TR-69-224
c. Task No. 735101	9b. OTHER REPORT NO(S) (Any other numbers that may be assigned this report)
d.	

10. DISTRIBUTION STATEMENT This document is subject to special export controls and each transmittal to foreign governments or foreign nationals may be made only with prior approval of the Metals and Ceramics Division (MAM), Air Force Materials Laboratory, Wright-Patterson AFB, Ohio 45433.

11. SUPPLEMENTARY NOTES	12. SPONSORING MILITARY ACTIVITY
	Metals and Ceramics Division Air Force Materials Laboratory Wright-Patterson AFB, Ohio 45433

13. ABSTRACT A comparison of the properties of two high strength columbium base alloys, Cb-1(Cb-30W-1Zr-0.06C-0.04N) and B-88 (Cb-28W-2Hf-0.067C) was made to reconcile the reported variation in mechanical properties of the two compositions. Studies of recrystallization, grain growth and response to thermal-mechanical processing were carried out to characterize the material. The alloys were quite similar in their response to thermal treatment with the exception that Cb-1 showed aging response in the temperature range 1000-1200°C. The aging behavior was attributed to the precipitation of a zirconium nitride or carbonitride. The 1315°C creep-rupture properties of the two alloys were quite similar when compared in equivalent structural conditions, with Cb-1 being slightly superior to B-88. The ductile-brittle transition of B-88 was approximately 50°C lower than that of Cb-1.

Studies of methods to increase the intermediate temperature (1200-1600°F) yield strength of creep resistant columbium alloys were also carried out. Prestraining was shown to be an effective means of increasing the yield strength in this temperature range. Prestraining a Cb-22W-2Hf-0.06C alloy 9% at 1400°F raised the 1400°F yield strength from 50,000 psi to 95,000 psi. Detailed studies of recovery behavior of prestrained specimens were conducted to permit prediction of the effect of protective coating thermal cycles on residual strain hardening.

The precipitation hardening behavior of a Cb-W-Hf-C-N alloy was also investigated to determine if the intermediate temperature strength of a creep resistant Cb alloy could be increased without degrading high temperature rupture properties. A Cb-22W-2Hf-0.05C-0.04N alloy exhibited pronounced aging response in the 1000-1200°C temperature range. A double aging peak was observed. Transmission photomicroscopy studies showed the hardness peaks correlated with the presence of a high density of small coherent precipitates, presumably a hafnium nitride or carbonitride.

DD FORM 1 NOV 65 1473

UNCLASSIFIED

Security Classification

14. KEY WORDS	LINK A		LINK B		LINK C	
	ROLE	WT	ROLE	WT	ROLE	WT
Alloy Development						
Columbium						
High Temperature Mechanical Properties						
Thermal-Mechanical Processing						

END